OPTIMAL PLACEMENT AND SIZING OF VAR COMPENSATORS IN POWER SYSTEMS USING IMPROVED AND GLOBAL HARMONY SEARCH ALGORITHMS

REZA SIRJANI

THESIS SUBMITTED IN FULFILMENT OF THE DEGREE OF DOCTOR OF PHILOSOPHY

FACULTY OF ENGINEERING AND BUILT ENVIROMENT
UNIVERSITI KEBANGSAAN MALAYSIA
BANGI

2013

PENEMPATAN DAN PENSAIZAN OPTIMUM PEMAMPAS VAR DALAM SISTEM KUASA MENGGUNAKAN ALGORITMA CARIAN HARMONI LEBIH BAIK DAN GLOBAL

REZA SIRJANI

TESIS YANG DIKEMUKAKAN UNTUK MEMPEROLEH IJAZAH
DOKTOR FALSAFAH

FAKULTI KEJURUTERAAN DAN ALAM BINA
UNIVERSITI KEBANGSAAN MALAYSIA
BANGI

2013

DECLARATION

I hereby declare that the work in this thesis is my own except for quotations and summaries which have been duly acknowledged.

2 January 2013

REZA SIRJANI
P49861

ACKNOWLEDGMENTS

All praises to Allah for the strengths and His blessing in completing this thesis. I deeply acknowledge the contribution of Prof.Dr.Azah Mohamed, without whose constant guidance, forbearance and utmost patience, this thesis would never have been possible. I could not have imagined having a better supervisor for my PhD, and without her common-sense, knowledge, perceptiveness and expertise in a wide variety of subjects, I would have never understood the merits of analyzing difficult problems from the basic principles.

My special thanks to my co-supervisor Dr.Hussain Shareef for his invaluable guidance, concern and support. He has always given me a word of support.

A big ”thank-you” to my beloved wife , Badieh who had to bear with me through the entire process and provided me constant encouragement and reassurance whenever needed. I am grateful for her endless love, prayers and care.

My deepest gratitude goes to my parents who have been a continuous source of support and motivation. I am thankful that they have always required high standards in my education. I also wish to thank my parents-in-law for their encouragement and support in helping motivate me to complete my PhD.

I would like to dedicate this thesis to my soulmate, my angel and my love, Badieh for her continuous love, affection, support and inspiration.

ABSTRACT

Reactive power compensation has been widely used to increase the steady state transmittable power by controlling the voltage profile along the transmission lines in power systems. A number of reactive compensation devices such as shunt capacitor, static Var compensator (SVC) and static synchronous compensator (STATCOM) have long been applied by electric power utilities for this purpose. However, the benefits of reactive power compensation depend greatly on the placement and size of the compensators. For the purpose of finding optimal placement and sizing of Var compensators, two novel optimization techniques, namely, the improved harmony search (IHS) algorithm and the global harmony search algorithm (GHS) are applied for generating new solution vectors so as to enhance the accuracy and convergence of the conventional harmony search (HS) algorithm. In this research, the IHS and GHS algorithms are used together with the backward/forward sweep power flow method and radial harmonic power flow for determining the optimal placement and sizing of capacitors in radial distribution networks for minimizing the power loss and total cost by considering mutual coupling, load unbalancing and harmonics. The IHS and GHS algorithms are also employed to determine the optimal location and size of Var compensators such as shunt capacitor, SVC and STATCOM in transmission networks to enhance voltage stability and improve voltage profile by minimizing power loss and total cost. A comparative study has been done to evaluate the effectiveness of the different Var compensators. To implement the developed IHS and GHS algorithms, the backward/forward sweep power flow and radial harmonic power flow methods in an open source environment, a Matlab based software tool named as Optimal Placement of Shunt Var Compensators has been developed. To validate the accuracy of the IHS and GHS algorithms, the three-phase 10 bus and 34 bus radial distribution systems were used for optimal capacitor placement and the 57 bus and 118 bus transmission systems were used for optimal placement of various Var compensators. The optimal capacitor placement results show that the IHS and GHS algorithms increase the net saving up to 27% and give greater reduction in power loss and total costs compared to genetic algorithm (GA), particle swarm optimization (PSO) and the conventional HS algorithm. The results of optimal placement and sizing of different Var compensators in transmission systems show that the IHS and GHS algorithms give lower power loss, better voltage profile and improved voltage stability compared to GA, PSO and conventional HS algorithm. The comparative study results show that although SVC and STATCOM are expensive compared to shunt capacitor, the effect of installing STATCOM is better than SVC and the effect of installing SVC is better than shunt capacitor in achieving power loss reduction, voltage profile improvement and voltage stability margin enhancement.

ABSTRAK

Pemampasan kuasa reaktif telah digunakan secara meluas untuk meningkatkan penghantaran kuasa keadaan mantap dengan mengawal profil voltan di sepanjang talian penghantaran dalam sistem kuasa. Beberapa peranti pemampasan reaktif seperti kapasitor pirau, pemampas statik Var (PSV) dan pemampas segerak statik (PSS) telah lama digunakan oleh utiliti kuasa elektrik untuk tujuan tersebut. Walau bagaimanapun, manfaat pemampasan kuasa reaktif sangat bergantung kepada lokasi dan saiz pemampas. Bagi menentukan kedudukan dan saiz pemampas Var yang optimum, satu algoritma carian harmoni lebih baik (CHLB) dan algoritma carian harmoni global (CHG) telah dicadangkan untuk menghasilkan vektor penyelesaian baru bagi memperbaiki ketepatan dan penumpuan berbanding algoritma carian harmoni (CH) konvensional. Dalam kajian ini, algoritma CHLB dan CHG telah digunakan bersama dengan kaedah aliran kuasa sapuan ke hadapan/ke belakang dan aliran kuasa harmonik untuk menentukan kedudukan optimum dan saiz kapasitor dalam rangkaian agihan jejari bagi tujuan meminimakan kehilangan kuasa dan jumlah kos serta mengambil kira faktor saling gandingan, ketak-seimbangan beban dan harmonik. Algoritma CHLB dan CHG turut digunakan untuk menentukan lokasi dan saiz optimum bagi pemampas Var seperti kapasitor pirau, PSV dan PSS dalam rangkaian penghantaran untuk tujuan meningkatkan kestabilan, memperbaiki profil voltan, meminima kehilangan kuasa dan keseluruhan kos. Satu kajian perbandingan telah dilakukan untuk menilai keberkesanan pelbagai pemampas Var. Bagi melaksanakan algoritma CHLB dan CHG berserta dengan aliran kuasa sapuan ke hadapan /ke belakang dan jejarian harmonik, sejenis perisian sumber terbuka berasaskan Matlab yang dinamakan sebagai Penempatan Optimum Pemampas Pirau Var (OPSVC) telah dibangunkan. Untuk mengesahkan ketepatan algoritma CHLB dan CHG, sistem agihan jejari tiga-fasa 10 bas dan 34 bas telah digunakan untuk menentukan lokasi optimum kapasitor dan sistem penghantaran 57 bas dan 118 bas telah digunakan untuk menentukan lokasi optimum pelbagai pemampas Var. Keputusan penempatan optimum kapasitor menunjukkan bahawa algoritma CHLB dan CHG meningkat penjimatan sehingga 27% dan memberikan pengurangan kehilangan kuasa dan jumlah kos yang lebih besar berbanding dengan algoritma genetik (AG), pengoptimuman kuruman zarah (PKZ) dan algoritma CH konvensional. Keputusan penentuan lokasi dan saiz yang optimum bagi pelbagai pemampas Var menunjukkan bahawa algoritma CHLB dan CHG memberi kehilangan kuasa yang lebih rendah, profil dan kestabilan voltan yang lebih baik berbanding dengan AG, PKZ dan algoritma CH. Keputusan kajian perbandingan menunjukkan bahawa walaupun kos pemasangan PSV dan PSS adalah mahal berbanding dengan kapasitor pirau, kesan PSS adalah lebih baik daripada PSV dan kesan PSV pula adalah lebih baik daripada kapasitor pirau untuk mencapai pengurangan kehilangan kuasa, pembaikan profil voltan dan peningkatan jidar kestabilan voltan.

TABLE OF CONTENTS

		Page
DECLARATION		iii
ACKNOWLEDGMENTS		iv
ABSTRACT		v
ABSTRAK		vi
CONTENTS		vii
LIST OF TABLES		xii
LIST OF FIGURES		xiv
LIST OF ABBREVIATIONS		xvii
LIST OF SYMBOLS		xix
CHAPTER I	**INTRODUCTION**	
1.1	Research Background	1
1.2	Problem Statement	4
1.3	Objectives of Research and Scope of Works	5
CHAPTER II	**LITERATURE REVIEW**	
2.1	Reactive Compensation Devices in Power Systems	8
	2.1.1 Shunt Capacitors	9
	2.1.2 Static Var Compensator	10
	2.1.3 Static Compensator	12
	2.1.4 Comparison of Shunt Capacitor, SVC and STATCOM	15
2.2	Review of Heuristic Optimization Techniques for Optimal Placement and Sizing of Capacitors in Distribution Systems	17
	2.2.1 Fuzzy Logic	17
	2.2.2 Evolutionary Computation	18
	2.2.3 Hybrid Artificial Intelligent Techniques	21
	2.2.4 Other Optimization Techniques	22
2.3	Heuristic Optimization Techniques for Optimal Placement and Sizing of SVC and STATCOM	22
	2.3.1 Evolution Strategy	23
	2.3.2 Genetic Algorithms	23

	2.3.3 Simulated Annealing	24
	2.3.4 Particle Swarm Optimization	24
	2.3.5 Harmony Search Algorithm	25
	2.3.6 Hybrid Artificial Intelligent Techniques	26
	2.3.7 Other Optimization Techniques	26
2.4	Chapter Summary	27
CHAPTER III	**HEURISTIC OPTIMISATION TECHNIQUES**	
3.1	Introduction	28
3.2	Genetic Algorithm	29
3.3	Particle Swarm Optimization	32
3.4	Harmony Search Algorithm	35
	3.4.1 Initialization of the Optimization Problem	37
	3.4.2 Initialization of the Harmony Memory	37
	3.4.3 Improvisation a New Harmony from the HM set	38
	3.4.4 Updating HM	39
	3.4.5 Checking stopping criterion	39
	3.4.6 Advantages of Harmony Search Algorithm	40
3.5	Improved Harmony Search Algorithm	41
3.6	Global Harmony Search Algorithm	43
3.7	Chapter Summary	47
CHAPTER IV	**OPTIMAL PLACEMENT AND SIZING OF CAPACITORS IN RADIAL DISTRIBUTION SYSTEMS**	
4.1	Introduction	48
4.2	Optimal Capacitor Placement and Sizing Formulation	49
4.3	Backward/Forward Sweep Power Flow	51
4.4	Harmonic Power Flow	54
4.5	Optimal Capacitor Placement and Sizing Method without Considering Mutual Coupling, Load Unbalance and Harmonics	60
	4.5.1 Application of IHS Algorithm for Optimal Capacitor Placement	60
	4.5.2 Application of GHS Algorithm for Optimal Capacitor Placement	64

4.6	Optimal Capacitor Placement and Sizing Method Considering Mutual Coupling, Load Unbalance and Harmonics	66
	4.6.1 Application of IHS Algorithm for Optimal Capacitor Placement in Three Phase Radial Distribution Systems	66
	4.6.2 Application of GHS Algorithm for Optimal Capacitor Placement in Three Phase Radial Distribution Systems	69
4.7	Chapter Summary	72
CHAPTER V	**OPTIMAL PLACEMENT AND SIZING OF VAR COMPENSATORS IN TRANSMISSION SYSTEMS**	
5.1	Modal Analysis for Determining Var Compensator Placement	73
5.2	Problem Formulation for Optimal Sizing of Var Compensators	76
	5.2.1 Operational Constrains	77
	5.2.2 Fitness Function	78
5.3	Optimal Placement and Sizing of SVC Using IHS and GHS Algorithms	79
	5.3.1 Application of IHS Algorithm for Optimal Placement and Sizing of SVCs	80
	5.3.2 Application of GHS Algorithm for Optimal Placement and Sizing of SVCs	82
5.4	Optimal STATCOM Placement and Sizing Method	84
	5.4.1 Application of IHS Algorithm for Optimal Placement and Sizing of STATCOM	85
	5.4.2 Application of GHS Algorithm for Optimal Placement and Sizing of STATCOM	87
5.4	Software Tool for Optimal Placement and Sizing of Shunt Var compensators inPower Systems	89
	5.5.1 Programming Language	89
	5.5.2 Software Structure	90
5.5	Chapter Summary	91

CHAPTER VI RESULTS AND DISCUSSION

6.1 Results of Optimal Capacitor Placement and Sizing in Radial Distribution Systems 93

6.1.1 Optimal Capacitor Placement Results for the 10 Bus Test System 94
6.1.2 Optimal Capacitor Placement Results for the 34 Bus Test System 96
6.1.3 Optimal Capacitor Placement Results for the Unbalanced 10 Bus Test System with Harmonics Considerations 98
6.1.4 Optimal Capacitor Placement Results for the Unbalanced 34 Bus Test System with Harmonics Considerations 102
6.1.5 Convergence Characteristics and Accuracy of Different Optimization Techniques for Optimal Placement and Sizing of Capacitors in the Unbalanced 34 Bus System 105

6.2 Results of Optimal SVC Placement and Sizing in Transmission Systems 106

6.2.1 Optimal SVC Placement Results for the 57 Bus Test System 107
6.2.2 Optimal SVC Placement Results for the 118 Bus Test System 113

6.3 Results of Optimal STATCOM Placement and Sizing in Transmission Systems 116

6.3.1 Optimal STATCOM Placement Results for the 57 Bus Test System 117
6.3.2 Optimal STATCOM Placement Results for the 118 Bus Test System 118

6.4 Comparative Study of the Effectiveness of Different Var Compensation Devices 120

6.4.1 Comparative Study Results for the 57 Bus Test System 120
6.4.2 Comparative Study Results for the 118 Bus Test System 124

6.5 Results on the Use of the OPSVC Software 127

6.5.1 Example of Using OPSVC for Analyis on a Radial Distribution System 127
6.5.2 Example of Using OPSVC for Analysis on a Transmission System 129

6.6	Chapter Summary	130
CHAPTER VII	**CONCLUSION AND FUTURE WORKS**	
7.1	Conclusion	132
7.2	Significant Contributions of the Research	134
7.3	Suggestions for Future Work	135
REFERENCES		136
APPENDIXES		
A	Partial Derivatives for STATCOM Model	147
B	IEEE 34 Bus Test System Data	149
C	Unbalanced 34 Bus Test System Data	150
D	IEEE 57 Bus Test System Data	154
E	IEEE 118 Bus Test System Data	156
F	MATLAB Codes for Backward/Forward Sweep Power Flow in Distribution Systems	161
G	MATLAB Codes for Harmonic Power Flow in Distribution Systems	164
H	Main Modules of the OPSVC Software	171
I	List of Publications	181

LIST OF TABLES

Table Number		Page
2.1	Comparison between SVC and STATCOM	16
6.1	Load and line data of the 10 bus test system	95
6.2	Comparison of capacitor placement results of the 10 bus system	96
6.3	Optimal capacitor placement results of the 34 bus system	97
6.4	Comparison of capacitor placement results of the 34 bus system	98
6.5	The load data for unbalanced 10 bus test system	99
6.6	Line impedances considering mutual coupling	99
6.7	The harmonic surce data for the unbalanced 10 bus test system	100
6.8	Capacitor placement results of the unbalanced 10 bus system considering mutual coupling, load unbalance and harmonic effects	101
6.9	Comparison of results of different optimization techniques for the unbalanced 10 bus system considering mutual coupling, load unbalance and harmonic effects	101
6.10	Capacitor placement results of the unbalanced 34 bus system by considering mutual coupling, load unbalance and harmonic effects	103
6.11	Comparison of results of different optimization techniques for unbalanced 34 bus system by considering mutual coupling, load unbalancing and harmonic effects	104
6.12	Accuracy of different optimization techniques for the optimal capacitor placement and sizing for unbalanced 34 bus test system	106
6.13	The participation factor values of all load buses in the 57 bus test system	108
6.14	Results of optimal SVC placement and size using different optimization techniques for the 57 bus test system	109
6.15	A comparison of objective function components after SVC installation in the 57 bus test system	110
6.16	Accuracy of different optimization techniques for the optimal SVC placement and sizing in the 57 bus test system	113
6.17	The participation factor values of critical buses in the 118 bus test system	113
6.18	Results of optimal SVC placement and size using different optimization techniques for the 118 bus test system	114
6.19	A comparison of objective function components after SVC installation in the 118 bus test system	115

6.20 A comparison of different optimization techniques for optimal placement and sizing of STATCOM in the 57 bus test system 117
6.21 A comparison of different optimization techniques in optimal placement and sizing of STATCOM in the 118 bus test system 118
6.22 Accuracy of different optimization techniques for the optimal STATCOM placement and sizing in the 118 bus test system 119
6.23 Cost comparison of Var compensators 122
6.24 Optimum size for single shunt Var compensator at the critical bus of the 57 bus test system 122
6.25 Comparing the effect of different Var compensators installed at the weakest bus of the 57 bus test system 123
6.26 The optimum size for single shunt Var compensator at the critical bus of the 118 bus test system 126
6.27 Comparing the effect of different Var compensators installed at the weakest bus in the 118 bus test system 126

LIST OF FIGURES

Figure Number		Page
2.1	Three phase shunt capacitor model	10
2.2	SVC building blocks	11
2.3	SVC connected to a transmission line	12
2.4	STATCOM representation (a) VSC connected to the AC network via a transformer (b) Shunt solid-state voltage source	13
3.1	Basic concept of PSO	33
3.2	Comparison between music improvisation and engineering optimization	36
3.3	The procedures of the conventional HS algorithm	40
3.4	Variation of a) PAR and b) bw with generation number	42
3.5	The procedures of the IHS algorithm	43
3.6	The schematic diagram of position updating	44
3.7	The procedures of the GHS algorithm	46
4.1	Simple radial distribution network	51
4.2	Flowchart of the backward/forward sweep power flow for radial distribution systems	53
4.3	A single line diagram of a distorted n-bus radial distribution system	54
4.4	Flowchart of the harmonic power flow algorithm	58
4.5	The IHS algorithm for solving the capacitor placement and sizing problem	63
4.6	The GHS algorithm for solving the capacitor placement problem	65
4.7	The IHS algorithm for solving the capacitor placement problem considering mutual coupling, load unbalance and harmonics	68
4.8	The GHS algorithm for solving the capacitor placement problem by considering mutual coupling, load unbalancing and harmonics	71
5.1	The IHS algorithm for solving the SVC placement problem	81
5.2	Procedures used in solving the optimal SVC placement and sizing problem using modal analysis and the GHS algorithm	83
5.3	Procedures used in solving the optimal STATCOM placement and sizing problem using modal analysis and the IHS algorithm	86
5.4	Procedures used in solving the optimal STATCOM placement and sizing problem using modal analysis and the GHS algorithm	88

5.5	Procedure in the OPSVC	91
6.1	Yearly costs of fixed capacitors	94
6.2	The 10 bus test system	94
6.3	The 34 bus test system	97
6.4	The three-phase 10 bus test system	98
6.5	Three-phase 34 bus test system	102
6.6	Convergence characteristics of different optimization techniques for the optimal placement and sizing of capacitors in the unbalanced 34 bus test system	105
6.7	Network configuration of the IEEE 57 bus test system	107
6.8	Voltage profiles before and after SVC placement in the 57 bus test system	111
6.9	Total voltage deviations before and after SVC placement in the 57 bus test system	111
6.10	Convergence characteristics of different optimization techniques for the optimal placement and sizing of SVCs in the 57 bus test system	112
6.11	Voltage profiles before and after SVC placement in the 118 bus test system	115
6.12	Total voltage deviations before and after SVC placement in the 118 bus test system	116
6.13	Convergence characteristics of different optimization techniques for the optimal placement and sizing of STATCOM in the 118 bus test system	119
6.14	Power loss versus Var compensator size after installing different devices in the 57 bus test system	120
6.15	Voltage deviation versus Var compensator size after installing different devices in the 57 bus test system	121
6.16	Smallest eigenvalue in the critical mode versus Var compensator size after installing the different devices in the 57 bus test system	121
6.17	Power loss versus Var compensator size after installing different devices in the 118 bus test system	124
6.18	Voltage deviation versus Var compensator size after installing the different devices in the 118 bus test system	125
6.19	Smallest eigenvalue versus Var compensator size after installing different devices in the 118 bus test system	125
6.20	Output display of the GUI for optimal capacitor placement in the 10 bus distribution system using the GHS algorithm	128
6.21	Voltage improvement after optimal capacitor placement in the 10 bus distribution system plotted by the OPSVC software	128

6.22 Output display of the GUI for optimal SVC placement in the 57 bus test system using the IHS algorithm 129

6.23 Voltage improvement after SVC placement in the 57 bus test system plotted by the OPSVC software 130

6.24 Voltage deviation before and after SVC placement in the the 57 bus test system plotted by the OPSVC software 130

LIST OF ABBREVIATIONS

AC:	Alternating Current
ACO:	Ant Colony Optimization
AI:	Artificial Intelligent
AIS:	Artificial Immune System
ANN:	Artificial Neural Network
BCO:	Bee Colony Optimization
BCP:	Before Capacitor Placement
DC:	Direct Current
DP:	Dynamic Programming
ES:	Evolution Strategy
FACTS:	Flexible AC Transmission System
GA:	Genetic Algorithm
GHS:	Global Harmony Search
GP:	Genetic Programming
GSA:	Gravitational Search Algorithm
GUI:	Graphical User Interface
HM:	Harmony Memory
HMCR:	Harmony Memory Considering Rate
HMS:	Harmony Memory Size
HS:	Harmony Search
HVDC:	High Voltage Direct Current
IHS:	Improved Harmony Search
LDS:	Low Discrepancy Sequences
LP:	Linear Programming
MATLAB:	Matrix Laboratory
NLP:	Non-Linear Programming
OPSVC:	Optimal Placement of Shunt Var Compensators
PAR:	Pitch Adjusting Rate
PSO:	Particle Swarm Optimization
SA:	Simulated Annealing
SQP:	Sequential Quadratic Programming

STATCOM:	Static Synchronous Compensator
SVC:	Static Var Compensator
TCR:	Thyristor Controlled Reactor
THD:	Total Harmonic Distortion
TS:	Tabu Search
TSC:	Thyristor Switched Capacitor
TSR:	Thyristor Switched Reactor
VSC :	Voltage Source Converter

LIST OF SYMBOLS

I^{abc} : Equivalent current injection of installed shunt capacitor

B_{svc}: Susceptance of the SVC

I_{svc}: Injected current of the SVC

Q_{svc} : Injected reactive power of the SVC

$pbest_i^k$: Best position ever visited by a particle i at the k^{th} iteration

$gbest^k$: Global best position in the entire swarm

bw: Band width

p_m : Genetic mutation probability

V_i : Voltage at bus i

V_{max}: Maximum bus voltage limit

V_{min} : Minimum bus voltage limit

R_i : Resistance of branch i.

P_i : Real powers at bus i.

$P_{loss}^{(Fund.)}$: Real power loss due to fundamental frequency

$P_{loss}^{(harmonics)}$: Real power loss due to harmonic frequencies

Q_i : Reactive powers at bus i

$[I]$: Bus current injection vector

$[B]$: Branch current vector

$[\Delta V]$: Voltage deviation

$[BIBC]$: Bus current injection to branch current matrix

$[BCBV]$: Branch current to bus voltage matrix

$[DLF]$: Voltage deviation to bus current injection matrix

P_{loss} : Total power loss

K_P : Equivalent annual cost of power loss

K_i^c: Annual capacitor installation cost

h : Harmonic order

h_0 : Lower limit of the harmonic order

H : Upper limit of the harmonic order

$[I^{(h)}]$: Vector of system harmonic currents at the h^{th} harmonic order

$[A_{ij}^{(h)}]$: The coefficient vector of harmonic currents for the branch between bus i and j at the h^{th} harmonic order

$[Ah_{ij}^{(h)}]$	:	The coefficient vector of the harmonic currents contributed by nonlinear loads and linear impedance for the branch between bus i and j at the h^{th} harmonic order
$[As_{ij}^{(h)}]$	:	The coefficient vector of harmonic currents absorbed by shunt capacitors for the branch between bus i and j at the h^{th} harmonic order
$Z_{ij}^{(h)}$	:	The branch impedance at the h^{th} harmonic order
$[HA^{(h)}]$	:	The relationship matrix between bus voltage vector and system harmonic current vector
$[HAs^{(h)}]$	:	Composed of the row vectors with respect to the buses of shunt capacitors
$Is_i^{(h)}$	:	The harmonic current of the shunt capacitor at bus i
$Z_{Si}^{(h)}$	:	The harmonic impedance of the shunt capacitor at bus i
L_v	:	Voltage deviation index
$\lambda_{Critical}$	:	Smallest eigenvalue
$Cost_{shunt}$	:	Total Var compensator cost
$\sum \Delta Loss_{base}$	:	The total active power loss in the network of the base system
$\sum V_{base}$	:	The total voltage deviation of the base system
$\lambda_{Critical(base)}$	:	The smallest eigenvalue of the base case
$Cost_{Max}$	:	The maximum cost

CHAPTER I

INTRODUCTION

1.1 RESEARCH BACKGROUND

Var compensation is defined as the management of reactive power to improve the performance of ac power systems. The concept of Var compensation embraces a wide and diverse field of both utility and customer problems, especially related with power quality issues, since most of power quality problems can be attenuated or solved with an adequate control of reactive power (Miller 1982; Dixon et al. 2006). In general, the problem of reactive power compensation is viewed from two aspects: load compensation and voltage support. In load compensation the objectives are to increase the value of the system power factor, to balance the real power drawn from the ac supply, compensate voltage regulation and to eliminate current harmonic components produced by large and fluctuating nonlinear industrial loads (Wanner et al. 1983; Bonnard 1985). Voltage support is generally required to reduce voltage fluctuation at a given terminal of a transmission line.

Reactive power compensation can be applied by means of either series or shunt compensation. Series compensation modifies the transmission or distribution system parameters, while shunt compensation changes the equivalent impedance of the load (Taylor 1999). In both cases, the reactive power that flows through the system can be effectively controlled, thus improving the performance of the overall ac power system. Shunt compensation is used to influence the natural electrical characteristics of transmission lines to increase the steady-state transmittable power and control the voltage profile along the line (Saranjeet 2009). Providing adequate reactive power support at the appropriate location not only leads to a reduction in the power loss and improvement in the voltage profile, but also solves voltage instability problems.

Reactive power compensation in transmission systems improves the stability of ac system by increasing the maximum active power that can be transmitted. It also helps to maintain a substantially flat voltage profile at all levels of power transmission, improves HVDC (High Voltage Direct Current) conversion terminal performance, increases transmission efficiency, controls steady-state and temporary overvoltages (Grudinin & Roytelman 1997), and can avoid disastrous blackouts (Grudinin & Roytelman 1997; Taylor 1999).

Many reactive compensation devices are used by modern electric power utilities in which each device has its own characteristics and limitations (Sode-Yome & Mithulananthan 2004). Traditionally, shunt capacitors are installed in power networks to compensate for reactive power. However, nowadays shunt capacitors are used for many purposes, such as power loss reduction, voltage profile improvement, and increasing the maximum transmitted power in cables and transformers. Among the reactive compensation devices, flexible AC transmission system (FACTS) devices play an important role in controlling the flow of reactive power to the power network, thereby affecting the system voltage fluctuations and stability (Azadani et al. 2008). The static Var compensator (SVC) is the most widely used shunt FACTS device in power networks due to its low cost and good performance in system enhancement. It is a shunt-connected static Var generator or absorber with an adjustable output, which allows the exchange of the capacitive or inductive current so as to provide voltage support. When installed at a proper location, the SVC can also reduce power losses. The static synchronous compensator (STATCOM) is also a shunt compensator and one of the important members of the FACTS family that are increasingly being used in long transmission lines in modern power systems. STATCOMs can have various applications in the operation and control of a power system, such as in power flow scheduling, reducing the number of unsymmetrical components that damp the power oscillations, and enhancing transient stability (Dixon et al. 2006). The shunt capacitor, SVC, and STATCOM are widely used to increase the static voltage stability margin and power transfer capability. However, SVC and STATCOM perform better than shunt capacitor in terms of reducing power loss and improving the voltage profile (Sode-Yome & Mithulananthan 2004).

Many techniques have been applied for solving the optimal capacitor placement problem in radial distribution systems. These techniques may be classified into the following categories: analytical, numerical programming, heuristic and artificial intelligence based techniques (Ng et al. 2000). Among these techniques, the heuristic optimization techniques have been widely applied in solving the optimal capacitor placement problem. The immune based optimization technique is used for selecting proper locations and ratings of capacitor banks in Huang (2000). Das (2000) applied genetic algorithm to determine the optimum capacitor locations and sizes of fixed and switched capacitors at various load levels. Fuzzy logic (Masoum et al. 2004) and particle swarm optimization (PSO) (Prakash & Sydulu 2007) have been applied to solve the capacitor placement problem by optimally locating and sizing the capacitors in radial distribution systems. In the above cases, the optimal capacitor placement problem is formulated as a nonlinear integer optimization problem by considering both capacitor location and size as discrete variables.

Several heuristic optimization techniques for determining optimal location and size of shunt FACTS devices have been reported in the literature, such as the genetic algorithm (GA), simulated annealing (SA), artificial immune system (AIS), and particle swarm optimization (PSO) techniques (Minguez et al. 2007). A solution algorithm based on SA is used to determine the location, types, and sizes of Var sources, as well as their settings at different loading conditions (Hsiao et al. 1993). The purchase, installation, and total costs of energy loss over the life of Var sources are minimized by considering the operational constraints (Hsiao et al. 1993). AIS technique has been applied to minimize the total loss and improve the voltage in a power system by determining the correct SVC placement (Ishak et al. 2004). GA is used to determine the best location of only one SVC in a power system, in which the objective function is to reduce the power loss, voltage deviation, and cost (Pisica et al. 2009). PSO has been used for optimal sizing and location of a STATCOM in a power system by considering voltage deviation constraints (Del Valle et al. 2006a). The application of PSO and continuation power flow (CPF) for the optimal allocation of multiple STATCOMs is presented in Azadani et al. (2008). The goal of the optimization is to improve the voltage profile, minimize the total power loss, and maximize the system loadability. The performance of an enhanced PSO technique is compared with classical optimization approaches in Del Valle et al. (2009) for determining optimal allocation of STATCOM devices. The PSO technique is also applied to obtain the optimal locations of SVCs in the IEEE 30 bus system (Sundareswaran et al. 2010). A relatively new technique using sensitivity analysis and a genetic algorithm has been developed to optimally locate STATCOMs in a distribution network (Samimi & Golkar 2011). In this optimal problem formulation, the objective function takes into account voltage stability, reduction of active power losses, and reduction of system reactive power.

1.2 PROBLEM STATEMENT

The benefits of reactive power compensation greatly depend on the placement and size of the added compensators. The installation of Var compensators at many buses is impossible and unnecessary because of economical consideration. Thus, it is important to determine the optimal location for installing Var compensators in power systems. Identifying the best location for Var compensators involves the calculation of steady-state optimal power flow for a power system. However, the optimal power flow problem becomes highly complex for large sized power systems due to the nonlinearity of the load flow equations, and an extensive computation has to be undertaken in order to solve it.

Many methods for optimally locating and sizing capacitors in a distribution system, consider the system to be balanced with no noise (Zhezhelenko et al. 2007). In real life, distribution systems are unbalanced due to mutual coupling between phase conductors and loading at different phases (Ghose & Goswam 2003; Ejal & Elhawary 2010). In addition, due to the widespread use of harmonic-producing equipment in distribution systems, harmonics are propagated throughout the systems. Therefore, it is important to solve the optimal capacitor placement problem by taking into account system unbalance and harmonics. Installation of shunt capacitors without considering the presence of harmonic sources in the system may lead to increased harmonic distortion levels due to resonance between capacitors and the various inductive elements in the system (Ejal & Elhawary 2010).

There are some drawbacks in the use of previous heuristic optimization techniques for determining optimal location and size of shunt Var compensators in power system. For instance, the disadvantages of GA are such as divergence and local optima problems and the PSO has difficulty in finding the optimal design parameters. In addition, the accuracy of both techniques depends on the initial conditions and the parameter values selected. Therefore, there is a need to explore on the use of more effective optimization techniques for solving the problem in determining optimal location and sizing of shunt Var compensation devices.

1.3 OBJECTIVES OF RESEARCH AND SCOPE OF WORKS

This research focuses on the development of effective heuristic optimization techniques for finding optimal placement and sizing of Var compensators in power systems. The objectives of the research are described as follows:

i. To develop an effective heuristic optimization technique in terms of speed and accuracy for determining optimal location and sizing of shunt capacitors in a radial distribution system by considering mutual coupling, load unbalancing and harmonics.

ii. To develop an effective heuristic optimization technique for determining optimal location and sizing of shunt Var compensators in transmission systems by maximizing power loss reduction and voltage stability margin.

iii. To determine and validate the most effective reactive compensating device among shunt capacitor, SVC and STATCOM for power loss reduction, voltage improvement and voltage stability enhancement.

The initial work carried out in this research focuses on the development of a relatively new meta-heuristic optimization technique known as harmony search (HS) algorithm (Geem et al. 2001) which is based on inspiration by musicians in improvising their instrument pitches to find better harmony. It has several advantages in which it does not require initial value settings for the decision variables and it can handle both discrete and continuous variables. An improved harmony search (IHS) algorithm (Mahdavi et al. 2007) is also developed to enhance the performance and accuracy of the HS algorithm. To solve complex optimization problems in power systems, a novel global harmony search (GHS) algorithm (Zou et al. 2010 a,b) which is a modified version of the HS algorithm is applied and developed in this research.

The IHS and GHS algorithms are first applied for determining optimal location and sizing of shunt capacitors in radial distribution systems. These optimization techniques are used together with the backward/forward sweep power flow method and harmonic power flow for determining optimal placement and sizing of capacitors in radial distribution systems. The IHS and GHS algorithms are also applied for determining optimal location and sizing of shunt reactive power compensators such as SVC and STATCOM in a transmission system. Here, the optimization problem is decomposed into two sub-problems, in which the first sub-problem deals with determining suitable locations for placement of shunt Var compensation devices using the modal analysis method and the second sub-problem is solved for determining optimal placement of the devices using the IHS and GHS algorithms.

The next part of the research work presents a comparative study on the effectiveness of installing reactive power compensators, such as shunt capacitor, SVC and STATCOM in transmission systems. Single shunt capacitor, SVC and STATCOM is installed separately at the critical bus. The effects of installing the different reactive power compensators are then investigated in terms of power loss reduction, voltage profile improvement, and voltage stability margin improvement. A MATLAB-based power system software tool is then developed by incorporating optimization features, named as OPSVC for optimal placement and sizing of shunt Var compensators in both distribution and transmission systems.

The scopes of works in this research are as follows:

i. For optimal capacitor placement in electrical distribution systems, the problem is limited to determine the best size and location of fixed shunt capacitors in a radial distribution system by minimizing the costs incurred due to power loss and capacitor installation.

ii. The performance of the IHS and GHS algorithms for determining optimal location and sizing of shunt capacitors in radial distribution systems are validated on three-phase 10-bus and 34-bus distribution systems by considering mutual coupling, load unbalancing and harmonics.

iii. For determining optimal location and sizing of shunt reactive power compensators such as SVC and STATCOM in a transmission system , a multi-criterion objective function is defined for the purpose of enhancing voltage stability, improving voltage profile and minimizing power loss and total cost.

iv. The IHS and GHS algorithms are tested on the 57-bus and 118-bus test systems so as to evaluate their effectiveness in minimizing power loss and enhancing voltage stability.

v. A comparison is also made among the optimization techniques; GHS algorithm, IHS algorithm, GA, PSO and conventional HS algorithm, in solving the optimal placement and sizing problem of shunt Var compensators.

CHAPTER II

LITERATURE REVIEW

2.1 REACTIVE COMPENSATION DEVICES IN POWER SYSTEMS

Many reactive compensation devices are used by electric power utilities and each device has its own characteristics and limitations. Shunt capacitors in power systems are generally used to supply reactive power for the purpose of loss minimization and voltage profile improvement. This method of reactive compensation, although it is economical and reasonably reliable, does not adequately address the needs presented by modern power systems (Quillen 2009). Recently, new technologies have emerged which may provide opportunities to address the shortcomings of shunt capacitor based reactive power compensation. The new capabilities offered by the advances in computer-based controls and the increased power handling capabilities of semiconductors make new technologies for reactive power compensation feasible (Quillen 2009). Among these new technologies, power electronics based equipment or Flexible AC Transmission Systems (FACTS) provide proven technical solutions to voltage stability problems. Especially, due to the increasing need for power quality and voltage stability improvement, shunt dynamic Var compensators such as Static Var Compensators (SVC) and Static Synchronous Compensators (STATCOM) have become feasible alternatives to a fixed reactive source, and therefore have received intensive interests. However, these new technologies do not come without their drawbacks. These technologies are very expensive and also complicated in comparison to shunt capacitors (Sode-Yome & Mithulananthan 2004). Further development is needed to reduce the perceived complexity and lower the costs of these systems.

2.1.1 Shunt Capacitor

Shunt capacitor banks are normally installed in transmission or distribution networks for the purpose of improving lagging power factor and bringing it close to unity. Therefore, they are usually located at the load buses to provide local reactive power and on distribution feeders for feeder voltage control purposes (Taylor 1998; Salloum 2011). Shunt capacitor banks have the following advantages: low implementation and maintenance cost, flexibility in installation and operation and require simple control schemes (Cutsem et al. 1994; Taylor 1998; Salloum 2011).

However, shunt capacitor banks have the following limitations and disadvantages (Cutsem et al. 1994; Taylor 1998 ; Salloum 2011):

i. Output reactive power produced by a capacitor is directly proportional to the voltage squared. Consequently, the reactive power output is reduced at low voltages when it is likely to be needed most, such as after a large disturbance.

ii. Mechanical switching by a capacitor is slow compared to power system transients. As a result, shunt capacitor banks are not capable of improving transient voltage instability.

iii. Due to energizing of shunt capacitor banks during period of voltage decay following a large disturbance, some parts of a power system may encounter very high over-voltages.

Three phase shunt capacitors are represented by their equivalent current injections (Chen et al. 1991; Ejal 2008). Figure 2.1 shows a three phase shunt capacitor with its equivalent current injection circuit.

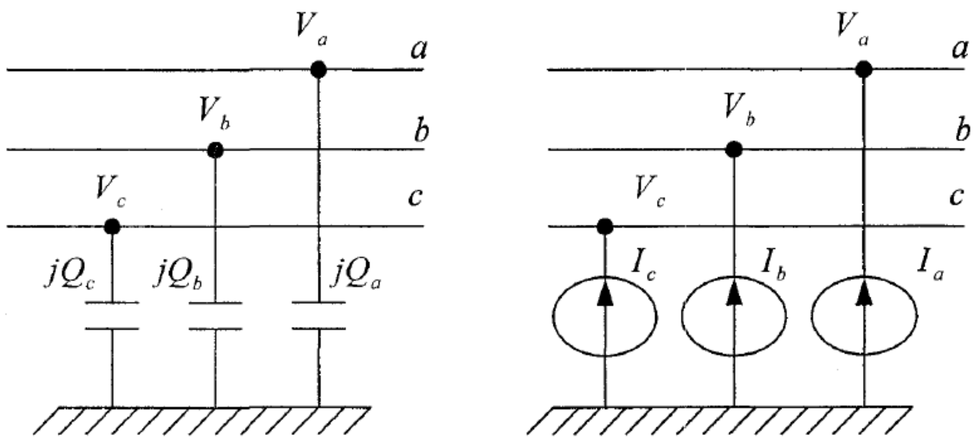

(a)

Three phase shunt capacitor (b) Equivalent current injections

Figure 2.1 Three phase shunt capacitor model

Normally, shunt capacitors are specified by their reactive power injections in terms of kVar ratings as well as the rated terminal voltage. The equivalent current injections of a shunt capacitor can be determined once both the reactive power output and the terminal voltage are calculated (Ejal 2008).

$$I^{abc} = \frac{-jQ^{abc}}{(V^{abc})^*} \tag{2.1}$$

where I^{abc} is the equivalent current injection of installed shunt capacitor.

2.1.2 Static Var Compensator

Static Var Compensator (SVC) is a shunt-connected static Var generator/load whose output can be adjusted to exchange capacitive or inductive current to maintain or control a specific power system variable (Thukaram & Lomi 2000; Mithulananthan et al. 2003). It can continuously provide the reactive power required to control dynamic voltage oscillations under various system conditions and thereby improve power transmission and distribution stability. Installing SVC at one or more suitable points in the network can increase transfer capability and reduce losses while maintaining a smooth voltage profile under different network conditions. In addition, SVC can mitigate active power oscillations through voltage amplitude modulation. The first commercial SVC was installed in 1972 for an electric arc furnace operation. Later in 1979, it was installed at the transmission network. Since then it is widely used and has been considered as the most accepted FACTS device (Zhang et al. 2006a). In principle, SVC consists of Thyristor Switched Capacitor (TSC), Thyristor Switched Reactor (TSR) and Thyristor Controlled Reactor (TCR) as shown in Figure 2.2. The coordinated control of a combination of these devices varies the reactive power produced by the SVC (Zhang et al. 2006a).

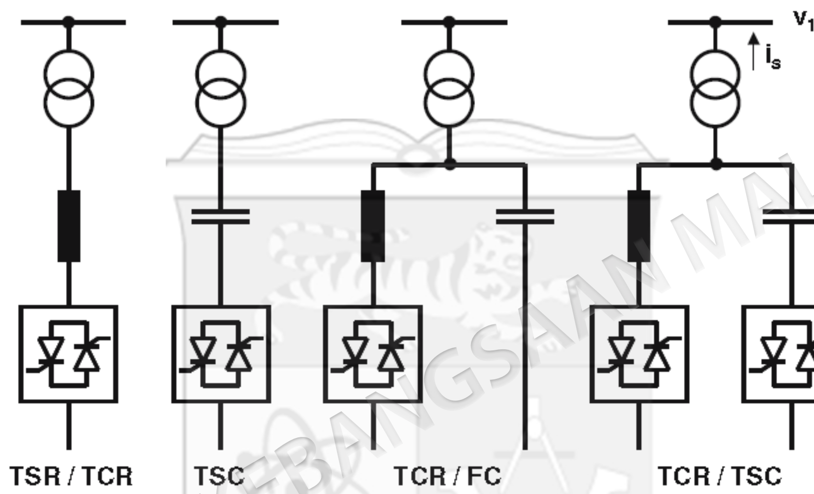

Figure 2.2 SVC building blocks (Source: Zhang et al. 2006a)

In its simplest form, SVC consists of a TCR in parallel with a bank of capacitors. From operational perspective, it behaves like a shunt-connected variable reactance, which either generates or absorbs reactive power to regulate the voltage magnitude at the point of connection to the AC network. It is used extensively to provide fast reactive power and voltage regulation support. The thyristor's firing angle control enables SVC to provide an almost instantaneous response speed. As an important component for voltage control, it is usually installed at the receiving node of transmission lines. Figure 2.3 shows an SVC that has been considered as a shunt branch with a compensated reactive power, Q_{SVC}, set by available inductive and capacitive susceptances (Etemadzadeh et al. 2010). From the figure, the current drawn and the reactive power injected by the SVC can be expressed as,

$$I_{SVC} = jB_{SVC} \times V \tag{2.2}$$

$$Q_{SVC} = -jB_{SVC} \times V^2 \tag{2.3}$$

where B_{svc}, I_{svc}, and Q_{svc} are the susceptance, injected current, and injected reactive power of the SVC, respectively.

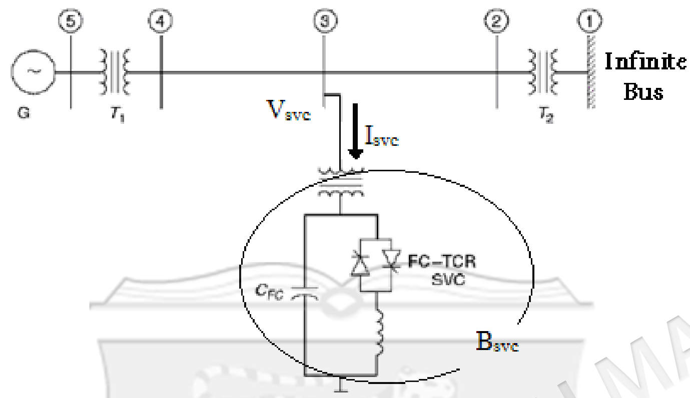

Figure 2.3 SVC connected to a transmission line

SVC size is expressed as the amount of reactive power supplied to a bus whose voltage is 1 p.u. SVC either operates in a capacitive state (generating reactive power and injecting it into the network) or in an inductive state (where the SVC absorbs reactive power from the network) (Pisica et al. 2009).

2.1.3 Static Compensator

In 1999, the first SVC with a voltage source converter went into operation and the device is better known as static compensator (STATCOM) (Zhang et al. 2006a). STATCOM is a voltage-source, converter-based device that converts a DC input voltage into an AC output voltage to compensate for the active and reactive needs of the system. It is usually used to control the transmission system voltage through shunt compensation of the reactive power. It has better characteristic than SVC due to the fact that when the system voltage drops, the STATCOM maximum reactive power output is not affected by the voltage magnitude. Therefore, STATCOM exhibits constant current characteristics even when the voltage is low (Quillen 2009).

Typically, a STATCOM consists of a coupling transformer, an inverter, and a DC capacitor. For an ideal steady-state analysis, the active power exchange between the AC system and the STATCOM is assumed negligible, and only reactive power is exchanged between them (Acha et al. 2004 ; Shaygan et al. 2011). The schematic representation of STATCOM and its equivalent circuit are shown in Figure 2.4 (a) and (b), respectively.

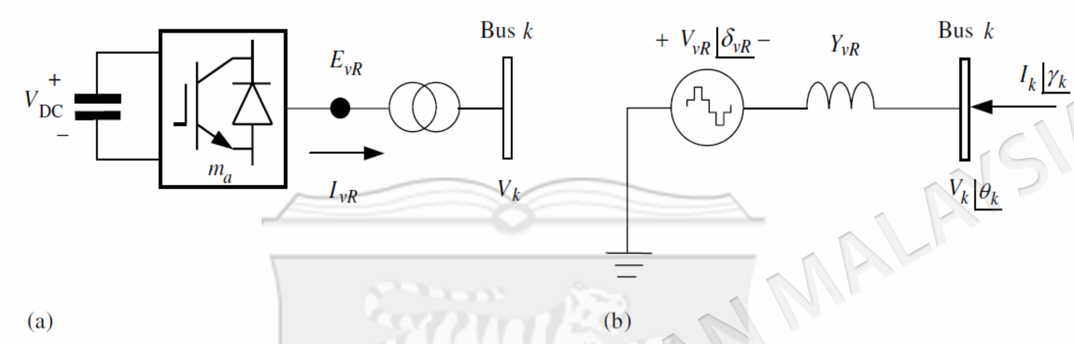

Figure 2.4 STATCOM representation (a) VSC connected to the AC network via a transformer (b) Shunt solid-state voltage source
Source: Acha et al. 2004

In Figure 2.4(a), the shunt-connected transformer is assumed to be ideal. STATCOM is implemented so that the active power flow between the AC source and the Voltage Source Converter(VSC) is controlled by a phase angle, and the reactive power flow is determined mainly by the magnitude of the voltage source (V_k) and the VSC output fundamental voltage (V_{vR}). VSC generates reactive power when $V_{vR} > V_k$ and consumes reactive power when $V_{vR} < V_k$. During normal operation, a small amount of active power flows into the VSC to compensate for the power losses inside the VSC, and δ is kept slightly larger than zero for lagging power factor (Acha et al. 2004). The STATCOM equivalent circuit shown in Figure 2.4(b) is used to derive the mathematical model of the controller for inclusion in the power flow algorithm. The power flow equations for bus i of the power system with no FACTS controllers are given by,

$$P_i = \sum_{m=1}^{n} \left(V_i^2 G_{ii} - V_i V_m [G_{im} \cos(\theta_i - \theta_m) + B_{im} \sin(\theta_i - \theta_m)] \right) \tag{2.4}$$

$$Q_i = \sum_{m=1}^{n} \left(- V_i^2 B_{ii} + V_i V_m [G_{im} \cos(\theta_i - \theta_m) - B_{im} \sin(\theta_i - \theta_m)] \right) \tag{2.5}$$

With the addition of a STATCOM connected at bus k, the system power flow equations remain the same as the equations of a system without a STATCOM for all buses given by (2.4) and (2.5) except for bus k. The power flow equations for the STATCOM in a two-bus system shown in Fig. 2.4 (b) are derived by first considering the voltage source and the complex power which are given by,

$$E_{vR} = V_{vR}(\cos\delta_{vR} + j \ \sin\delta_{vR}) \tag{2.6}$$

$$S_{vR} = V_{vR}I_{vR}^{*} = V_{vR}Y_{vR}(V_{vR}^{*} - V_{k}^{*}) \tag{2.7}$$

By substituting (2.6) into (2.7), the active and reactive power equations at the converter terminal and bus k are obtained as follows (Shaygan et al. 2011):

$$P_{vR} = V_{vR}^2 G_{vR} - V_k V_{vR}[G_{vR}\cos(\delta_{vR} - \theta_k) + B_{vR}\sin(\delta_{vR} - \delta_k)] \tag{2.8}$$

$$Q_{vR} = -V_{vR}^2 B_{vR} + V_k V_{vR}[B_{vR}\cos(\delta_{vR} - \theta_k) - G_{vR}\sin(\delta_{vR} - \delta_k)] \tag{2.9}$$

$$P_k = V_k^2 G_{vR} - V_k V_{vR}[G_{vR}\cos(\theta_k - \delta_{vR}) + B_{vR}\sin(\delta_k - \delta_{vR})] \tag{2.10}$$

$$Q_k = -V_k^2 B_{vR} + V_k V_{vR}[B_{vR}\cos(\theta_k - \delta_{vR}) - G_{vR}\sin(\theta_k - \delta_{vR})] \tag{2.11}$$

These equations for two-bus power system are obtained.Thus, for an n-bus power system, the active and reactive power equations at bus k (i.e. the bus where the STATCOM is connected) are given as follows:

$$P_K = V_{vR}^2 G_{vR} - V_K V_{vR}[G_{vR}\cos(\delta_{vR} - \theta_K) + B_{vR}\sin(\delta_{vR} - \delta_K)] + \\ + \sum_{m=1}^{n}\left(V_K^2 G_{KK} - V_K V_m[G_{Km}\cos(\theta_K - \theta_m) + B_{im}\sin(\theta_K - \theta_m)]\right) \tag{2.12}$$

$$Q_K = -V_K^2 B_{vR} + V_K V_{vR}[B_{vR}\cos(\theta_K - \delta_{vR}) - G_{vR}\sin(\theta_K - \delta_{vR})] + \\ + \sum_{m=1}^{n}\left(-V_K^2 B_{KK} + V_K V_m[G_{Km}\cos(\theta_K - \theta_m) - B_{Km}\sin(\theta_K - \theta_m)]\right) \tag{2.13}$$

Using these power equations, the linearised STATCOM model is derived as shown in (2.14), where the voltage magnitude V_{vR} and phase angle δ_{vR} are considered as state variables (Zhang et al. 2006a):

$$\begin{bmatrix} \Delta P_K \\ \Delta Q_K \\ \Delta P_{vR} \\ \Delta Q_{vR} \end{bmatrix} = \begin{bmatrix} \frac{\partial P_K}{\partial \theta_K} & \frac{\partial P_K}{\partial V_K} V_K & \frac{\partial P_K}{\partial \delta_{vR}} & \frac{\partial P_K}{\partial V_{vR}} V_{vR} \\ \frac{\partial Q_K}{\partial \theta_K} & \frac{\partial Q_K}{\partial V_K} V_K & \frac{\partial Q_K}{\partial \delta_{vR}} & \frac{\partial Q_K}{\partial V_{vR}} V_{vR} \\ \frac{\partial P_{vR}}{\partial \theta_K} & \frac{\partial P_{vR}}{\partial V_K} V_K & \frac{\partial P_{vR}}{\partial \delta_{vR}} & \frac{\partial P_{vR}}{\partial V_{vR}} V_{vR} \\ \frac{\partial Q_{vR}}{\partial \theta_K} & \frac{\partial Q_{vR}}{\partial V_K} V_K & \frac{\partial Q_{vR}}{\partial \delta_{vR}} & \frac{\partial Q_{vR}}{\partial V_{vR}} V_{vR} \end{bmatrix} \times \begin{bmatrix} \Delta \theta_K \\ \frac{\Delta V_K}{V_K} \\ \Delta \delta_{vR} \\ \frac{\Delta V_{vR}}{V_{vR}} \end{bmatrix} \tag{2.14}$$

The Jacobian elements in Equation (2.14) are given in explicit form in Appendix A.

2.1.4 Comparison of Shunt Capacitor, SVC and STATCOM

Shunt capacitor, SVC and STATCOM increase the static voltage stability margin and power transfer capability, with the SVC and STATCOM providing better loss reduction and voltage profile improvement than the shunt capacitor. The increase in losses with a shunt capacitor under lightly loaded conditions is due to poor voltage profile (Sode-Yome & Mithulananthan 2004). To solve the voltage control problem at the shunt capacitor bus, a remote voltage control scheme is usually implemented. In general, SVC and STATCOM behave better than a shunt capacitor; however, these controllers are expensive compared to the shunt capacitor (Sode-Yome & Mithulananthan 2004). A complete cost–benefit analysis has to be carried out to justify the economic viability of the SVC and STATCOM. Shunt capacitors are relatively inexpensive to install and maintain, and installing them in load areas increases voltage stability. However, during low-voltage conditions, Var support drops due to the fact that reactive power delivered by a shunt capacitor is proportional to the square of the terminal voltage (Kundur 1994; Coevering et al. 1996; Sode-Yome & Mithulananthan 2004).

Despite the relatively high initial costs, SVC has been widely used in power systems because of its fast and precise voltage regulation capabilities which help improve system voltage instability following a large disturbance. As mentioned before, a major disadvantage of SVC is that at its maximum output it behaves as a regular shunt capacitor and the reactive power produced is directly proportional to the square of the voltage. To overcome this problem, STATCOM which is similar to a synchronous condenser is used. STATCOM has an internal voltage source which provides constant output current even at very low voltages. Therefore, the output reactive power of the STATCOM is linearly proportional to the bus voltage. Table 2.1 describes a comparison between SVC and STATCOM.

Table 2.1 Comparison between SVC and STATCOM

SVC	**STATCOM**
Acts as a variable susceptance	Acts as a voltage source behind a reactance
Sensitive to harmonic resonance in transmission systems	Insensitive to harmonic resonance in transmission systems
Higher generation of harmonics	Lower generation of harmonics
Somewhat slower response during transients	Fast response (within ms) and better performance during transients
Has difficulty operating with a very weak ac system	Can maintain a stable voltage even with a very weak ac system

2.2 REVIEW OF HEURISTIC OPTIMIZATION TECHNIQUES FOR OPTIMAL PLACEMENT AND SIZING OF CAPACITORS IN DISTRIBUTION SYSTEMS

The problem of locating and sizing shunt capacitors in distribution systems has been a challenge for power system planners and researchers. The unbalanced operating conditions and the presence of harmonic sources in distribution systems further complicate the capacitor placement and sizing problem (Ejal 2008). Many techniques have been developed for solving the capacitor placement problem, namely, analytical techniques, numerical programming, heuristic or artificial intelligence (AI) based techniques (Ng et al. 2000). Among these techniques, heuristic optimization techniques have been widely applied to solve the optimal capacitor placement problem. AI is a powerful knowledge-based approach that can address the nonlinearity of practical systems (Eslami et al. 2011). Developing solutions using AI based approach offers two major advantages: i) the development time is much shorter than when using more traditional approaches and ii) the systems are very robust, i.e., relatively insensitive to noisy and/or missing data (Eslami et al. 2011). This section presents the heuristic optimization techniques that are used in solving the optimal capacitor placement and sizing problems.

2.2.1 Fuzzy Logic

Masoum et al. (2004a) applied fuzzy logic for solving the discrete optimization problem of fixed shunt capacitor placement and sizing under harmonic conditions. Power and energy losses due to installed capacitors and the cost of fixed capacitors are used as the objective function. Kannan (2008) and Saranya (2011) developed fuzzy expert system to determine suitable candidate nodes for determining the optimal capacitor sizes in distribution systems. Bhattacharya et al. (2009) formulated new fuzzy membership functions to identify probable capacitor locations in radial distribution systems. A new algorithm for selecting capacitor nodes was presented, and simulated annealing technique was employed for final sizing of the capacitors. However , fuzzy logic has some diadvantages such as : It is hard to develop a model from a fuzzy system and it requires more fine tuning and simulation before operational.

2.2.2 Evolutionary Computation

Different types of evolutionary computation based optimization techniques have been used to search for optimal or near optimal solutions for optimal capacitor placement in radial distribution networks (Khajehzadeh et al. 2011). These evolutionary computation techniques include Tabu search (TS), simulated annealing (SA), ant colony optimization (ACO), harmony search (HS), genetic algorithm (GA), and particle swarm optimization (PSO). TS is based on the hill-climbing method which evaluates the final solution by repeating the process of creating solution candidates in the neighborhood around the initial solution and selecting the best solution among the candidates (Eslami et al. 2011). The hill-climbing method stops if the solution is not improved and therefore it can be easily trapped in a local minimum (Mori et al. 2005). Optimal capacitor placement has been solved with a hybrid method that utilizes TS and other heuristic techniques such as genetic algorithm and simulated annealing. (Gallego et al. 2001). Mori et al. (2005) applied a variable neighborhood TS technique for capacitor placement in distribution systems. An optimization technique that exploits the resemblance between a minimization process and crystallization in a physical system is simulated annealing (SA). Ghose et al. (2003) applied SA for solving optimal capacitor placement problem considering unbalance and the presence of harmonics in a distribution system. A modified SA technique has been developed for optimal placement and sizing of fixed capacitor banks in a distribution network (Elmitwally 2011). SA is very slow, especially if the cost function is expensive to compute.

Another optimization technique that is inspired by the behavior of ants in nature such that the ants can find the shortest path from their home to food is the ant colony algorithm (Eslami et al. 2011). Annaluru et al. (2004) applied the ant colony algorithm to solve the capacitor placement and sizing problem, in which the Newton-Raphson power flow method was used to calculate the cost function. Chang (2008) solved the optimal capacitor placement problem, the optimal feeder reconfiguration problem, and a combination of the two using the ant colony algorithm. In the implementation of the ant colony optimization for the problem, capacitors should be in discrete values and not in continuous values which are usually more accurate. A disadvantage of the ant colony algorithm is that it has low speed because all paths must be reviewed by the ants.

The optimal capacitor placement and sizing is also solved by using genetic algorithm (GA) which searches for an optimal solution using the principle of evolution based on a certain string which is judged and propagated to form the next generation (Goldberg 1989). A GA-based method that incorporates nonlinear load models for the problem of finding optimal shunt capacitors in distribution systems has been reported by Abou-Ghazala (2003). The optimization problem was formulated such that the optimal solution did not result in severe resonant conditions at harmonic frequencies. Another GA-based method was developed for solving the discrete optimization problem of fixed shunt capacitor placement and sizing in the presence of voltage and current harmonics (Masoum et al. 2004b). The problem of simultaneous placement and sizing of both capacitor banks and voltage regulators in unbalanced distribution system in the presence of linear and nonlinear loads, using GA is discussed in Carpinelli et al. (2006). The problem is formulated as a mixed integer program that accounts for imbalance and incorporates network losses and costs of capacitor, voltage regulator and harmonic distortion. Reddy et al. (2007) applied GA and a power loss index to determine suitable candidate nodes in distribution systems for capacitor installation. The power loss index is used to determine the suitability of capacitor placement at each node. The buses with the highest suitability are identified for capacitor placement. Carpinelli et al. (2009) applied GA for the optimal sizing and setting of capacitors in unbalanced multi-converter distribution systems. Swarnkar et al. (2010) presented an efficient method for determining the optimal number, location, and sizing of fixed and switched shunt capacitors in radial distribution systems using GA. However, GA which is one of the early heuristic optimization techniques used for solving the optimal capacitor placement problem, has some drawbacks too, such as divergence and local optima problems.

Particle swarm optimization (PSO) which involves simulating social behavior among individuals or particles has been used for solving the capacitor placement problem in radial distribution systems (Yu et al. 2004). The target problem is reformulated by a comprehensive objective function and a set of equality and inequality constraints with consideration of the harmonic effects, different load levels, and practical aspects of fixed or switched capacitor banks. Prakash & Shydulu (2007) presented a PSO-based parallel search technique to estimate the required level of shunt capacitive compensation to improve the voltage profile of the system and reduce active power loss. AlHajri et al. (2007) applied PSO technique for solving the fixed capacitor placement and sizing problem by formulating two sub-problems considering discrete variables and some practical constraints. The binary PSO has been used in solving the discrete optimization problem for optimal capacitor placement in the presence of nonlinear loads in Khalil et al. (2007). In this optimization problem, the objective function maximizes the net savings from peak power and energy reduction while taking capacitor cost into account. Zhezhelenko et al. (2009) extended the work reported in Khalil et al. (2007) by including the effect of mutual coupling, load unbalancing, and harmonics on the capacitor placement problem in distribution systems. Oo (2008) made a comparative study on the use of PSO and the two variants of evolutionary PSO techniques for solving optimal capacitor placement in radial distribution system. The optimal capacitor placement considering voltage stability enhancement has been reported in Kim et al. (2009). Ejal & Elhawary (2010) combined a discrete version of PSO with a radial distribution power flow (RDPF) algorithm to form a hybrid PSO algorithm. PSO is employed to find the global optimal solution, while the RDPF algorithm was used to calculate the objective function and to verify the bus voltage limits. Afaghzadeh et al. (2011) applied binary PSO for solving the optimal capacitor placement problem in a radial distribution network by considering harmonic distortion of voltage sources in the problem formulation. From the literature, it is noted that although PSO techniques are widely used for solving the optimal capacitor placement problem, it still has disadvantages, such as difficulty in finding the optimal design parameters and selecting the appropriate initial conditions and parameters for an accurate solution. The PSO is the most widely used optimization technique due to its advantages which include simple implementation, small computational load, and fast convergence. PSO is efficient for solving many problems which are difficult to find accurate mathematical models. However, the PSO technique is prone to relapse into local minima and premature convergence when solving complex optimization problems (Khajehzadeh et al. 2011).

2.2.3 Hybrid Artificial Intelligent Techniques

To create a hybrid intelligent system, two or more AI techniques are applied. During the last decade, hybrid intelligent systems have been applied in engineering applications. A combinatorial optimization problem with a non-differentiable objective function has been formulated and solved using simulating annealing, GA, TS and hybrid GA-fuzzy logic algorithms (Al-Mohammed & Elamin 2003). Hsiao et al. (2004) applied combined fuzzy-GA method for solving the capacitor placement problem in distribution systems. Here, three distinct objectives were considered; minimize the total cost of energy loss and capacitors, increase the margin loading of feeders and improve the voltage profile. A GA-based fuzzy multi-objective approach for optimal capacitor placement while improving voltage profile and maximizing net savings in a radial distribution system has been presented (Das 2008). This study attempted to maximize net savings and minimize node voltage deviations. A GA-fuzzy logic algorithm has been proposed for solving the discrete optimization problem of fixed shunt capacitor placement and sizing in the presence of voltage and current harmonics (Ladjavardi et al. 2008). Fuzzy logic and PSO have been applied to determine optimal locations and sizes of shunt capacitors for reactive power compensation of radial distribution systems, respectively (Reddy et al. 2008). A fuzzy decision function with bacterial foraging algorithm creates a powerful optimization tool for solving capacitor allocation problem considering both loss minimization and voltage improvement (Tabatabaei et al. 2011). Mohkami et al. (2011) determined the optimal placement of capacitors using bacterial foraging with PSO by considering a multi-objective function. The bacterial foraging-PSO rechnique was also applied to solve the optimal placement of capacitor banks to reduce cost of energy losses and improve voltage profile (Hooshmand et al. 2011). . Due to the limitations of GA and PSO, recently many hybrid techniques or multi-stage methodologies have been developed to find optimal location and size of shunt capacitors. In most of these hybrid techniques, a fuzzy approach is used to find the optimal capacitor locations, while other optimization techniques such as PSO, GA and bacteria foraging algorithm are used to find the optimal capacitor sizes (Passino 2002).

2.2.4 Other Optimization Techniques

An artificial neural network (ANN)-based method for optimally switching the switchable capacitors installed in a power distribution system has been developed by Das et al. (2001). This method is much faster than the conventional optimization techniques, even for a realistic number of capacitors in the system. Passino (2002) applied bacteria foraging algorithm for solving the optimal capacitor placement problem. Huang et al. (2008) developed a two-stage immune algorithm which embeds compromised programming to solve the multi-objective capacitor placement problem. The concept of the non-inferior set is applied to obtain a set of optimal compromise solutions from which the decision maker can choose one. Haghdar & Shayanfar (2010) presented the use of a generalized pattern search method for calculating the placement and sizing of capacitor and DG in distribution networks. The method is considered more precise and leads to faster results than GA-based methods. Capacitor placement and sizing was performed by using loss sensitivity factors and plant growth simulation algorithm in Rao et al. (2011). The plant growth simulation algorithm is used to estimate the required level of shunt capacitive compensation to improve voltage profile of the system.

2.3 HEURISTIC OPTIMIZATION TECHNIQUES FOR OPTIMAL PLACEMENT AND SIZING OF SVC AND STATCOM

Static Var Compensator (SVC) and Static Synchronous Compensator (STATCOM) are two components of Flexible AC Transmission System (FACTS) devices, that play an important role in voltage and angle stability control in power networks. Due to economic considerations, identifying best location for installing SVC and STATCOM has become important. The techniques used to optimize the allocation of these devices in power systems can be classified as using loss sensitivity analysis, modal analysis and continuation power flow, optimal power flow and heuristic optimization technique (Zhang et al. 2006b). Among these optimization techniques, the heuristic optimization techniques have been widely applied in solving the optimal SVC and STATCOM placement problem.

2.3.1 Evolution Strategy

The main search procedure in the evolution strategy (ES) is the mutation operator that generates random samples around search points selected from a population of different search points (Santiago & Maldonado 2006). ES was developed to obtain the best points for operating SVC, STATCOM, and UPFC with the objective of reducing system losses and taking into account voltage drop constraints and operation limits of the devices (Dominguez-Navarro et al. 2007). ES was also used to find the optimal placement of FACTS devices such as SVC, TCSC and UPFC in power systems (Rezaee-Jordehi & Joorabian 2011). The goal of the optimization is to maximize system loadability.

2.3.2 Genetic Algorithms

Talebi et al. (2005) applied GA for determining optimal SVC placement for the purpose of load balancing during a specific period of time. A GA based optimization procedure has been implemented to find the best placement, type, and size of selected FACTS devices for the reduction of total financial losses in the network due to voltage sags (Zhang & Milanovic 2007). A GA based allocation algorithm for optimal placement of FACTS devices considering cost function of these devices and system losses was presented in Baghaee et al. (2008). A messy GA-based optimization scheme for voltage stability enhancement of power systems under critical operation conditions was presented in Huang & Negnevistky (2008). An application of GA has been presented for finding the best location of an SVC within a power network with the objective of reducing power losses and reducing voltage deviations and costs (Pisica et al. 2009). An optimization technique termed as the queen bee assisted GA has been explored to obtain optimal placement of FACTS devices for voltage profile enhancement (Sundareswaran et al. 2009). The non-dominated sorting GA was used for continuous, discrete and multiple placement of five reactive power compensator devices in the IEEE 57-bus test system (Belazzoug & Boudour 2010). GA was also used for solving both the inter-area congestion and oscillation issues in a high voltage transmission system by installing FACTS devices (Berizzi et al. 2011). An approach based on sensitivity analysis and GA was developed to optimally locate STATCOMs in distribution networks (Samimi & Golkar 2011). However ,GA which is considered as one of the first global optimization technique used for solving optimal placement of FACTS devices, has some drawbacks such as divergence and local optima problems (Khajehzadeh et al. 2011).

2.3.3 Simulated Annealing

A method based on simulated annealing (SA) and Lagrange multiplier techniques for optimal placement of SVCs was presented in (Chang & Huang, 1997). Gitizadeh & Kalantar (2008) presented the use of SA and sequential quadratic programming (SQP) for optimally locating TCSC and SVC in transmission systems. The problem is formulated according to the SQP problem in the first stage to accurately evaluate the static security margin in the presence of TCSC and SVC, and in the next stage a SA based optimization method is used to find the optimal solution. However SA is is very slow, especially for computing multi-criterion objective functions.

2.3.4 Particle Swarm Optimization

Del Valle et al. (2006) demonstrated the application of PSO for determining optimal sizing and location of STATCOM in a power system, considering voltage deviation constraints at each bus. Hernandez et al. (2006) demonstrated the feasibility of applying PSO for optimal allocation of STATCOM in a 45-bus section of the Brazilian power system. A modified PSO approach has been developed for determining global or near global optimum solution for optimal location of TCSC and SVC (Pirayesh et al. 2007). Saravanan et al. (2007) applied PSO for determining optimal placement of single and multi-type FACTS devices by minimizing the installation cost of FACTS devices and improving system loadability. Azadani et al. (2008) presented an approach for optimal placement and sizing of STATCOM in power systems using PSO and CPF in order to improve voltage profile, minimize system total losses, and maximize system loadability. Panda & Padhy (2008) also applied PSO to determine the optimal location and controller parameters of STATCOM but for transient stability improvement following a severe disturbance. Del Valle et al. (2009) applied enhanced PSO algorithm for determining optimal sizing and location of STATCOM in a power system considering voltage deviation constraints and economic criteria. Non-dominated sorting PSO has been used to solve a multi-objective optimization problem for optimizing the location and size of SVC and TCSC in order to maximize static voltage stability margin, reduce power losses, and minimize load voltage deviations (Benabid & Boudour 2007; Benabid et al. 2009a; Benabid et al. 2009b). Laifa & Boudour (2009) applied multi-objective PSO to solve a mixed continuous-discrete multi-objective optimization problem in order to find optimal location of SVC. The applicability and effectiveness of using heuristic optimization techniques such as GA, PSO, and evolutionary PSO for determining optimal placement of SVC devices was investigated in Eghbal et al. (2009).

Many other works have been carried using PSO in determining optimal location of SVC for different objectives such as for transmission loss reduction (Jumaat et al. 2011), minimizing voltage deviation and active power loss reduction (Tibin et al. 2011), minimizing total power loss and maximizing total transfer capability (Rao & Kumar 2011). A methodology has been presented for attaining maximum instantaneous wind penetration by optimal placement and setting of FACTS controllers (Sreedharan et al. 2011). To find optimal location and sizing of STATCOM in a power system for voltage profile improvement, variations of PSO algorithms have been developed, namely, classical PSO, PSO time varying inertia weight, PSO random inertia weight, and PSO time varying acceleration coefficients (Varshney et al. 2011). Comparing the performance of these PSO algorithms, the PSO time varying acceleration coefficients was found to be superior in terms of computational speed and quality of solution. PSO is efficient for solving many problems which are difficult to find accurate mathematical models. However, the PSO algorithm is prone to relapsing into local minima and premature convergence when solving complex optimization problems (Ejal 2008).

2.3.5 Harmony Search Algorithm

The harmony search (HS) algorithm which is an optimization technique that is inspired by musicians improvising their instrument pitches to find better harmony (Geem et al. 2001) has been applied to determine the optimal location of FACTS devices in a power system to improve power system security (Kazemi et al. 2009). Three types of FACTS devices, namely UPFC, TCSC, and SVC were considered. HS algorithm was also applied for optimal placement of multi-type FACTS devices such as SVC, thyristor controlled phase angle regulator and UPFC (Parizad et al. 2009).

2.3.6 Hybrid Artificial Intelligence Techniques

A combination of the micro-GA and FL has been used to optimize the various parameters of FACTS devices such as SVC, TCSC, UPFC and thyristor controlled phase angle regulator (Baskaran & Palanisamy 2006). Mohamadi and Jazaeri (2007) developed the hybrid PSO-GA algorithm to overcome the drawbacks of implementing PSO and GA individually. A combination of modified SA and PSO has been developed to determine optimal placement of FACTS devices with the objective of minimizing total losses in a power system (Majumdar et al. 2009). Khandani et al. (2011) presented a hybrid GA -sequential quadratic programming for optimal placement of SVC with the objective of maximizing total transfer capability of power transactions between source and sink areas in a power system. As for the hybrid techniques or multi-stage methods for finding optimal location and sizing of SVC and STATCOM, numerical analyses are usually used to find suitable location for SVC or STATCOM, while the heuristic optimization techniques such as PSO and GA are used to find the optimal size of SVC and STATCOM.

2.3.7 Other Optimization Techniques

AIS technique was used to determine optimal location of SVC in order to minimize loss in the system (Ishhak et al. 2004). An optimization algorithm based on the low discrepancy sequences (LDS) has been employed to solve optimal placement of FACTS devices in a power network by minimizing the costs of both active and reactive power generation (Alabduljabbar & Milanovi 2006). The LDS is a uniform scattering of points in a space bounded originally between 0 and 1. An artificial intelligence technique was implemented to determine optimal location of a STATCOM by Karimi et al. (2006). A group search optimizer with multiple producers has been used for reactive power dispatch incorporating FACTS devices in which a non-linear constrained multi-objective optimization problem is formulated (Wu et al. 2008). The group search optimizer is inspired by group-living which is a phenomenon of the animal kingdom. A multi-start Benders decomposition technique is applied to determine optimal placement of SVC by maximizing the loading margin of a transmission network (Minguez et al. 2007). The technique was proven to be efficient in identifying optimal or near-optimal solutions and robust with regards to computational speed.

2.4 CHAPTER SUMMARY

This chapter presents the models, characteristics, advantages and disadvantages of the currently available and most commonly used shunt-compensation devices such as shunt capacitor, SVC and STATCOM. A comprehensive analysis of the heuristic optimization techniques that solve the optimal shunt Var compensator placement problem is also presented. Various heuristic optimization techniques that have been used to address the optimal placement and sizing of shunt capacitors in distribution systems and FACTS devices in transmission system are reviewed and discussed with respect to their advantages and limitations.

CHAPTER III

HEURISTIC OPTIMIZATION TECHNIQUES

3.1 INTRODUCTION

Many engineering problems in various fields have been formulated as optimization problems and solved using various optimization techniques. The conventional mathematical optimization techniques, such as linear programming (LP), non-linear programming (NLP), and dynamic programming (DP), have been frequently used for solving optimization problems (Geem et al. 2001). All the three programming techniques can guarantee global optima in simple and ideal models. However, in real world problems, there are some drawbacks in the conventional optimization techniques. The disadvantage of LP is that considerable losses occur when a linear ideal model from a non-linear real world problem is developed (Shyr 2008 ; Guo et al. 2010). As for the limitation of DP, an increase in the number of variables would exponentially increase the number of evaluations of the recursive functions and tax the core-memory which results in curse of dimensionality. The disadvantages of NLP are that if the functions used in computation are not differentiable, the solving algorithm may not find an optimum solution and careful attention is also required in selecting the initial values in order to guarantee convergence to the global optimum and not into local optima (Geem et al. 2001). Therefore, to overcome the above deficiencies of mathematical optimization techniques, heuristic optimization techniques based on simulation have been introduced. These techniques allow a near optimum solution to be found within a reasonable computation time and with reasonable use of memory without any loss of subtle nonlinear characteristics of the model and without any requirement of complex derivatives or careful choice of initial values (Glover 1989).

In the past few decades several heuristic optimization techniques which are based nature inspired analogy have been developed. These techniques are mostly population based metaheuristics also called global optimization algorithms because of their applicability to solve a wide range of problems. Some popular heuristic optimization techniques include evolution strategies (ES) (Rechenberg 1965), evolutionary programming (EP) (Fogel et al. 1966), genetic algorithm (GA) (Holland 1975a, b), genetic programming (GP) (Smith 1980), simulated annealing (SA) (Kirkpatrick et al. 1983), artificial immune system (AIS) (Farmer et al. 1986),Tabu search (TS) (Glover 1989; Glover 1990), ant colony optimization (ACO) (Dorigo & Maniezzo1992), particle swarm optimization (PSO) (Kennedy & Eberhart 1995), Harmony Search (HS) algorithm (Geem et al. 2001), bee colony optimization (BCO) (Nakrani & Tovey 2004) and gravitational search algorithm (GSA) (Rashedi et al. 2009). Among these optimization techniques, GA and PSO are the most widely used techniques for solving complex and intricate optimization problems in various fields.

3.2 GENETIC ALGORITHM

Genetic algorithm is an adaptive heuristic search algorithm premised on the evolutionary ideas of natural selection and genetic. The basic concept of GA is designed to simulate processes in natural system necessary for evolution, specifically those that follow the principles first laid down by Charles Darwin of survival of the fittest (Holland 1975a, b). As such it represents an intelligent exploitation of a random search within a defined search space to solve a problem. In GA, a population of strings called as chromosomes, which encode candidate solutions (called as individuals) to an optimization problem, evolves toward better solutions. Traditionally, solutions are represented in binary as strings of 0s and 1s, but other encodings are also possible. The evolution usually starts from a population of randomly generated individuals and happens in generations. In each generation, the fitness of every individual in the population is evaluated, multiple individuals are stochastically selected from the current population (based on their fitness), and modified (recombined and possibly randomly mutated) to form a new population. The new population is then used in the next iteration of the algorithm. Commonly, the algorithm terminates when either a maximum number of generations has been produced, or a satisfactory fitness level has been reached for the population. If the algorithm has terminated due to a maximum number of generations, a satisfactory solution may or may not have been reached.

The procedure for implementing GA is described as follows (Shyr 2008):

Step 1: Initialization. The algorithm starts with a set of solutions (represented by chromosomes) called population. A set of chromosomes is randomly generated.

Step 2: Evaluation. For every chromosome, its fitness value is calculated and analyzed individually. Comparing with the existing best fitness value, if one chromosome can generate better fitness, renew the values of the defined vector and variable with this chromosome and its fitness value; otherwise, keep their values unchanged.

Step 3: Selection. Population selection within the algorithm utilizes the principle of survival of the fittest, which is based on the Darwinian's concept of natural selection (Holland, 1975a,b). A random number generator is employed to generate random numbers whose values are between 0 and 1.

Step 4**:** Crossover. The crossover operation is one of the most important operation in GA. The basic idea is to combine some genes from different chromosomes. A GA recombines of bit strings by copying segments from chromosomes pairs.

Step 5: Mutation. Some useful genes are not generated during the initial step and therefore to overcome this difficulty, mutation is considered. The basic mutation operator randomly generates a number as the crossover position and then changes the value of this gene randomly.

Step 6: Stopping criteria. Steps 2-5 are repeated until a predefined number of generations has been reached. The optimal solution can be generated after termination.

Some rapid GA-based methods for the optimal sizing and setting of capacitors in unbalanced multi-converter distribution systems have been used and compared to obtain a good solution with tolerable computational efforts (Carpinelli et al. 2009).

One technique is based on micro-GA while the other two techniques are based on the inherent structure theory of networks and the sensitivity analysis, which are used to determine a set of feasible candidate nodes to which the GA is applied. The three techniques have been compared with a simple GA method using the IEEE 34-node unbalanced test system. The problem of simultaneous placement and sizing of both voltage regulators and capacitor banks in unbalanced distribution system in the presence of linear and nonlinear loads, using GA is discussed in Carpinelli et al. (2006). The problem is formulated as a mixed integer program that accounts for imbalance and incorporates network losses, cost of the capacitors/voltage regulators, and cost of harmonic distortions. GA is also applied to determine the best location of only one SVC in a power system in which the objective function is defined for reducing power loss, voltage deviation and cost (Pisica et al. 2009). A GA was employed to seek the optimal solution for sizing and placing STATCOMs across the IEEE 14-bus network, while a correcting power ratio was defined for adapting the optimized values with those obtained by the average model (Tavakoli et al 2005).

The advantages and disadvantages of GA are described as follows (Shyr 2008 ; Khajehzadeh et al. 2011).

The advantages of GA:

i. It can solve every optimisation problem which can be described with the chromosome encoding.
ii. It solves problems with multiple solutions.
iii. Since GA execution technique is not dependent on the error surface, it can be used for solving multi-dimensional, non-differential, non-continuous, and even non-parametrical problems.
iv. GA is a technique which is easy to understand and it practically does not demand the knowledge of mathematics.
v. GA is easily transferred to existing simulations and models.

The disadvantages of GA:

i. Certain optimisation problems cannot be solved by GA probably due to poorly known fitness functions which generate bad chromosome blocks.

ii. There is no absolute assurance that a GA will find a global optimum.

iii. GA cannot assure constant optimisation response times. In addition, the difference between the shortest and the longest optimisation response times is much larger than with conventional gradient methods. This disadvantage limits the use of GA in real time applications.

iv. GA application in real time control is limited because of random solutions and convergence. This means that while the entire population is improving, there is no assurance that an individual within this population will converge to its specified value. Therefore, it is unreasonable to use GA for on-line control in real systems without testing it first on a simulation model.

3.3 PARTICLE SWARM OPTIMIZATION

Particle swarm optimization (PSO) is a metaheuristic optimization technique which is based on population inspired by bird flocking and fish schooling (Kennedy & Eberhart 1995). Initially, PSO is used for solving continuous nonlinear optimization problems but now it has been extended to solve constrained nonlinear optimization problems with both discrete and continuous variables (Hu et al. 2004; Ejal 2008).The fundamental idea behind the PSO algorithm is that a population called a swarm is randomly generated. The swarm consists of individuals called particles. Each particle in the swarm represents a potential solution of the problem considered. Each particle moves through a dimensional search space at a random velocity. Each particle updates its velocity and position according to the following equations:

$$v_{id}^{k+1} = wv_{id}^{k} + c_1 r_1 (pbest_i^k - x_{id}^k) - c_2 r_2 (gbest^k - x_{id}^k) \tag{3.1}$$

$$x_{id}^{k+1} = x_{id}^{k} + v_{id}^{k+1} \tag{3.2}$$

where,

w : inertia weight

c_1, c_2 : acceleration constants

r_1, r_2 : two random numbers in the range of [0,1]

$pbest_i^k$: best position ever visited by a particle i at the k^{th} iteration

$gbest^k$: global best position in the entire swarm.

The basic concept of PSO is illustrated in Figure 3.1. Each particle modifies its velocity and position according to its own past flying experience and that of the rest of the swarm. If particle i, is randomly placed in two dimensional search space at the point (x_i^k), this particle flies through the problem search space with a random velocity (v_i^k). The particle remembers the best position achieved so far and stores it as ($pbest_i^k$). Then, each particle shares information with its neighboring particles. In other words, each particle compares its best position with those attained by other particles. Finally, each particle stores the best position achieved in the entire swarm as $gbest^k$ (Hu et al. 2004 ; Ejal 2008).

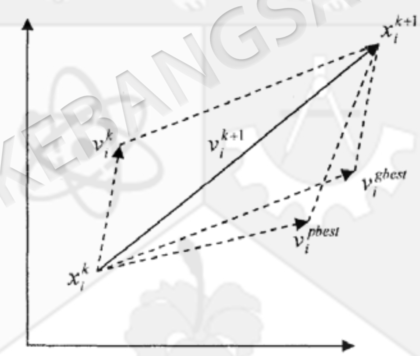

Figure 3.1 Basic concept of PSO

The implementation of the PSO algorithm can be described by the following steps (Eberhart & Shi 2001 ; Ejal 2008):

Step 1: Randomly initialize a swarm of particles in a D-dimensional search space.

Step 2: Evaluate the fitness of the entire swarm.

Step 3: Record the best position of each particle, *pbest* and the global best position, *gbest*.

Step 4: Update the velocity vector and position vector of each particle.

Step 5: Repeat steps (2-4) until a stopping criterion is satisfied.

A discrete PSO algorithm is applied to optimally locate and size a fixed single-phase capacitor in a balanced radial distribution system (Al-Hajri et al. 2007). For this case, the problem is considered as a nonlinear integer optimization problem with both capacitor location and size having discrete values and the Newton-Raphson power flow method is used to calculate the cost function. A PSO based algorithm was used to obtain the minimum voltage deviation and active power loss by optimally locating the SVC device. This approach showed a step-by-step application of the PSO algorithm to solve the problem of optimal placement in a medium size power network. The algorithm was easy to implement and was able to find the optimal solution with regard to the global best position and size of the SVC. The PSO technique has been used to solve a multi-objective optimization problem of minimizing total power loss and maximizing the total transfer capability simultaneously through optimal placement and rating of the SVC (Rao et al. 2011). Hernandez et al. (2006) demonstrated the feasibility of the application of the PSO technique to the optimal allocation of a STATCOM in a 45-bus section of the Brazilian power system. The technique was able to find the best location for the STATCOM in order to optimize the system voltage profile with a low degree of uncertainty.

From the literature, it is noted that PSO has advantages and disadvantages which are described as follows (Bai 2010; Rini et al. 2011).

The advantages of PSO:

i. PSO is based on intelligence which can be applied for both scientific research and engineering use.

ii. PSO have no overlapping and mutation calculation and the search can be carried out based on the speed of a particle. In the development of several generations, only the most optimist particle can transmit information onto the other particles, and the speed of the researching is very fast.

iii. The calculation in PSO is very simple compared with other optimization techniques and its optimization ability is stronger.

iv. PSO adopts real number code, and it is decided directly by a solution. The number of the dimension is equal to the constant of a solution (Bai 2010 ; Rini et al. 2011).

The disadvantages of PSO:

i. PSO easily suffers from partial optimism, which reduces the accuracy and speed of finding the velocity and position vectors.

ii. PSO has difficulty in finding optimal design parameters and its accuracy depends on the initial conditions and the parameter values selected.

iii. PSO application cannot work out on problems such as scattering and non-coordinate system with moving rules of particles in the energy field (Bai 2010; Rini et al. 2011).

3.4 HARMONY SEARCH ALGORITHM

Recently, a meta-heuristic optimization algorithm inspired by playing music has been developed and it is called as harmony search (HS) algorithm (Geem et al. 2001). It is based on meta-heuristic which combine rules and randomness to imitate natural phenomena. HS algorithm is inspired by the operation of orchestra music to find the best harmony between components which are involved in the operation process, for obtaining optimal solution. As musical instruments can be played with some discrete musical notes based on player experience or based on random processes in improvisation, optimization design variables can be considered as discrete values based on computational intelligence and random processes (Lee & Geem 2005). Music players improve their experience based on aesthetics standards while design variables in computer memory can be improved based on objective function. The performance of music seeks a best state or excellent harmony determined by aesthetic estimation, as the optimization process seeks a best state determined by objective function evaluations. The combination of pitches in the ensemble provides aesthetic estimation. Evaluation of the objective function is performed by comparing the values produced by decision variables, which corresponds to harmony which can be improved via repetition. In this analogy, the objective function values can be improved iteration by iteration. As the optimization process looks for finding a global solution that is determined by the objective function, musical performances follow to find pleasing harmony which is determined by the aesthetic standard (Geem et al. 2001).

Figure 3.2 shows a comparison of information between musical improvisation and engineering optimization. In music improvisation, each musician plays within possible pitches to make a harmony vector. If all the pitches create good harmony, the musician saved them in memory and increases good or better harmony for next time. Similarly, in the field of engineering optimization, at first each decision variable value is selected within the possible range and formed a solution vector. If all decision variable values lead to a good solution, each variable that has been experienced is saved in memory, and it increases the possibility of good or better solutions for next time. The advantages of HS algorithm are that it can consider discontinuous functions as well as continuous functions because it does not require differential gradients; it does not require initial value setting for the variables; it is free from divergence and may escape local optima (Lee & Geem 2005).

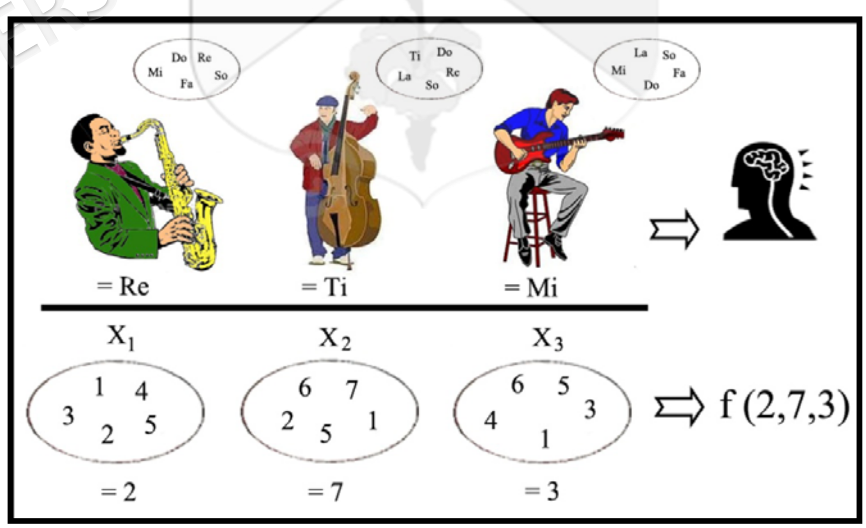

Figure 3.2 Comparison between music improvisation and engineering optimization

In the HS algorithm, it looks for a vector or a path of X which can reduce the computational function cost or shorten the path. The computational procedures of the HS algorithm are described as follows (Geem et al. 2001; Lee & Geem 2005):

Step 1: Initialization of the optimization problem.

Step 2: Initialization of the harmony memory (HM).

Step 3: Improvisation of a new harmony from the HM set.

Step 4: Updating the HM.

Step 5: Repeat steps 3 and 4 until the end criterion is satisfied.

3.4.1 Initialization of the Optimization Problem

Consider an optimization problem which is described as,

Minimize $F(x)$ subject to $x_i \in X_i$, $i=1,2,3,.....N.$

where, $F(x)$: objective function

x : set of each design variable (x_i)

X_i : set of the possible range of values for each design variable ($xL_i < X_i < xU_i$) .

N : number of design variables

Here, other parameters in the HS algorithm have to be also specified. The paraemters are such as the harmony memory size (HMS) or the number of solution vectors in the harmony memory; harmony memory considering rate (HMCR); pitch adjusting rate (PAR); number of decision variables (N); number of improvisations (NI) and the stopping criterion (Geem et al. 2001; Lee & Geem 2005).

3.4.2 Initialization of the Harmony Memory

The HM matrix is filled with as many randomly generated solution vectors as HMS and it is sorted by the values of the objective function, $f(x)$ (Geem et al. 2001; Lee & Geem 2005). The HM matrix is given by,

$$HM = \begin{bmatrix} x_1^1 & x_2^1 & \dots & x_{N-1}^1 & x_N^1 \\ x_1^2 & x_2^2 & \dots & x_{N-1}^2 & x_N^2 \\ . & . & . & . & . \\ . & . & . & . & . \\ . & . & . & . & . \\ x_1^{HMS-1} & x_2^{HMS-1} & \dots & x_{N-1}^{HMS-1} & x_N^{HMS-1} \\ x_1^{HMS} & x_2^{HMS} & \dots & x_{N-1}^{HMS} & x_N^{HMS} \end{bmatrix} \begin{matrix} \Rightarrow & f(x^{(1)}) \\ \Rightarrow & f(x^{(2)}) \\ . & . \\ . & . \\ . & . \\ \Rightarrow & f(x^{(HMS-1)}) \\ \Rightarrow & f(x^{(HMS)}) \end{matrix} \tag{3.3}$$

3.4.3 Improvisation a New Harmony from the HM set

A new harmony vector, $x' = (x_1', x_2', \dots, x_n')$, is generated based on three rules, namely, random selection, memory consideration and pitch adjustment (Lee & Geem 2005).

These rules are described as follows:

i) Random Selection: When HS determines the value x_i' for the new harmony, $x' = (x_1', x_2', \dots x_n')$, it randomly picks any value from the total value range with a probability of (1-HMCR). Random selection is also used for the previous memory initialization.

ii) Memory Consideration: When HS determines the value x_i', it randomly picks any value x_i^j from the HM with a probability of HMCR since j= {1, 2,…, HMS}.

$$x'_i \leftarrow \begin{Bmatrix} x'_i \in \{x_i^1, x_i^2, \dots, x_i^{HMS}\} & \text{with probablity } HMCR \\ x'_i \in X_i & \text{with probablity } (1-HMCR) \end{Bmatrix} \tag{3.4}$$

iii) Pitch Adjustment: Every component of the new harmony vector $x' = (x_1', x_2', \dots x_n')$, is examined to determine whether it should be pitch-adjusted.

After the value x_i' is randomly picked from HM in the above memory consideration process, it can be further adjusted into neighboring values by adding a certain amount to the value, with probability of PAR. This operation uses the PAR parameter, which is the rate of pitch adjustment given as follows:

$$x'_i \leftarrow \begin{cases} Yes & with\ probablity\ PAR \\ No & with\ probablity\ (1-PAR) \end{cases} \quad (3.5)$$

The value of (1-PAR) sets the rate of doing nothing. If the pitch adjustment decision for x_i' is yes, x_i' is replaced by,

$$x'_i \leftarrow x'_i \pm bw \quad (3.6)$$

where *bw* is the arbitrary distance bandwidth for a continuous design variable.
In this step, pitch adjustment or random selection is applied to each variable of the new harmony vector in turns.

3.4.4 Updating HM

If the new harmony vector $x' = (x_1', x_2', ...x_n')$ is better than the worst harmony in the HM, from the viewpoint of the objective function value, the new harmony is entered in the HM and the existing worst harmony is omitted from the HM (Kazemi et al. 2009).

3.4.5 Checking Stopping Criterion

If the stopping criterion which is based on the maximum number of improvisations is satisfied, computation is terminated. Otherwise, Steps 3 and 4 are repeated.

The conventional HS algorithm is described in terms of a flow chart as shown in Figure 3.3.

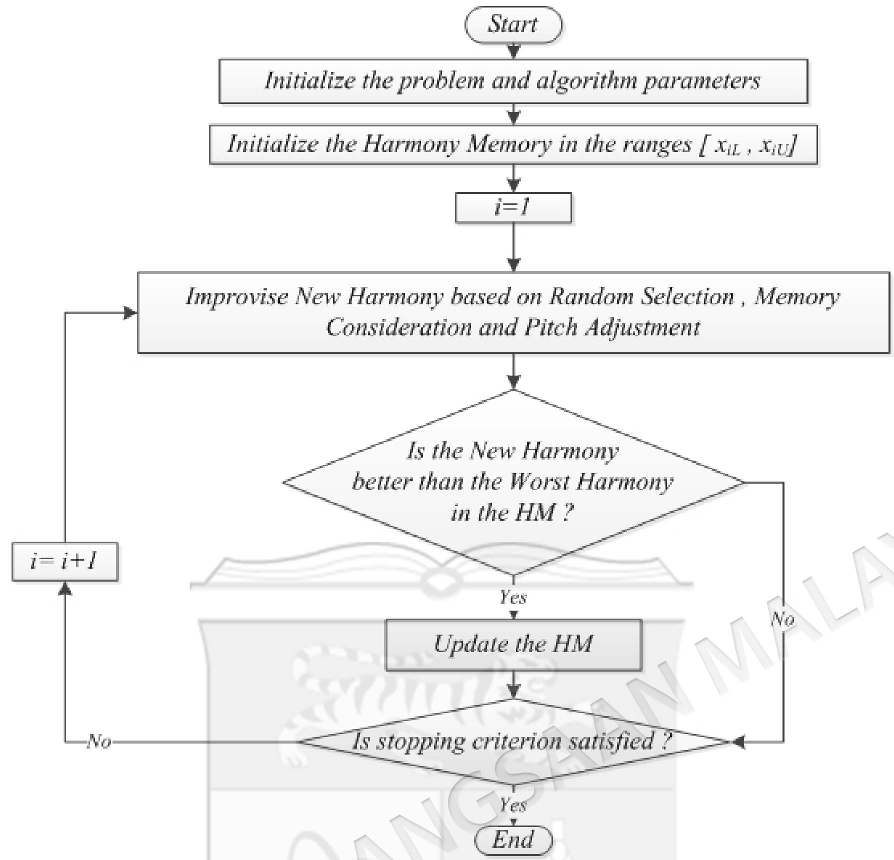

Figure 3.3 The procedures of the conventional HS algorithm

3.4.6 Advantages of Harmony Search Algorithm

The HS algorithm has the following merits (Geem et al. 2001; Lee & Geem 2005):

i. HS does not require differential gradients, thus it can consider discontinuous functions as well as continuous functions.
ii. HS can handle discrete variables as well as continuous variables.
iii. HS does not require initial value setting for the variables.
iv. HS is free from divergence.
v. HS may escape local optima.
vi. HS may overcome the drawback of GA building block theory which works well only if the relationship among variables in a chromosome is carefully considered. If neighbor variables in a chromosome have weaker relationship than remote variables, the building block theory may not work well because of

crossover operation. However, HS explicitly considers the relationship using ensemble operation.

vii. HS has a novel stochastic derivative applied to discrete variables, which uses musician's experiences as a searching direction.

viii. Certain HS variants do not require algorithm parameters such as HMCR and PAR, thus novice users can easily use the algorithm.

3.5 IMPROVED HARMONY SEARCH ALGORITHM

The IHS algorithm was developed by Mahdavi et al. (2007) and has been successfully applied to various benchmarking tests and standard engineering optimisation problems (Gil-Lopez et al. 2012). Numerical results have proven that the IHS algorithm can give better solutions than the conventional HS algorithm and other heuristic optimization techniques (Del-Ser et al. 2012). The conventional HS algorithm uses fixed values for both *PAR* and *bw*. These values are set in the initialisation step and cannot be changed during new generations. The main drawback of the conventional HS algorithm is the large number of iterations the algorithm needs to find an optimal solution. Small *PAR* values combined with large *bw* values can lead to poor performance of the algorithm, and a large number of iterations is needed to find an optimum solution. Small *bw* values in the final generations improve the fine-tuning of solution vectors. Therefore, using large *PAR* values and small *bw* values usually leads to an improvement in achieving the best solution in the final generation in which the algorithm converges to an optimal solution vector (Mahdavi et al. 2007). The key difference between the IHS and conventional HS algorithms is in the way the *PAR* and *bw* values are adjusted. To improve the performance of the HS algorithm and eliminate the drawbacks associated with using fixed values of *PAR* and *bw*, the IHS algorithm uses variable *PAR* and *bw* values in the improvisation step. The *PAR* value changes dynamically with the generation number as shown in Figure 3.4 and is expressed as (Mahdavi et al. 2007):

$$PAR(gn) = PAR_{\min} + \frac{(PAR_{\max} - PAR_{\min})}{NI} \times gn \qquad (3.7)$$

where PAR is the pitch adjustment rate for each generation, PAR_{min} is the minimum pitch adjustment rate, PAR_{max} is the maximum pitch adjustment rate, NI is the number of solution vector generations and gn is the generation number.

The bandwidth at each generation parameter, *bw* changes dynamically with the generation number as shown in Figure 3.4 and is given by,

$$bw(gn) = bw_{max}\, exp(c \cdot gn) \tag{3.8}$$

$$c = \frac{Ln\left(\frac{bw_{\max}}{bw_{\min}}\right)}{NI} \tag{3.9}$$

where bw_{min} and bw_{max} are the minimum and maximum bandwidth, respectively.

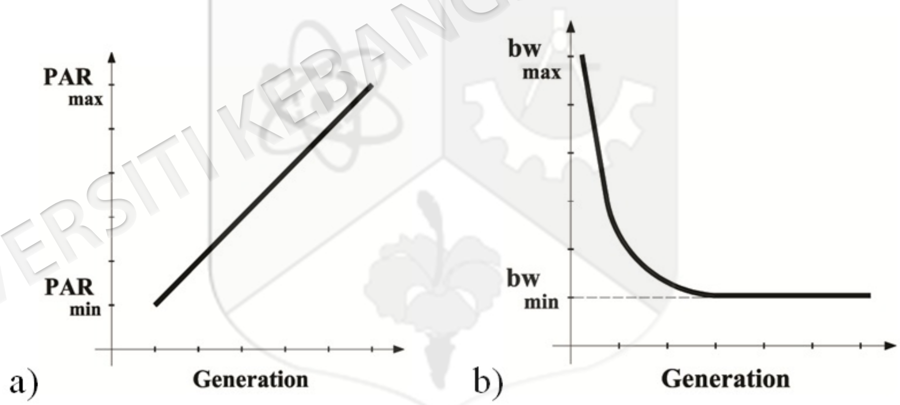

Figure 3.4 Variation of a) PAR and b) *bw* with generation number

The IHS algorithm is described in terms of a flow chart as shown in Figure 3.5.

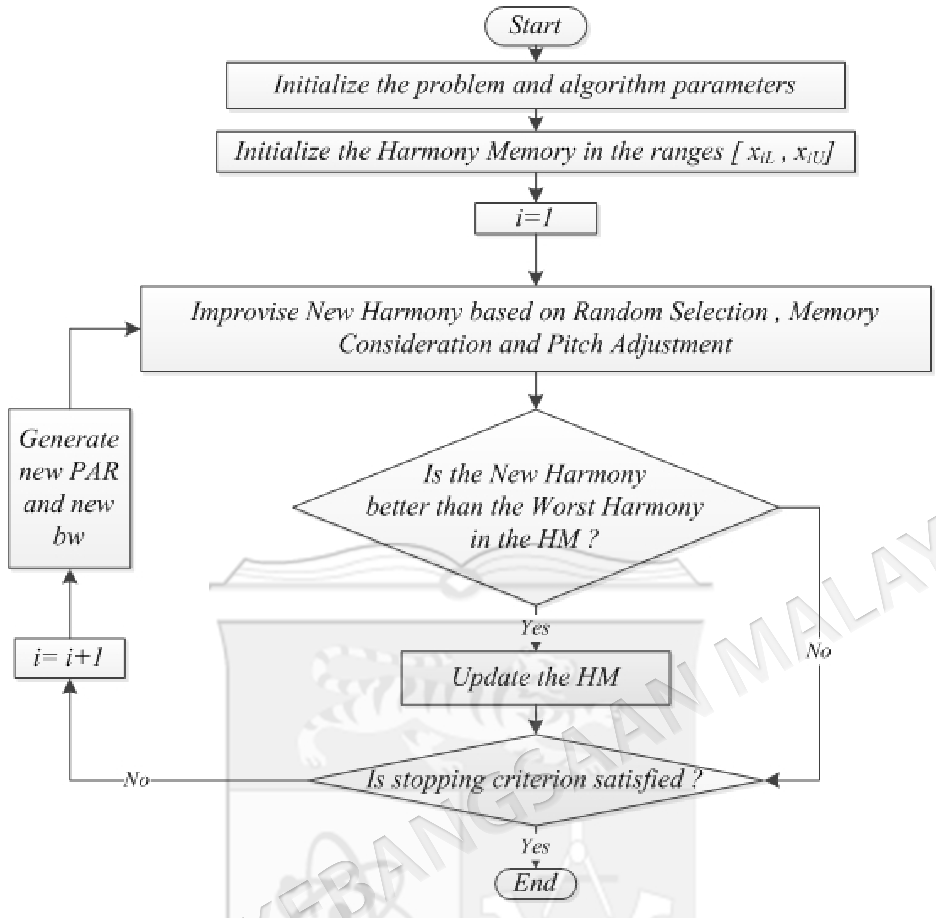

Figure 3.5 The procedures of the IHS algorithm

3.6 GLOBAL HARMONY SEARCH ALGORITHM

Inspired by the swarm intelligence of particle swarm, a novel global harmony search algorithm (GHS) is proposed by Zou et al. (2010 a,b) to solve optimization problems. The GHS algorithm includes two important operations; position updating and genetic mutation with a small probability. The new approach modifies the improvisation step of the HS such that the new harmony can mimic the global best harmony in the HM. The GHS and the HS algorithms are different in three aspects described as as follows (Zou et al. 2010a):

i. The HMCR and PAR are excluded from the GHS algorithm and genetic mutation probability (p_m) is included in the GHS algorithm.

ii. The GHS algorithm modifies the improvisation step of the HS algorithm and this modification is represented by the following pseudo code.

For** each i* $\in$ *[1, N]* ***do

$x_R = 2 \times x^{best}_i - x^{worst}_i$

if $x_R > x_{iU}$ *then* $x_R = x_{iU}$
elseif $x_R < x_{iL}$ *then* $x_R = x_{iL}$

$x'_i = x^{worst}_i + r_{1i} \times (x_R - x^{worst}_i)$ *%position updating*

if $r_{2i} \leq p_m$ *then* $x'_i = x_{iL} + r_{3i} \times (x_{iU} - x_{iL})$ *%genetic mutation*

End

Here, "*best*" and "*worst*" are the indexes of the global best harmony and the worst harmony in HM, respectively. r_{1i}, r_{2i} and r_{3i} are all the uniformly generated random numbers in [0,1]. r_{1i} is used for position updating, r_{2i} determines whether the GHS should carry out genetic mutation, and r_{3i} is used for genetic mutation. Figure 3.6 illustrates the principle of position updating (Zou et al. 2010a).

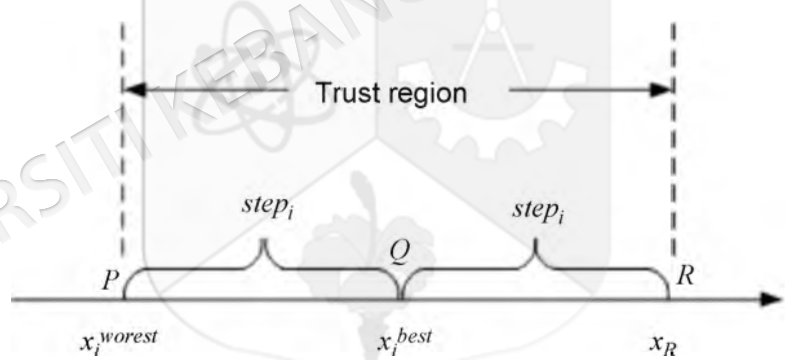

Figure 3.6 The schematic diagram of position updating (Zou et al. 2010a)

$step_i = |x^{best}_i - x^{worst}_i|$ is defined as adaptive step of the i[th] decision variable. The region between *P* and *R* is defined as trust region for the i[th] decision variable. The trust region is actually a region near the global best harmony. In the early stage of optimization, all solution vectors are sporadic in solution space, so most trust regions are wide, which is beneficial to the global search of the GHS; while in the late stage of optimization, all non-best solution vectors are inclined to move to the global best solution vector, so most solution vectors are close to each other. Here, most trust regions are narrow, which is beneficial to the local search of the GHS algorithm. A reasonable design for adaptive step can guarantee that the proposed algorithm has strong global search ability in the early stage of optimization, and has strong local search ability in the late stage of optimization. Dynamically adjusted $step_i$ keeps a balance between the global search and the local search (Zou et al. 2010a,b). As for genetic mutation operation with a small probability, it is carried out for the worst harmony of HM after updating position, so as to enhance the capacity of escaping from the local optimum for the proposed algorithm.

iii. The GHS algorithm replaces the worst harmony x^{worst} in HM with the new harmony x' even if x' is worse than x^{worst}.

For clarity, the GHS algorithm is described in terms of a flow chart as shown in Figure 3.7. In modified improvisation steps , adaptive step and trust region are defined for the GHS, and according to these two factors, a novel position updating equation is designed to make the worst harmony of harmony memory move to the global best harmony in each iteration.Using position updating equation can accelerate the convergence rate of the GHS, however, it also accelerates the premature convergence of the GHS and make it get into the local optimum. To overcome these disadvantages, genetic mutation with a small probability is introduced in the GHS algorithm (Zou et al. 2010a,b) .

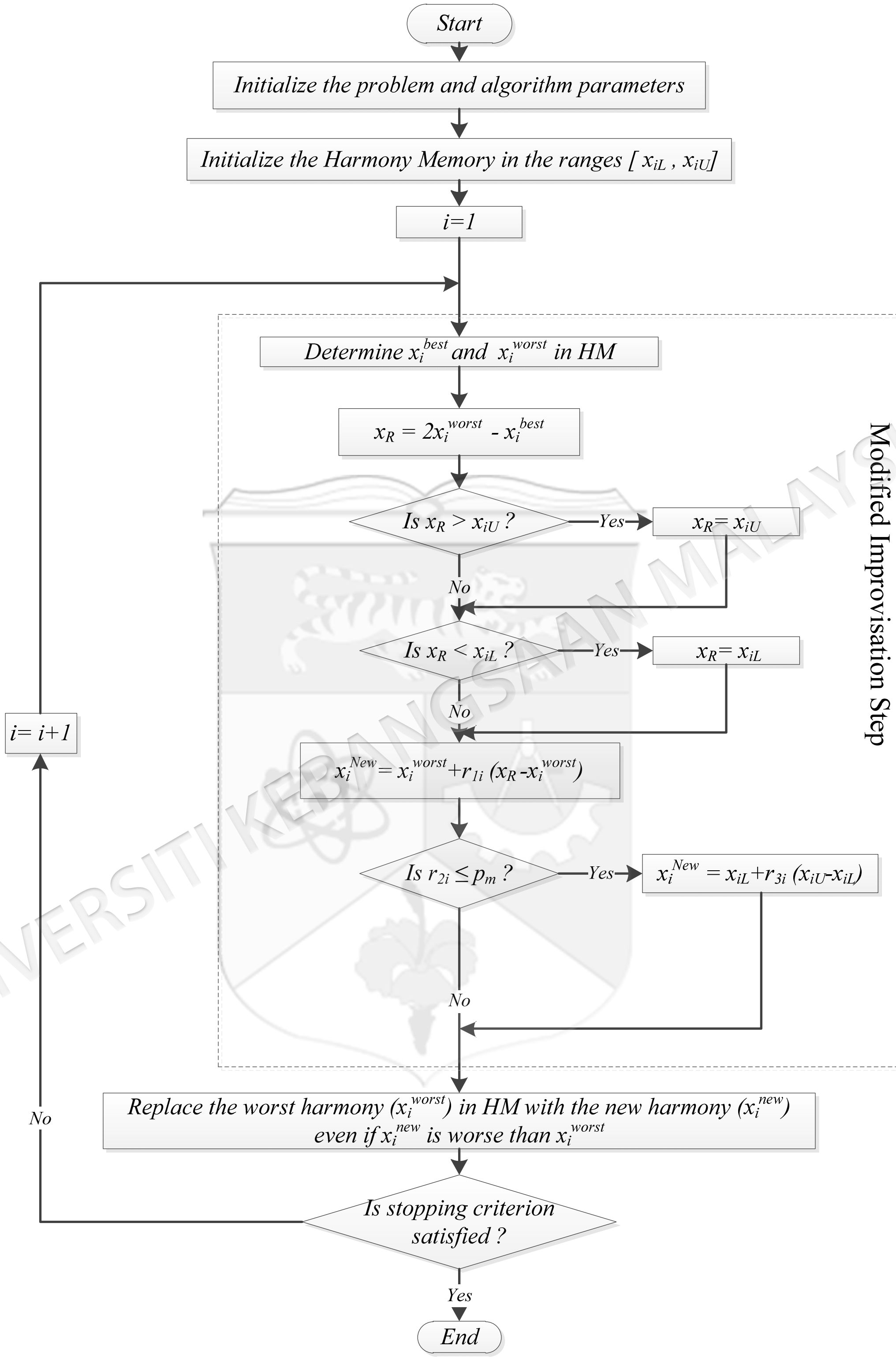

Figure 3.7 The procedures of the GHS algorithm

3.7 CHAPTER SUMMARY

In this chapter, the background theories of existing optimization techniques such as GA, PSO and HS algorithm are described. GA has some drawbacks such as divergence and local optima problems and PSO has difficulty in finding the optimal design parameters. The accuracy of GA and PSO depends on the initial conditions and the parameter values selected. The HS algorithm has several advantages over GA and PSO in which it does not require initial value settings for the decision variables, and that it is free from divergence. The two modified HS algorithm, namely, IHS and novel GHS algorithms are also described. IHS algorithm employs a method for generating new solution vectors so as to enhance accuracy and convergence of the conventional HS algorithm. The GHS algorithm which is inspired by swarm intelligence of the PSO technique, modifies the improvisation step of the HS algorithm, such that new harmony can mimic the global best harmony in the HM. In addition, the GHS algorithm notably consumes less average time than the IHS algorithm (Zou et al. 2010a,b).

CHAPTER IV

OPTIMAL PLACEMENT AND SIZING OF CAPACITORS IN RADIAL DISTRIBUTION SYSTEMS

4.1 INTRODUCTION

Shunt capacitors in distribution networks are used to provide reactive power compensation in distribution networks to reduce power losses and to maintain a voltage profile within acceptable limits. However, the installation of shunt capacitors in distribution networks requires consideration of their appropriate location and size. Capacitor placement is important to maximize loss reduction by properly installing shunt capacitors while minimizing shunt capacitor costs (Ng et al. 2000). The problem of locating and sizing shunt capacitors in distribution systems has been a challenge for power system planners and researchers. Many published papers and reports were found in the literature that addressed this issue. Different formulations have been utilized to solve this difficult combinatorial problem (Ejal 2008). The unbalanced operating conditions and the presence of harmonic sources in distribution systems further complicate the capacitor placement and sizing problem. These issues have been neglected in many of the studies conducted on the capacitor optimization problem. Installing shunt capacitors without considering the presence of harmonic sources in the system may lead to increased harmonic distortion levels due to resonance between the capacitors and the various inductive elements in the system (Ejal & El-Hawary 2010). Therefore, in this study, harmonics and unbalance have been considered in solving the optimal capacitor placement and sizing problem.

4.2 OPTIMAL CAPACITOR PLACEMENT AND SIZING FORMULATION

One of the goals in radial distribution systems is to determine the optimal location and size of shunt capacitors by maximizing loss reduction and minimizing total cost incurred due to power loss and capacitor installation. To solve the optimal capacitor placement and sizing problem, the following objective function, F, is considered (Ng et al. 2000).

F = Minimize {Yearly Power Loss Cost + Yearly Capacitor Cost} (4.1)

Subject to:

$$\text{Cost of Yearly Power Loss} = K_P P_{loss} \tag{4.2}$$

$$\text{Cost of Yearly Capacitor Cost} = \sum_{i=1}^{n} K_i^c Q_i^c \tag{4.3}$$

The total real power loss in (4.1) is given by

$$P_{loss} = P_{loss}^{(Fund.)} + P_{loss}^{(harmonics)} \tag{4.4}$$

in which,

$$P_{loss}^{(harmonics)} = \sum_{h=h_0}^{H} P_{loss}^{(h)} \tag{4.5}$$

where $P_{loss}^{(Fund.)}$ and $P_{loss}^{(harmonics)}$ are the total power losses of the fundamental and harmonic components, respectively. n is the number of candidate locations for capacitor placement, K_P is the equivalent annual cost per unit of power loss ($/(kW-year)), K_i^c is the annual capacitor installation cost, and $i = 1, 2,...,n$ are the indices of the buses selected for compensation. h_0 and H are the lower and upper limits of the harmonic order, respectively.

In addition to the objective function, the constraints of the optimization model must be defined. In real applications, limits are placed on the choice of control variables (Ejal & El-Hawary 2010). The constraints are associated with the bus voltages, the total harmonic distortion levels, and the shunt capacitors to be installed. These constraints are described as follows:

i. Bus Voltage Limits: The bus voltage magnitudes must be kept within acceptable operating limits throughout the optimization process (IEEE Std 18-1992):

$$V_{\min} \le |V_i| \le V_{\max} \quad (4.6)$$

where V_{min} is the lower bound of bus voltage limits, V_{max} is the upper bound of bus voltage limits, and V_i is the rms value of the bus voltage.

ii. Total Harmonic Distortion Limits: The total harmonic distortion at each bus must be maintained less than or equal to the maximum allowable harmonic distortion level (IEEE Std 519-1992):

$$THD_i(\%) \le THD_{\max}(\%) \quad (4.7)$$

where THD_{max} is the maximum allowable harmonic distortion level at each bus.

The total harmonic distortion at each bus is given by,

$$THD_i(\%) = \frac{100}{|V_i^1|}\sqrt{\sum_{h=h_0}^{H} |V_i^h|^2} \quad (4.8)$$

where V_i is the rms value of the bus voltage, h_0 and H are the lower and upper limits of the harmonic order, respectively.

iii. Number and Sizes of Shunt Capacitors: Commercially available capacitors come in discrete sizes in which the shunt capacitors are multiple integers of the smallest capacitor size available:

$$Q_{ci} \le LQ_0 \qquad L = 1,2,\ldots,nc\,, \tag{4.9}$$

where Q_0 is the smallest capacitor size available.

4.3 BACKWARD / FORWARD SWEEP POWER FLOW

To solve the optimal capacitor placement and sizing problem for three-phase radial distribution networks, a simpler power flow method known as the backward/forward sweep power flow is used for computing the power loss (Teng 2000). In this power flow method, the relationship between bus current injections, [I] and branch currents, [B] as shown in a simple radial distribution network of Figure 4.1 is represented by the matrix [BIBC] which is given by,

$$[B]= [BIBC]\ [I] \tag{4.10}$$

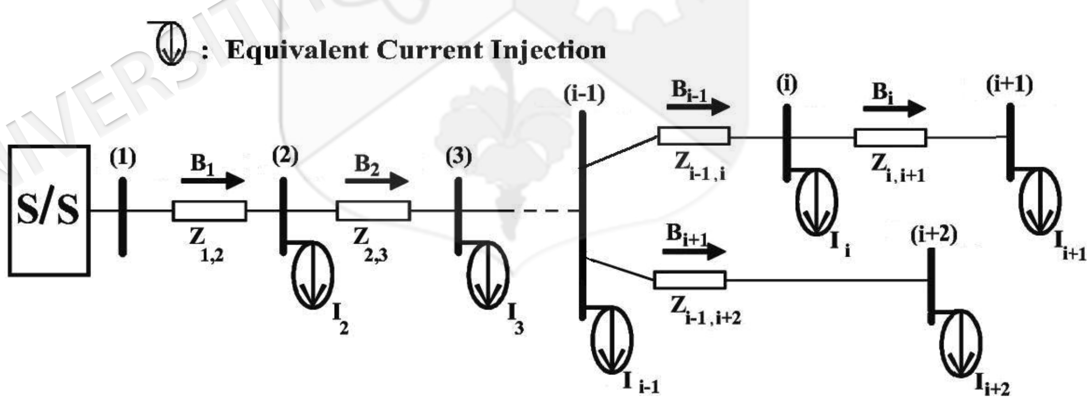

Figure 4.1 Simple radial distribution network

The backward current sweep can be used to build the coefficient vectors. For example, if a bus current flows through the branch, then the corresponding position in the coefficient vector will be 1. Therefore, the coefficient vector will consist of only 0 and 1. The relationship between the branch currents, *[B]* and bus voltages, *[ΔV]* is represented by the matrix *[BCBV]*. The matrices *[BIBC]* and *[BCBV]* are then multiplied to obtain the relationship between the voltage deviation, *[ΔV]* and the bus current injections, *[I]*, which is represented by the matrix *[DLF]*,

$$[\Delta V] = [BCBV]\,[B] = [BCBV]\,[BIBC]\,[I] = [DLF]\,[I] \tag{4.11}$$

The backward/forward sweep power flow method (Teng 2000) at the k^{th} iteration considers the following equations:

$$I_i^k = \left(\frac{P_i + jQ_i}{V_i^k}\right)^* \tag{4.12}$$

$$\left[\Delta V^{k+1}\right] = [DLF]\left[I^k\right] \tag{4.13}$$

where k is the iteration count.

After the power flow is converged, the total power loss of the fundamental component is calculated. The total power loss is given by,

$$P_{loss}^{(Fund.)} = \sum_{i=1}^{nb} Ploss_i = \sum_{i=1}^{nb} \left|B_i\right|^2 R_i \tag{4.14}$$

$\left|B_i\right|$ is the magnitude of the i^{th} branch current and R_i is the resistance of branch i.

The backward/forward sweep power flow algorithm is described in terms of a flowchart as shown in Figure 4.2.

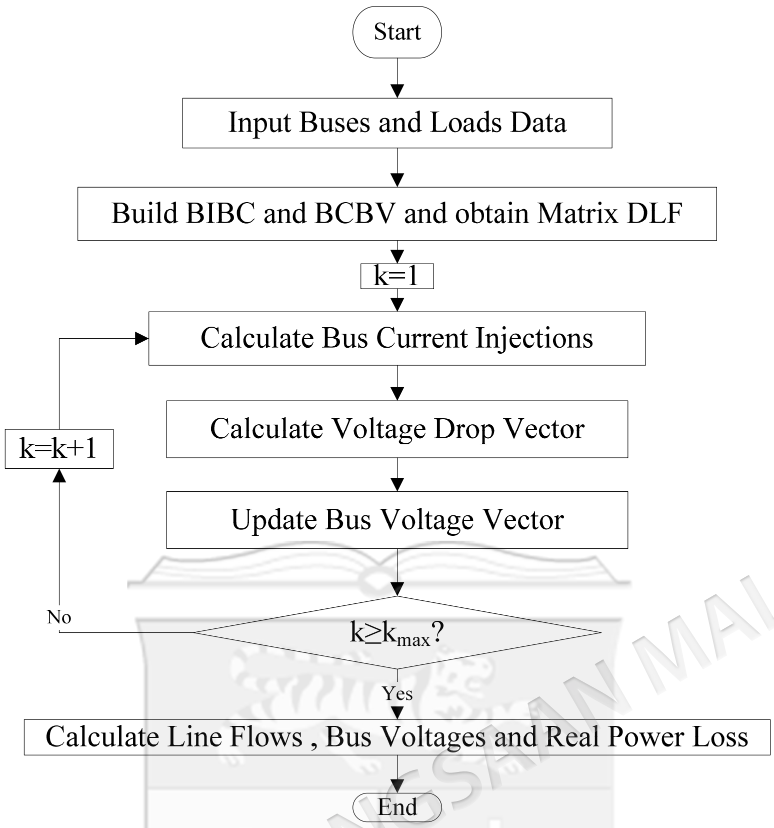

Figure 4.2 Flowchart of the backward/forward sweep power flow for radial distribution systems

This method can be best described by the following steps:

1) Set the iteration index k = 1 .

2) Initialize the bus voltage vector.

3) Form the *[DLF]* matrix

4) Calculate the bus current injections

5) Compute the voltage drop vector

6) Update the bus voltage vector

7) Repeat steps (4-6) until a predetermined tolerance is reached

8) Calculate the total real power loss

The codes written in Matlab for the backward/forward sweep power flow method are given in Appendix F.

4.4 HARMONIC POWER FLOW

It is necessary to perform harmonic power flow calculations at different harmonic orders so that harmonic losses, harmonic voltages and bus voltage THD can be calculated. A simple harmonic power flow that uses backward and forward sweep method to calculate harmonic branch currents and harmonic nodal voltages has been developed in Teng & Chang (2007). This method has definite advantages over other harmonic power flow methods in which the computational time required to compute branch currents and nodal voltages at harmonic frequencies are much smaller than the traditional harmonic power flow method (Ejal 2008). The full three phase representations of system components are included and the method is suitable for performing harmonics studies in large size distribution systems (Ejal 2008).

To describe the different stages of the harmonic power flow algorithm development, a distorted n-bus radial distribution system is considered as shown in Figure 4.3 (Ejal 2008).

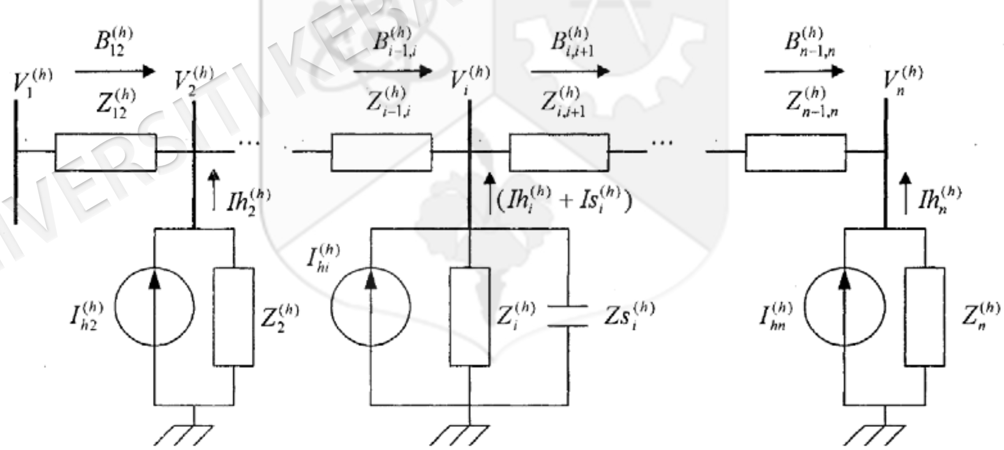

Figure 4.3 A single line diagram of a distorted n-bus radial distribution system

In Figure 4.3, bus 1 represents the main substation or the supply source and is modeled as a slack bus. The (2-n) load buses consist of linear and nonlinear loads. The system harmonic currents can be divided into two categories, namely, harmonic currents contributed by nonlinear loads and linear impedance and harmonic currents absorbed by shunt capacitors (Teng & Chang 2007). The system harmonic currents can be expressed in vector form as:

$$\left[I^{(h)}\right]=\begin{bmatrix} Ih^{(h)} \\ . \\ . \\ . \\ Is^{(h)} \end{bmatrix} \tag{4.15}$$

where $[I^{(h)}]$ is the vector of system harmonic currents at the h^{th} harmonic order. $[Ih^{(h)}]$ and $[Is^{(h)}]$ are the vectors of harmonic currents contributed by nonlinear loads and linear impedance, and harmonic currents absorbed by shunt capacitors at the h^{th} harmonic order, respectively. For a distribution system with harmonic sources and shunt capacitors, the $[Ih^{(h)}]$ is a m×1 vector; the $[Is^{(h)}]$ is a n×1 vector; and the $[I^{(h)}]$ is a (m+n)×1 vector (Teng & Chang 2007).

Next, a coefficient vector is defined to record whether the system harmonic currents flow through the branch. The coefficient vector for the branch between bus *i* and *j* is given by

$$\left[A_{ij}^{(h)}\right]=\begin{bmatrix} Ah_{ij}^{(h)} \\ . \\ . \\ . \\ As_{ij}^{(h)} \end{bmatrix} \tag{4.16}$$

where $[A_{ij}^{(h)}]$ is the coefficient vector of harmonic currents for the branch between bus *i* and *j* at the h^{th} harmonic order. $[Ah_{ij}^{(h)}]$ and $[As_{ij}^{(h)}]$ are the coefficient vectors of the harmonic currents contributed by nonlinear loads and linear impedance, and harmonic currents absorbed by shunt capacitors for the branch between bus *i* and *j* at the h^{th} harmonic order, respectively.

The backward current sweep can be used to build the coefficient vectors. For example, if bus harmonic current flows through a branch, then the corresponding position in the coefficient vector will be 1. Therefore, the coefficient vector will consist of 0 and 1 only (Teng & Chang 2007). The branch current resulting from system harmonic currents can be easily calculated using,

$$B_{ij}^{(h)} = \left[A_{ij}^{(h)}\right]^T \left[I^{(h)}\right] \tag{4.17}$$

The branch voltage drop resulting from system harmonic vector is expressed as

$$\Delta V_{ij}^{(h)} = Z_{ij}^{(h)} \left[A_{ij}^{(h)}\right]^T \left[I^{(h)}\right] \tag{4.18}$$

where $Z_{ij}^{(h)}$ is the branch impedance at the h^{th} harmonic order.

After calculating the voltage drop, the forward voltage sweep is utilized to obtain the harmonic bus voltages with respect to harmonic bus current injections as follows (Ejal 2008) :

$$\left[V^{(h)}\right] = \left[HA^{(h)}\right]\left[I^{(h)}\right] \tag{4.19}$$

where $[HA^{(h)}]$ is the relationship matrix between bus voltage vector $[V^{(h)}]$and system harmonic current vector, $[I^{(h)}]$. The bus voltages of shunt capacitors can be written as

$$\left[Vs^{(h)}\right] = \left[HAs^{(h)}\right]\left[I^{(h)}\right] \tag{4.20}$$

where $[HAs^{(h)}]$ is composed of the row vectors with respect to the buses of shunt capacitors. The elements of (n-1) columns in the vector $[HAs^{(h)}]$ are associated with the harmonic currents of the nonlinear and linear loads, while the last element in $[HAs^{(h)}]$ is related to the harmonic current of the shunt capacitor at bus i. Therefore, $[HAs^{(h)}]$ can be written in the form of:

$$\left[HAs^{(h)}\right] = \left[HA_{Sh}^{(h)} : HA_{Ss}^{(h)}\right] \tag{4.21}$$

The voltage at the shunt capacitor is;

$$Vs_i^{(h)} = -Is_i^{(h)} \times Zs_i^{(h)} \tag{4.22}$$

where $Is_i^{(h)}$ is the harmonic current of the shunt capacitor at bus *i* and $Z_{Si}^{(h)}$ is the harmonic impedance of the shunt capacitor at bus *i*.

Substituting (4.21) and (4.22) into (4.20), the following equation is obtained.

$$\left[Vs^{(h)}\right] = \left[HAs^{(h)}\right]\left[I^{(h)}\right] \Rightarrow$$

$$-\begin{bmatrix} Zs_1.Is_1 \\ \vdots \\ Zs_n.Is_n \end{bmatrix} = \left[HA_{Sh}^{(h)} : HA_{Ss}^{(h)}\right]\begin{bmatrix} Ih^{(h)} \\ \vdots \\ Is^{(h)} \end{bmatrix} \Rightarrow$$

$$\underbrace{\left(\left[HA_{Ss}^{(h)}\right] + \begin{bmatrix} Zs_1^{(h)} & & \\ & \ddots & \\ & & Zs_n^{(h)} \end{bmatrix}\right)}_{HLF^{(h)}}.\left[Is^{(h)}\right] = -\left[HA_{Sh}^{(h)}\right]\left[Ih^{(h)}\right] \tag{4.23}$$

Equation (4.23) can also be expressed as,

$$\left[HLF^{(h)}\right]\left[Is^{(h)}\right] = -\left[HA_{Sh}^{(h)}\right]\left[Ih^{(h)}\right] \tag{4.24}$$

If n shunt capacitors are installed in a radial distribution system, [$HLF^{(h)}$] will be a square matrix of (n × n) dimension. Instead of solving linear equations of a full distribution system, the proposed harmonic power flow method method only needs to solve the linear equations with n dimension thus making the method efficient.
The bus voltage at the k^{th} iteration and the h^{th} harmonic order can be expressed as:

$$\left[V^{(h),k+1}\right] = \left[V^{(h),0}\right] + \left[V^{(h),k}\right] \tag{4.25}$$

The harmonic power flow method is described in terms of a flowchart as shown in Figure 4.4.

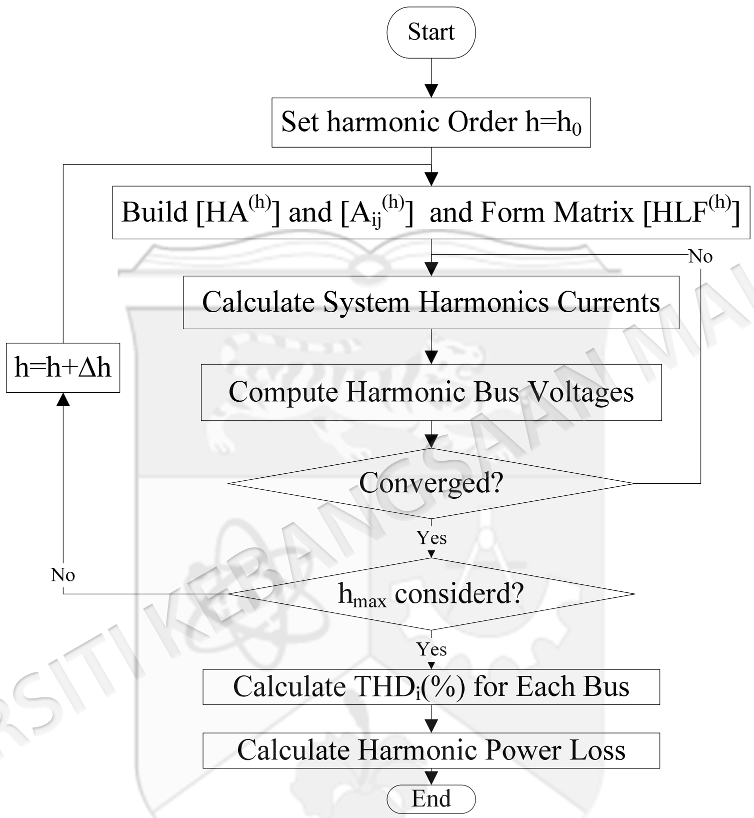

Figure 4.4 Flowchart of the harmonic power flow algorithm

The steps involved in the harmonic power flow algorithm are described as follows (Teng & Chang 2007; Ejal 2008):

i. Set the harmonic order to the smallest value of interest ($h=h_0$).
ii. Build the coefficient vector of system harmonic current flows through each branch.
iii. Form the relationship matrix $[HA^{(h)}]$ between the harmonic bus voltages and system harmonic currents.

iv. For n shunt capacitors, build the [$HLF^{(h)}$] matrix for all harmonic frequencies of interest.

v. Calculate the harmonic currents of shunt capacitors.

vi. Compute the harmonic bus voltage vector at the k^{th} iteration.

vii. Repeat steps (iv) and (v) until a stopping criterion for convergence is met. The stopping criterion is given by ($\left|V_i^{(h),k+1} - V_i^{(h),k}\right| \leq \varepsilon$).

viii. Repeat steps (i) to (vii) until all the harmonic orders are considered.

ix. Calculate the rms values of the harmonic bus voltages.

x. Measure the voltage *THD (%)* at each bus.

The total real power loss formula for the h^{th} harmonic order is given by,

$$P_{loss}^{(h)} = \sum_{i=1}^{nb} Ploss_i^{(h)} = \sum_{i=1}^{nb} \sum_{h=h_0}^{H} \left|B_i^{(h)}\right|^2 R_i^{(h)} \tag{4.26}$$

where h is the harmonic order, h_0 and H are the lower and upper limits of the harmonic order, respectively. $\left|B_i^{(h)}\right|$ is the magnitude of the i^{th} branch current for the h^{th} harmonic order and $\left|R_i^{(h)}\right|$ is the i^{th} branch resistance for the h^{th} harmonic order.

The total power loss of harmonic components is given by,

$$P_{loss}^{(harmonics)} = \sum_{h=h_0}^{H} P_{loss}^{(h)} \tag{4.27}$$

The codes written in Matlab for the harmonic power flow method are given in Appendix G.

4.5 OPTIMAL CAPACITOR PLACEMENT AND SIZING METHOD WITHOUT CONSIDERING MUTUAL COUPLING, LOAD UNBALANCE AND HARMONICS

The proposed method for optimal capacitor placement and sizing at the buses is solved by using the IHS and GHS algorithms in which the optimal capacitor set $\{Q^c_{1,\ldots}, Q^c_{i,\ldots,} Q^c_N\}$ leads to maximum power loss reduction and cost saving. Here, the backward/forward sweep power flow is applied for computing the power loss.

4.5.1 Application of IHS Algorithm for Optimal Capacitor Placement

The IHS algorithm is used together with the backward/forward sweep power flow for determining the optimal placement and sizing of capacitors in radial distribution networks. The procedures for implementing the proposed optimal capacitor placement method are described as follows:

i. Input system parameters such as line and load data.
ii. Build the BIBC and BCBV matrices and compute the DLF matrix.
iii. Randomly add the capacitors for reactive power compensation at the load buses. Calculate the total power loss and total cost, respectively. Each capacitor set is considered as the harmony vectors. Initialize the arrays of harmony memory (HM) randomly as in (3.3). The number of columns in the HM is equal to number of buses in the test system. In this case, the optimal parameters of the test system, xL_i and xU_i are assumed to have minimum and maximum kVar values of capacitors, respectively. The harmony memory size (HMS) generally varies from 1 to 100 (Geem et al. 2001). In this study, the HMS is assumed 10 so as to solve the problem with smaller radius of convergence. Thus, HM matrix for optimal capacitor placement is given as,

$$HM = \begin{bmatrix} Q_1^{c\,(1)} & Q_2^{c\,(1)} & \cdots & Q_{N-1}^{c\ \ (1)} & Q_N^{c\,(1)} \\ Q_1^{c\,(2)} & Q_2^{c\,(2)} & \cdots & Q_{N-1}^{c\ \ (2)} & Q_N^{c\,(2)} \\ . & . & . & . & . \\ . & . & . & . & . \\ . & . & . & . & . \\ Q_1^{c\,(9)} & Q_2^{c\,(9)} & \cdots & Q_{N-1}^{c\ \ (9)} & Q_N^{c\,(9)} \\ Q_1^{c\,(10)} & Q_2^{c\,(10)} & \cdots & Q_{N-1}^{c\ \ (10)} & Q_N^{c\,(10)} \end{bmatrix}_{10\times N} \tag{4.28}$$

where $Q_i^{c(k)}$ is the added reactive power value at i_{th} bus in k_{th} row of the harmony memory. The size of HM matrix is 10 × N (number of load buses).

iv. Improvise a new harmony using the three rules of random selection, memory consideration and pitch adjustment. In order to find the optimal parameters of IHS, the best parameters which produce lowest fitness function value with suitable convergence are selected. Therefore, the optimal parameters which lead to the best trade-off between accuracy and speed of optimization are selected as: HMCR = 90% , PAR_{max}= 0.99, PAR_{min}= 0.4, bw_{max}=1 , bw_{min}=0.0001 and NI = 5000.

v. Run the backward/forward sweep power flow to calculate the bus current injections and bus voltages using (4.12) and (4.13), respectively.

vi. Calculate power loss and total cost.

vii. Check if the capacitor set (new harmony) gives less total cost than the worst harmony in the HM. If yes, the worst harmony is replaced with the new harmony in the HM. Otherwise, generate new *PAR* and new *bw* using (3.7) and (3.8), respectively and then return to step (iv). In this step, the capacitor set which consider the new harmony is [$Q^c{}_1{}^{New}$,…. ,$Q^c{}_i{}^{New}$,…., $Q^c{}_N{}^{new}$].The main objective function of the problem is minimization of total cost which includes power loss cost and investment cost. Any reduction in total power loss or total capacitor cost leads to less objective function value.

viii. Determine the optimal capacitor set (best harmony) which gives maximum power loss reduction and maximum cost saving.

The best solution to be found by the proposed harmony search algorithm is a (1×N) matrix where some of the values are 0 in the arrays. A value of 0 in the matrix means that there is no need to install capacitor at that bus. For example, consider the best solution shown below:

$$Best \quad Solution = [\ldots \quad 0 \quad Q_i^c \quad 0 \quad \ldots \quad 0 \quad Q_j^c \quad \ldots \quad 0 \quad Q_k^c \quad 0 \quad \cdots \quad 0] \qquad (4.29)$$

The solution indicates that the best capacitor placement are at buses i , j, k with reactive power values of Q_i^c ,Q_j^c and Q_k^c, respectively.

Figure 4.5 describes the procedures involved in solving the optimal capacitor placement problem using the IHS algorithm.

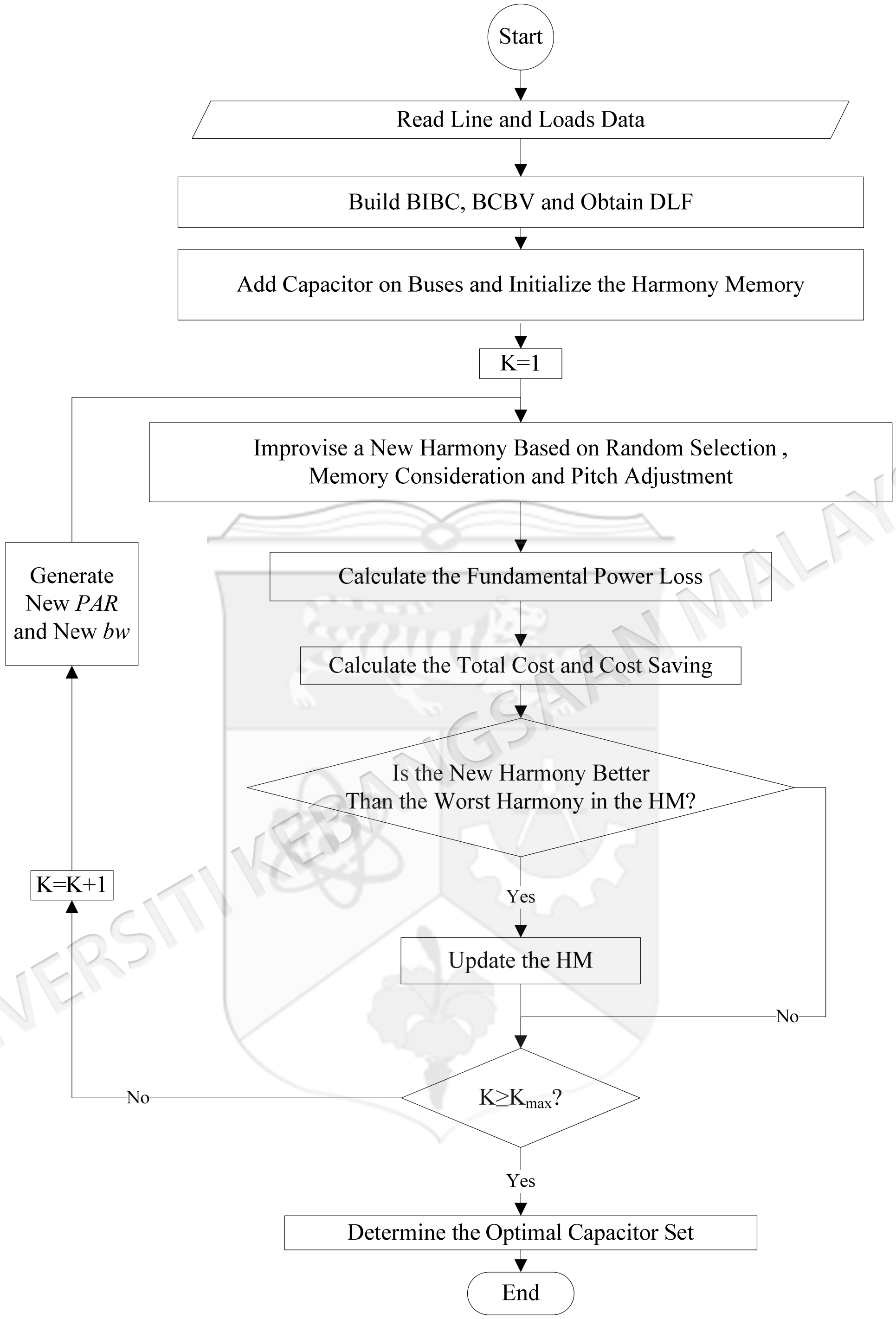

Figure 4.5 The IHS algorithm for solving the capacitor placement and sizing problem

4.5.2 Application of GHS Algorithm for Optimal Capacitor Placement and Sizing

The GHS algorithm is used together with the backward/forward sweep power flow for determining the optimal placement and sizing of capacitors in radial distribution networks. The procedures for implementing the proposed optimal capacitor placement method are described as follows:

i. Input system parameters such as line and load data.
ii. Build the BIBC and BCBV matrices and compute the DLF matrix.
iii. Randomly add the capacitors for reactive power compensation at the buses. Each capacitor set is considered a harmony vector. The HM arrays are randomly initialized using (3.3). The number of columns in the HM is equal to the number of buses in the test system. The optimal parameters of the test system, xL_i and xU_i, are assumed to have minimum and maximum values of capacitors in kVar, respectively. The HMS value is assumed to be 10.
iv. A new harmony is improvised through position updating and genetic mutation. In this step, the genetic mutation probability is assumed as p_m=0.2.
v. Run the backward/forward sweep power flow to calculate the bus current injections and bus voltages using (4.12) and (4.13).
vi. Calculate power loss and total cost.
vii. The worst harmony in HM is replaced with the new harmony.
viii. Determine whether the stopping criterion, maximum generation ≥5000, is satisfied. If not, return to step (iv).
ix. Determine the optimal capacitor set (best harmony) which gives maximum power loss reduction and maximum cost saving.

Figure 4.6 shows a schematic diagram of the procedures involved in solving the optimal capacitor placement and sizing problem using the GHS algorithm.

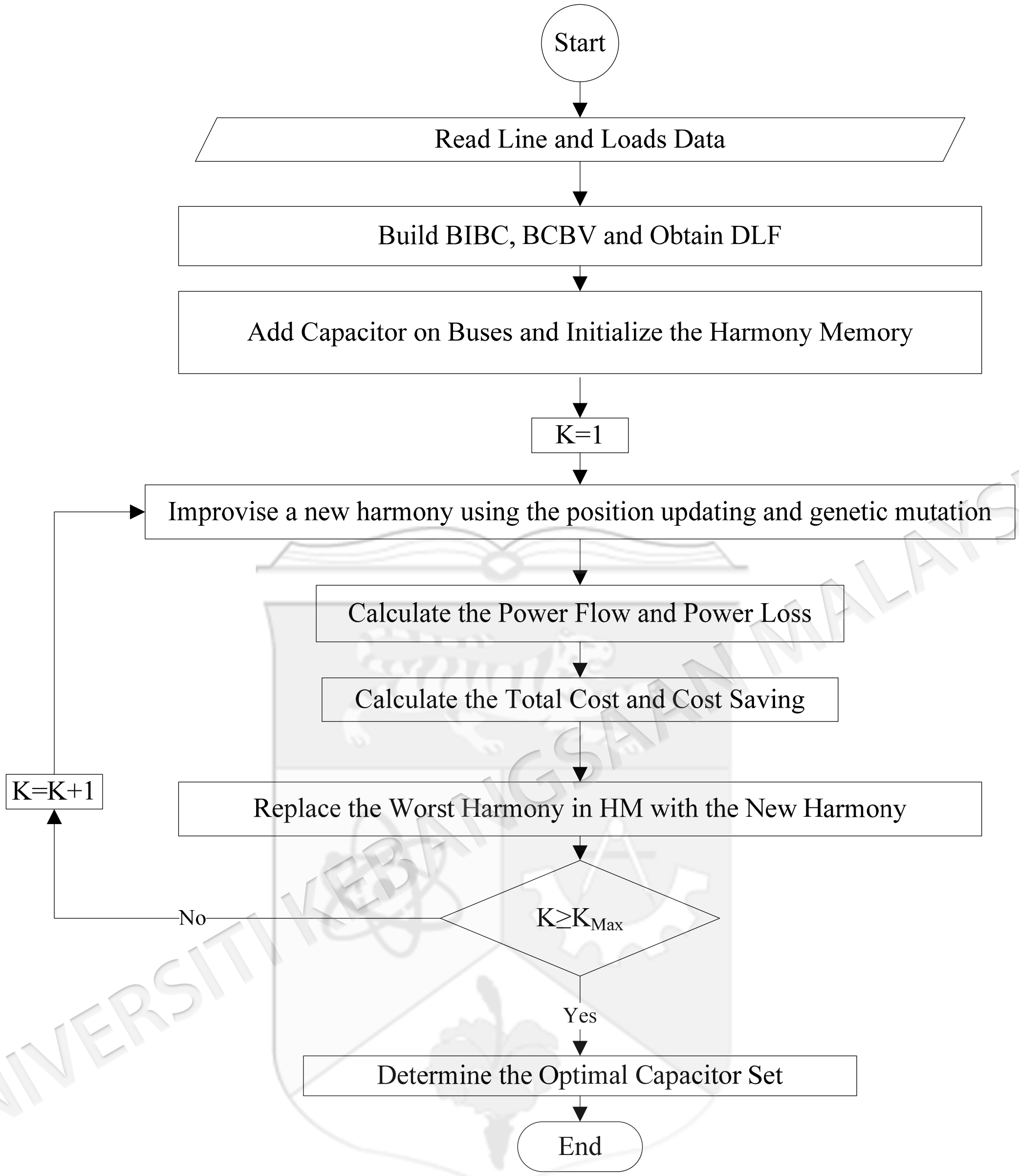

Figure 4.6 The GHS algorithm for solving the capacitor placement problem

4.6 OPTIMAL CAPACITOR PLACEMENT AND SIZING METHOD CONSIDERING MUTUAL COUPLING, LOAD UNBALANCE AND HARMONICS

Real life distribution networks are unbalanced both in respect of mutual coupling between phase conductors and loading on different phases (Ghose & Goswami 2004). Moreover, a considerable amount of harmonic distortion exists in distribution system. In this Section, the IHS and GHS algorithms are applied as two optimization techniques to solve the optimal location and sizing of the three phase capacitors at the load buses. The objective function of the optimization problem takes into account the total cost due to the reduction of power loss and capacitor installation costs.

4.6.1 Application of IHS Algorithm for Optimal Capacitor Placement in Three Phase Radial Distribution Systems

The IHS algorithm is used together with the backward/forward sweep power flow method and radial harmonic power flow for determining the optimal placement and sizing of capacitors in three phase radial distribution networks for minimizing the power loss and total cost by considering mutual coupling, load unbalance and harmonics. Inclusion of system unbalance increases the dimension of the problem as the three phases have to be considered instead of single phase balanced representation (Ghose & Goswami 2004). Consideration of harmonics, introduces more constraints in the problem, thus making the capacitor placement problem more complex compared with the balanced sinusoidal case (Ejal & Elahawary 2010). The procedures for implementing the proposed optimal capacitor placement method are described as follows:

i. Input system parameters such as network and harmonics data.
ii. Model the distribution system considering the effect of network unbalance and mutual coupling between phases.
iii. Build the BIBC and BCBV matrices and compute the DLF matrix for a three phase system.
iv. Randomly add the capacitors for reactive power compensation at the phases of buses. Calculate the total power loss and total cost, respectively. Each capacitor set is considered as the harmony vectors. Initialize the

arrays of HM as in (3.3), randomly. The optimal parameters of the test system are assumed such that the xL_i and xU_i which are the minimum and maximum kVar values, respectively. The HMS is assumed 10.

v. Improvise a new harmony using the three rules of random selection, memory consideration and pitch adjustment. Here, the optimal parameter values are selected as: HMCR = 90% , PAR_{max}= 0.99, PAR_{min}= 0.4, bw_{max}=1 , bw_{min}=0.0001 and NI = 5000. These optimal parameters lead to the best trade-off between accuracy and speed of optimization.

vi. Run the backward/forward sweep power flow to calculate bus current injections and bus voltages using (4.12) and (4.13).

vii. Calculate the fundamental power loss using the backward/forward sweep power flow method.

viii. Calculate harmonic power loss, injection currents and THD by using harmonic power flow for all harmonic orders.

ix. Check if $THD_i \le THD_{\max}$, if yes continue, otherwise, go to step (iv).

x. Calculate power loss and total cost.

xi. Check if the capacitor set (new harmony) gives less total cost than the worst harmony in the HM. If yes, the worst harmony is replaced with the new harmony in the HM. Otherwise, generate new *PAR* and new *bw* using (3.7) and (3.8), respectively and then return to step (v).

xii. Determine the optimal capacitor set (best harmony) which gives maximum power loss reduction and maximum cost saving. The optimal capacitor set includes the optimal value of three phase capacitors at each bus.

Figure 4.7 describes the procedures involved in solving the optimal capacitor placement problem using the IHS algorithm and the backward/forward sweep power flow method in terms of a flowchart.

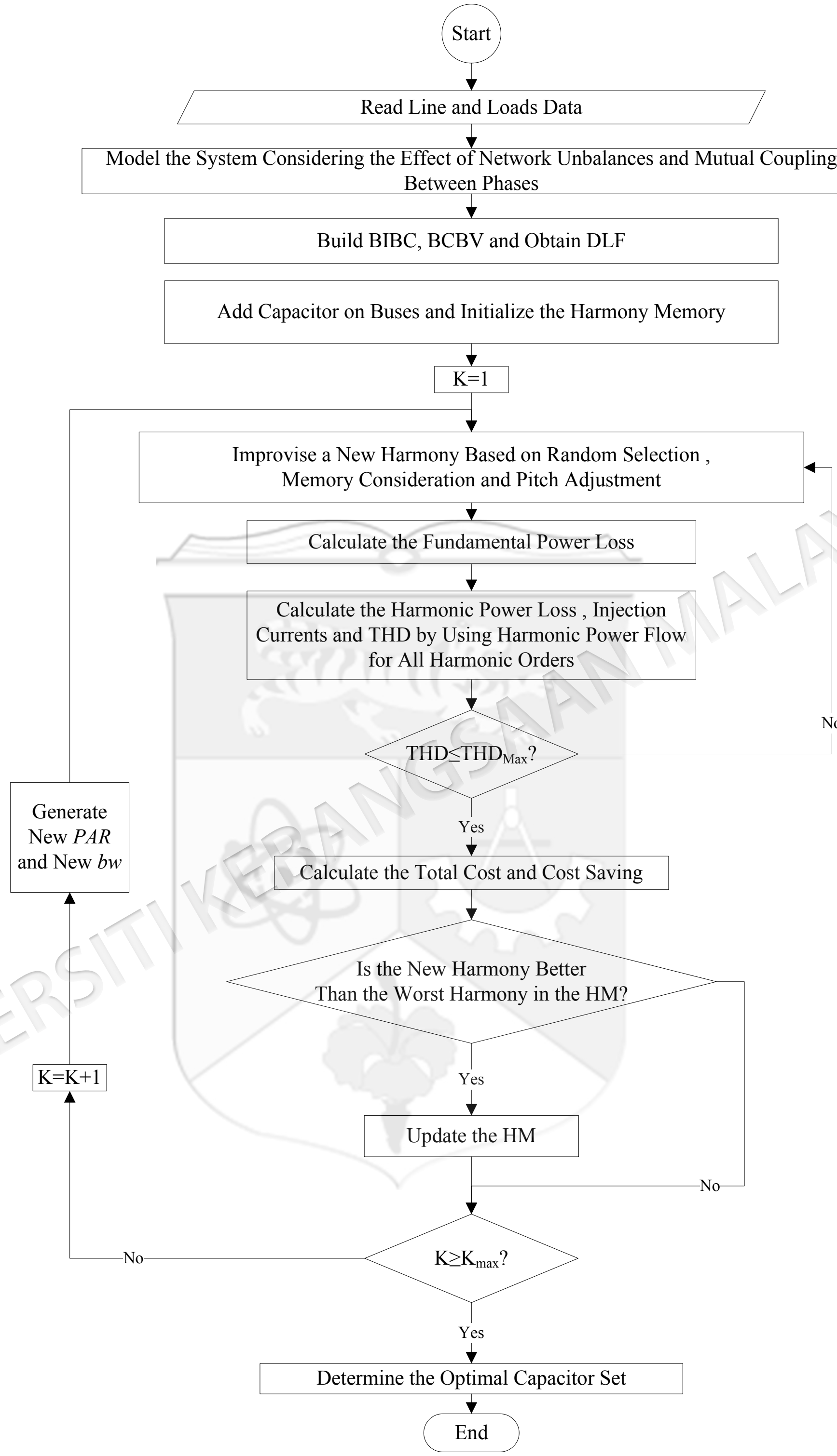

Figure 4.7 The IHS algorithm for solving the capacitor placement problem considering mutual coupling, load unbalance and harmonics

4.6.2 Application of GHS Algorithm for Optimal Capacitor Placement in Three Phase Radial Distribution Systems

The GHS algorithm is used together with the backward/forward sweep power flow method and radial harmonic power flow for determining the optimal placement and sizing of capacitors in radial distribution networks for minimizing the power loss and total cost by considering mutual coupling, load unbalance and harmonics. The procedures for implementing the proposed optimal capacitor placement method are described as follows:

i. Input system parameters such as network and harmonics data.
ii. Model the distribution system considering the effect of network unbalance and mutual coupling between the phases.
iii. Build the BIBC and BCBV matrices and compute the DLF matrix for a threephase system.
iv. Randomly add the capacitors for reactive power compensation at the buses. Each capacitor set is considered a harmony vector. The HM arrays are randomly initialized using (3.3). The optimal parameters of the test system, xL_i and xU_i, are assumed to have minimum and maximum values of capacitor sizes in kVar, respectively. The HMS value is assumed to be 10.
v. A new harmony is improvised through position updating and genetic mutation. In this step, the genetic mutation probability is assumed as p_m=0.2.
vi. Run the backward/forward sweep power flow to calculate the bus current injections and bus voltages using (4.12) and (4.13).
vii. Calculate the fundamental power loss using the backward/forward sweep power flow method.
viii. Calculate harmonic power loss, injection currents and THD by using harmonic power flow for all harmonic orders.
ix. Check if $THD_i \leq THD_{\max}$, if yes continue, otherwise, go to step (iv).
x. Calculate power loss and total cost.
xi. The worst harmony in HM is replaced with the new harmony.
xii. Check whether the stopping criterion, maximum generation ≥5000 is satisfied is assessed. If not, return to step (v).

xiii. Determine the optimal capacitor set (best harmony) which gives maximum power loss reduction and maximum cost saving. The optimal capacitor set includes the optimal values of the three phase capacitors at each bus.

Figure 4.8 describes the procedures involved in solving the optimal capacitor placement problem using the GHS algorithm and the backward/forward sweep power flow method in terms of a flowchart.

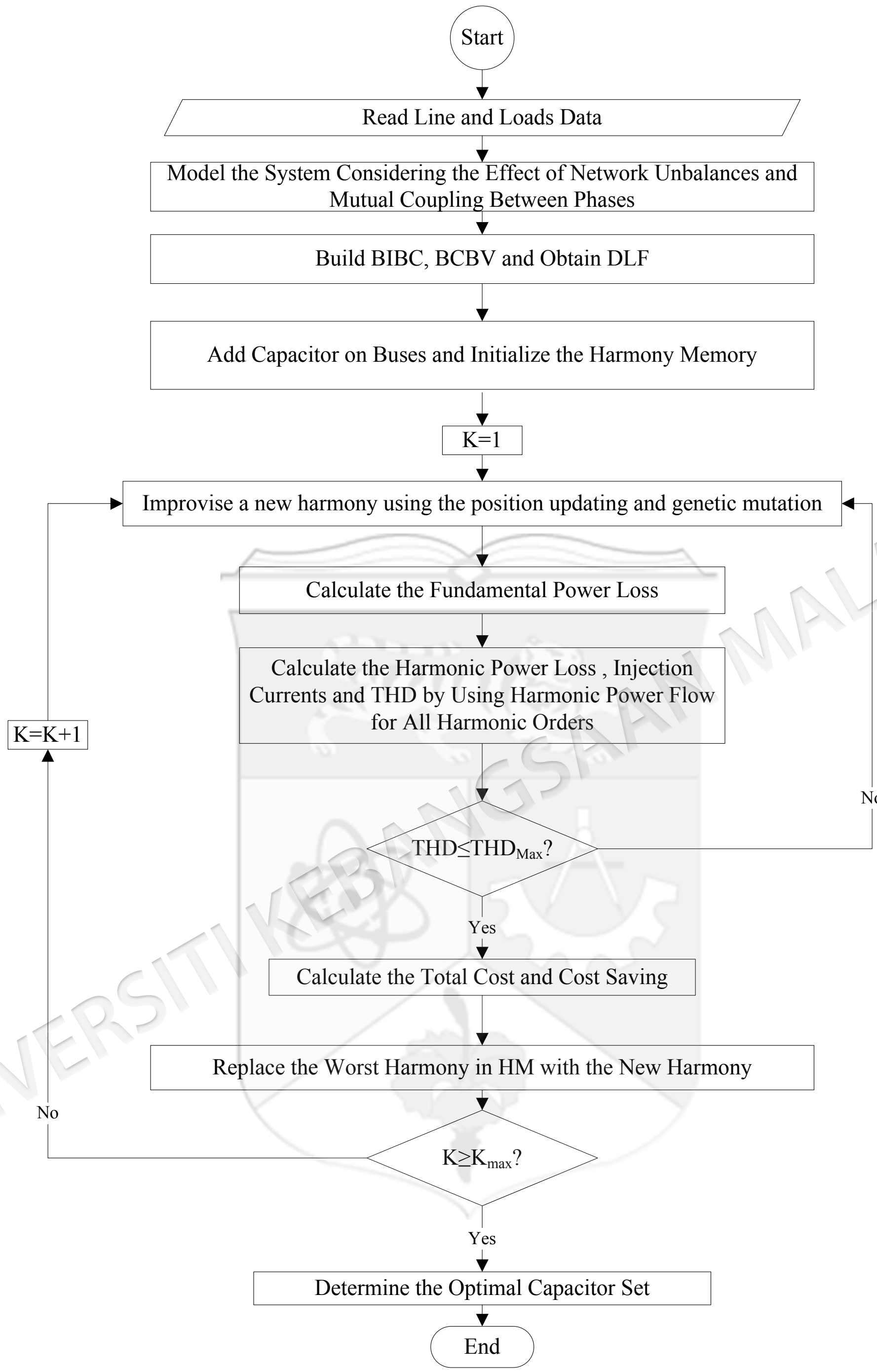

Figure 4.8 The GHS algorithm for solving the capacitor placement problem by considering mutual coupling, load unbalancing and harmonics

4.7 CHAPTER SUMMARY

In this chapter, the application of IHS and GHS algorithms as two novel optimization techniques for determining the optimal location and size of shunt capacitors in radial distribution networks has been presented. These IHS and GHS algorithms are considered as modified HS algorithms that employ new techniques for generating new solution vectors that enhances accuracy and convergence of the conventional HS algorithm. Mutual coupling, load unbalance and harmonics are also taken into account in solving the optimal capacitor placement and sizing problem. The backward/forward sweep power flow method and radial harmonic power flow method are also applied in solving the optimal capacitor placement and sizing problem in both single phase and three phase radial distribution systems.

CHAPTER V

OPTIMAL PLACEMENT AND SIZING OF VAR COMPENSATORS IN TRANSMISSION SYSTEMS

5.1 MODAL ANALYSIS FOR DETERMINING VAR COMPENSATOR PLACEMENT

Modal or eigenvalue analysis of the Jacobian (J) matrix of system load flow equation, near the point of voltage collapse, has been widely used to identify buses vulnerable to voltage collapse and locations for injecting reactive power into the system (Shayegan et al. 2011). The participation of each load in the critical mode determines the importance of the load in voltage collapse. The degree of participation is determined from an inspection of the entries of the left eigenvector of the critical mode. Right eigenvector components indicate the degree to which given variables are involved in a given mode. The use of both left and right eigenvector information leads to the notion of participation factors that indicate which generators should be motivated to inject more active or reactive power into the system (Zhang et al. 2006b). Here, modal analysis is used for determining optimal placement of VAR compensators which are normally installed in power transmission systems for voltage stability improvement.

In the modal analysis method, the Jacobian matrix of the operating point of a power system is calculated (Kundur 1994). For this purpose, the power flow equation linearized around the operating point is considered and given as follows:

$$\begin{bmatrix} \Delta P \\ \Delta Q \end{bmatrix} = \begin{bmatrix} J_{P\theta} & J_{PV} \\ J_{Q\theta} & J_{QV} \end{bmatrix} \begin{bmatrix} \Delta\theta \\ \Delta V \end{bmatrix} \tag{5.1}$$

where ΔP is the incremental change in the bus active power, ΔQ is the incremental change in the bus reactive power, $\Delta\theta$ is the incremental change in the bus voltage angle, and ΔV is the incremental change in the bus voltage magnitude. $J_{p\theta}$, J_{PV}, $J_{Q\theta}$, and J_{QV} are the Jacobian matrix elements representing the sensitivity of the power flow to bus voltage changes.

System voltage stability is affected by both *P* and *Q,* however, at each operating point, *P* can be kept constant and voltage stability can be evaluated by considering the incremental relationship between *Q* and *V*. If the active power *P* is kept constant in (5.1), then $\Delta P = 0$ and (5.1) becomes,

$$\Delta Q = J_R \Delta V \qquad (5.2)$$

where J_R is the reduced Jacobian matrix system given by

$$J_R = [J_{QV} - J_{Q\theta} J_{P\theta}{}^{-1} J_{PV}] \qquad (5.3)$$

The power network modes can be defined by the eigenvalues and eigenvectors of J_R which can be written as

$$J_R = \xi \ \Lambda \ \eta \qquad (5.4)$$

where ξ is the right eigenvector matrix of J_R, η is the left eigenvector matrix of J_R, and Λ is the diagonal eigenvalue matrix of J_R.

The inverse of J_R is then given by,

$$J_R{}^{-1} = \xi \ \Lambda^{-1} \ \eta \qquad (5.5)$$

Substituting (5.5) into (5.2) yields

$$\Delta V = (\xi \ \Lambda^{-1} \ \eta) \ \Delta Q \qquad (5.6)$$

or

$$\Delta V = \sum_i (\frac{\xi_i \ \eta)_i}{\lambda_i} \ \Delta Q \qquad (5.7)$$

where λ_i is the *i*th eigenvalue, ξ_i is the *i*th column right eigenvector of J_R, and η_i is the *i*th row left eigenvector of J_R. λ_i, ξ_i, and η_i define the i_{th} mode of the system. The *i*th modal reactive power variation is given by,

$$\Delta Q_{mi} = \kappa_i \xi_i \qquad (5.8)$$

where k_i is a normalization factor such that

$$\kappa_i^{\ 2} \sum_J \xi_{ij}^{\ 2} = 1 \tag{5.9}$$

and ξ_{ij} is the *j*th element of ξ_i.

The i_{th} modal voltage variation can therefore be written as

$$\Delta V_{mi} = \frac{1}{\lambda_i} \Delta Q_{mi} \tag{5.10}$$

From (5.10), the stability of mode *i* with respect to reactive power changes is defined by the modal eigenvalue, λ_i. Large values of λ_i suggest small changes in the modal voltage for reactive power changes. As the system is stressed, the value of λ_i becomes smaller, and the modal voltage becomes weaker. If the magnitude of λ_i is equal to zero, the corresponding modal voltage collapses because it undergoes an infinite change for a finite reactive power change. A system is therefore defined as voltage stable if all the eigenvalues of J_R are positive. The bifurcation or voltage stability limit is reached when at least one eigenvalue reaches zero, i.e., when one or more modal voltages collapse. If any of the eigenvalues are negative, the system is unstable. The magnitude of the eigenvalues provides a relative measure of the proximity of the system to voltage instability (Kundur 1994; Sharma & Ganness 2007).

The left and right eigenvectors corresponding to the critical modes in the system can provide information concerning the mechanism of voltage instability by identifying the elements involved in these modes. The bus participation factor that measures the participation of the k_{th} bus in the i_{th} mode can be defined as

$$P_{ki} = \xi_{ki}\ \eta_{ik} \tag{5.11}$$

Bus participation factors corresponding to critical modes can predict areas or nodes in the power system susceptible to voltage instability. Buses with large participation factors in the critical mode are the most critical system buses. Thus, by using the modal analysis method, the critical buses can be determined and these buses are considered as suitable location for Var compensators installation.

5.2 PROBLEM FORMULATION FOR OPTIMAL SIZING OF VAR COMPENSATORS

A multi-objective function consisting of shunt Var compensator cost is considered in searching for an optimal solution. This multi-objective function which not only maximizes voltage stability margin but also minimizes voltage deviation, active-power loss and cost which are described as follows:

Active power loss : The total active-power loss in a power system is given by (Pisica et al. 2009) :

$$P_{loss} = \sum_{l=1}^{n} R_l I_l^2 = \sum_{l=1}^{n} \sum_{j=1, i \neq j}^{n} [V_i^2 + V_j^2 - 2V_i V_j \cos(\theta_i - \theta_j)] Y_{ii} \cos\varphi_{ij} \tag{5.12}$$

where n is the number of lines, R_l is the resistance of line l, I_l is the current through line l, V_i and θ_i are the voltage magnitude and angle at node i, respectively, and Y_{ij} and φ_{ij} are the magnitude and angle of the line admittance, respectively.

Voltage deviation : The voltage improvement index of a power system is defined as the deviation from unity voltage magnitude at a bus. Thus, for a given system, the voltage improvement index is given by (Pisica et al. 2009):

$$L_v = \sqrt{\sum_{i=1}^{n} \left(\frac{V_{iref} - V_i}{V_{iref}} \right)^2} \tag{5.13}$$

where n is the number of buses, V_{iref} is the reference voltage at bus i, and V_i is the actual voltage at bus i.

Voltage stability margin : From the voltage stability viewpoint, critical modes with the lowest eigenvalues are considered very important. The minimum eigenvalue should be increased to maximize the voltage stability margin (Sharma & Ganness 2007).

Total injected reactive power: The total injected reactive power of Var compensator is given by (Azadani et al. 2008):

$$Q_{ST} = \sum_{j=1}^{ns} Q_j \tag{5.14}$$

where *ns* is the number of Var compensators, and Q_j is the injected reactive power of the Var compensators.

Investment cost: Shunt Var compensators are expensive devices and therefore the investment cost for installing such controllers must be considered to justify the economic viability of the devices. The total cost also depends on the size of fixed and controlled portion of the shunt controllers. The FACTS equipment cost represent only half of the total FACTS project cost. Other costs like civil works, installation, commissioning, insurance,engineering and project management constitute the other half of the FACTS project cost.

5.2.1 Operational Constraints

The objective of using shunt Var compensator is to control system variables such as the real and reactive line power flows and bus voltages, and therefore the following constraints are considered:

Power flow balance equations: The balance of active and reactive powers must be satisfied at each bus. Power balance with respect to a bus can be formulated as (Pisica et al. 2009) :

$$P_{Gi} - P_{Li} = V_i \sum_{j=1}^{b} [V_j [G'_{ij} \cos(\delta_i - \delta_j) + B'_{ij} \sin(\delta_i - \delta_j)]] \tag{5.15}$$

$$Q_{Gi} - Q_{Li} = V_i \sum_{j=1}^{b} [V_j [G'_{ij} \sin(\delta_i - \delta_j) - G'_{ij} \sin(\delta_i - \delta_j)]] \tag{5.16}$$

where P_{Gi} and Q_{Gi} are the generated active and reactive powers and P_{Li} and Q_{Li} are the load active and reactive powers at node i. The conductance G'_{ik} and the susceptance B'_{ik} represent the real and imaginary components of element Y'_{ij} of the $[Y'_{bb}]$ matrix, which are obtained by modifying the initial nodal admittance matrix.

Power flow limit: The apparent power that is transmitted through a branch l must not exceed its limiting value, $S_{l\,\max}$, which represents the thermal limit of a line or transformer in steady-state operation:

$$S_l \leq S_{l\max} \tag{5.17}$$

Bus voltage limits: For several reasons, such as stability and power quality, the bus voltages must be maintained within limits around its nominal value which is given by

$$V_{i\min} \leq V_{inom} \leq V_{i\max} \tag{5.18}$$

In practice, the accepted deviation can reach up to 10% of the nominal voltage value (IEEE Std 18-1992).

5.2.2 Fitness Function

The fitness function for solving the optimal sizing of Var compensator problem is calculated using the objective functions described in Section 5.2. The constraints of this problem do not explicitly contain the variables. Therefore, the effect of the constraints must be included in the fitness function value. The constraints are separately checked, and the violations are handled using a penalty function approach. Incorporating all of the constraints in the same mathematical function is impossible because the three objectives are different. Thus, an overall fitness function, in which each objective function is normalized with respect to the base system without a Var compensator, is considered. This fitness function is given by,

$$f(x) = \omega_1 \frac{P_{loss}}{\sum \Delta Loss_{base}} + \omega_2 \frac{L_v}{\sum \Delta V_{base}} + \omega_3 \frac{\lambda_{Crtical(base)}}{\lambda_{Critical}} + \omega_4 \frac{Cost_{shunt}}{Cost_{Max}}$$

$$- \chi_1 . \sum_{i=1}^{nr} bal_i - \chi_2 . \sum_{k=1}^{n} thermal_k - \chi_3 . \sum_{k=1}^{n} voltage_k \tag{5.19}$$

Subject to:

$$\omega_1 + \omega_2 + \omega_3 + \omega_4 = 1$$
$$0 < \omega_1, \omega_2, \omega_3, \omega_4 < 1 \tag{5.20}$$

where P_{loss}, L_{v}, $\lambda_{\text{Critical}}$, and $Cost_{\text{shunt}}$ are the total active power loss, voltage deviation index, smallest eigenvalue, and total Var compensator cost, respectively. ω_1, ω_2, ω_3, and ω_4 are the coefficients of the corresponding objective functions, $\sum \Delta Loss_{base}$ is the total active power loss in the network of the base system, $\sum V_{base}$ is the total voltage deviation of the base system , $\lambda_{\text{Critical(base)}}$ is the smallest eigenvalue of the base case, and $Cost_{\text{Max}}$ is the maximum cost.

The bal_i element in (5.19) is a factor equal to 0 if the power balance constraint at bus i is not violated; otherwise, bal_i is equal to 1. The sum of these violations represents the total number of buses in the network that do not follow constraints (5.15) and (5.16). This sum is multiplied by a penalty factor that increases the fitness function to an unacceptable value, which results in an unfeasible solution that must be discarded. The second and third sums in the fitness function represent the total number of violations of constraints (5.17) and (5.18), respectively, and are also multiplied by penalty factors. The last three sums in this fitness function are the measures of unfeasibility for each candidate solution. The penalty factors used in this study are χ_1, χ_2, and χ_3, and each is set to a value equals to 100 (Pisica et al. 2009).

5.3 OPTIMAL PLACEMENT AND SIZING OF SVC USING IHS AND GHS ALGORITHMS

The problem of optimal SVC placement and sizing in transmission systems is decomposed into two sub-problems. First, using the modal analysis method to determine the critical system buses (i.e., buses with large participation factors) and these buses are considered as suitable location for SVC installation. The optimal placement of SVC at the suitable buses is found by using the IHS and GHS algorithms in which the optimal SVC set $\{Q^{svc}_{1,\ldots}, Q^{svc}_{i,\ldots,} Q^{svc}_{N}\}$ leads to a maximum power loss reduction, minimum voltage deviation, maximum eigenvalue in critical mode and maximum cost saving. The formulation for the total SVC cost in US$/kVar is given by (Hsiao et al. 1993):

$$C_{SVC} = \sum_{k=1}^{n} 0.0003 Q_k{}^2 - 0.3051 Q_k + 127.38 \tag{5.21}$$

where Q_k is the reactive power capacity of k^{th} installed SVC, in MVar.

5.3.1 Application of IHS Algorithm for Optimal Placement and Sizing of SVCs

The procedures for implementing the IHS algorithm for determining optimal placement and sizing of SVC are described as follows:

i. Input system parameters such as bus, branch and generator data.

ii. Calculate the Jacobian matrix and eigenvalues of the system at base case.

iii. Calculate eigenvectors and bus participation factors for the smallest eigenvalue.

iv. Determine buses with large participation factors and consider them as possible locations for SVC installation.

v. Randomly place SVC for reactive power compensation at the allowed buses. Calculate total power loss, voltage deviation and total cost, respectively. Each SVC set is considered as the harmony vectors. Initialize the arrays of HM randomly using (3.3). The number of columns in the HM is equal to number of buses in the test system. In this case, the optimal parameters of the test system, xL_i and xU_i are assumed to have minimum and maximum of SVC size in MVar, respectively. The HMS is assumed 10.

vi. Improvise a new harmony using the three rules of random selection, memory consideration and pitch adjustment. In this step, the optimal parameters are selected as: HMCR = 90% , PAR_{max}= 0.99, $\mathrm{PAR}_{\mathrm{min}}$= 0.4, bw_{max}=1 , bw_{min}=0.0001 and NI = 5000. These optimal parameters lead to the best trade-off between accuracy and speed of optimization.

vii. Run power flow to calculate the bus voltages.

viii. Calculate power loss, voltage deviation, eigenvalues and total cost.

ix. Check if the SVC set (new harmony) gives lower fitness function value than the worst harmony in the HM. If yes, the worst harmony is replaced with the new harmony in the HM. Otherwise, generate new *PAR* and new *bw* using (3.7) and (3.8), respectively and then go to step (vi).

x. Determine the optimal SVC set (best harmony) which gives maximum power loss reduction, minimum voltage deviation, maximum voltage stability enhancement and maximum cost saving.

Figure 5.1 describes the procedures involved in solving the optimal SVC placement problem using the IHS algorithm.

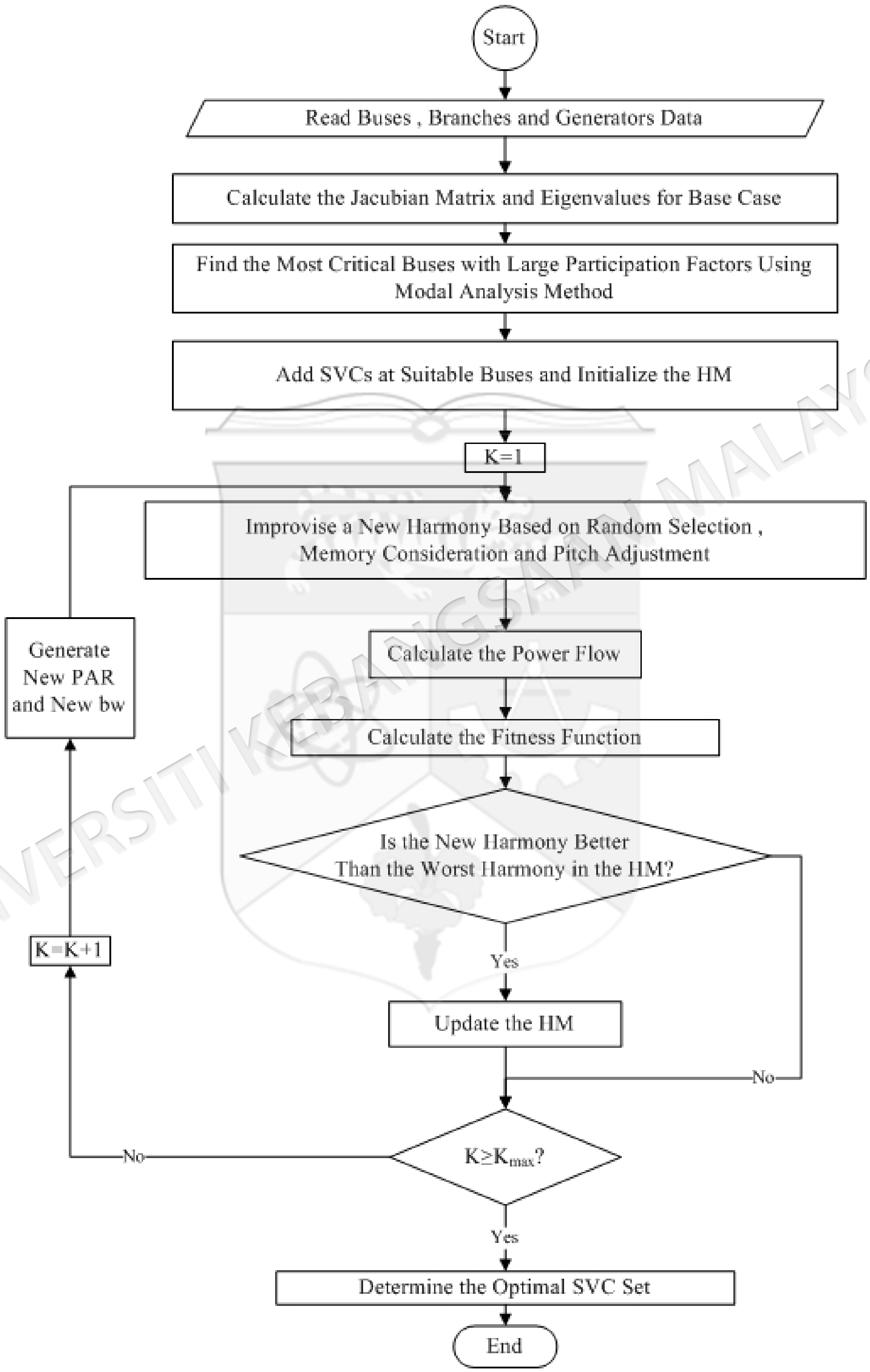

Figure 5.1 The IHS algorithm for solving the SVC placement problem

5.3.2 Application of GHS Algorithm for Optimal Placement and Sizing of SVCs

The procedures for implementing the GHS algorithm for the optimal placement and sizing of SVCs are described as follows:

i. Input the system parameters such as bus, branch, and generator data.
ii. Form the Jacobian matrix and calculate the eigenvalues for the base case.
iii. Calculate eigenvectors and bus participation factors for the smallest eigenvalue.
iv. Determine buses with large participation factors and possible buses for SVC installation.
v. Inject randomly Q^{SVC} at the buses with SVC. Calculate the total power loss, voltage deviation, smallest eigenvalue and total cost. Each SVC set is considered a harmony vector. The HM arrays are randomly initialized using (3.3). The number of columns in the HM is equal to the number of buses in the test system. The optimal parameters of the test system, xL_i and xU_i, are assumed to have minimum and maximum values of SVC size in MVar, respectively. The HMS value is assumed to be 10.
vi. Improvise a new harmony through position updating and genetic mutation. In this step, the genetic mutation probability is assumed as p_m=0.2.
vii. Run the power flow program to calculate power loss, voltage deviation and the eigenvalues.
viii. Calculate the total cost using (5.21).
ix. Calculate the objective function using (5.19).
x. Replace the worst harmony in HM with the new harmony.
xi. Evaluate whether the stopping criterion (maximum generation ≥5000) is satisfied. If not, return to step (vi) and repeat the procedure.
xii. The optimal SVC set (i.e., the best harmony) that provides the maximum power loss reduction, minimum voltage deviation, maximum voltage satiability enhancement, and minimum total cost is determined.

Figure 5.2 shows a schematic diagram of the procedures used in solving the optimal SVC placement and sizing problem using modal analysis and the GHS algorithm.

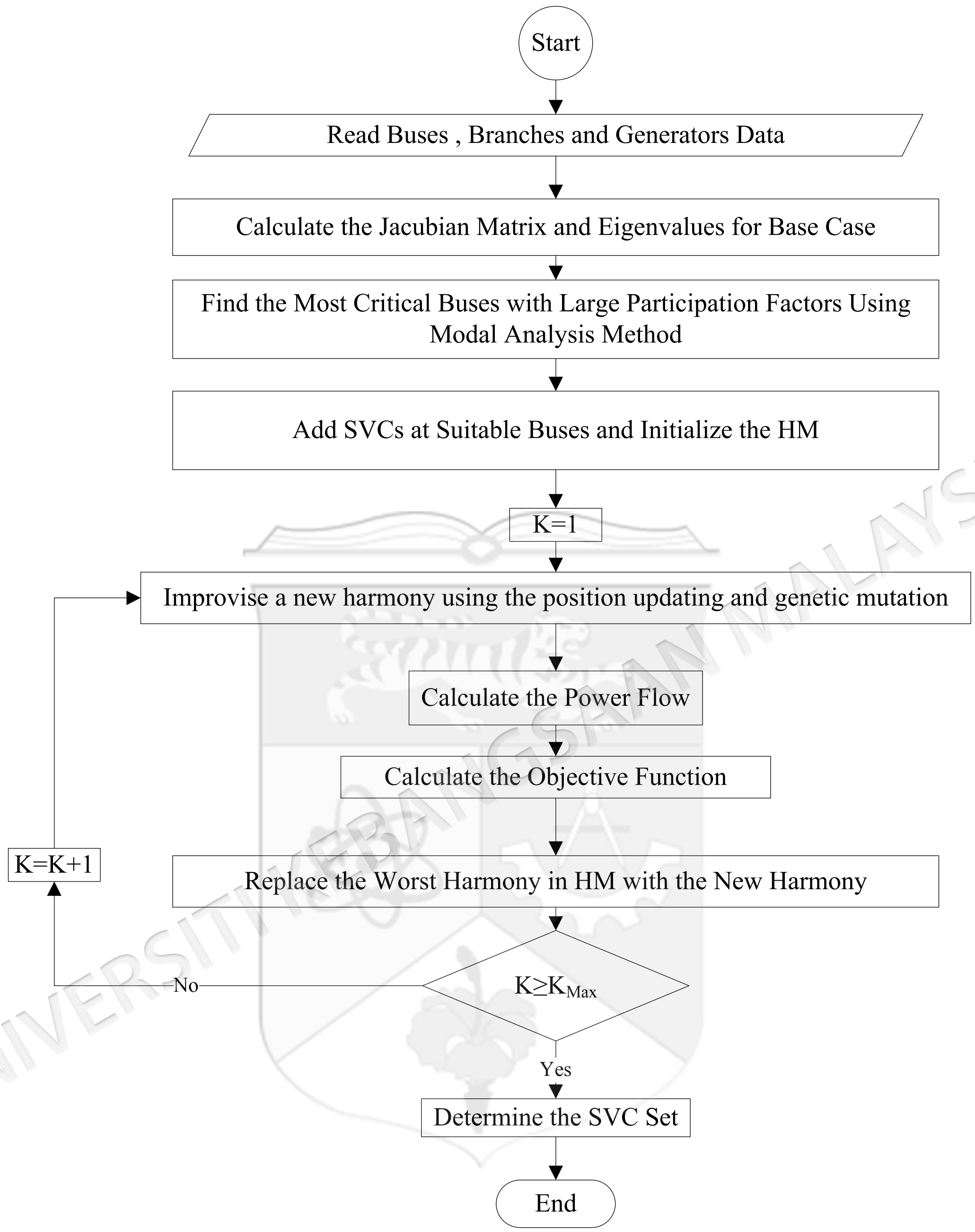

Figure 5.2 Procedures used in solving the optimal SVC placement and sizing problem using modal analysis and the GHS algorithm

5.4 OPTIMAL STATCOM PLACEMENT AND SIZING METHOD

STATCOM is an expensive device and therefore optimum placement and sizing of only one STATCOM in a transmission system is considered. For calculating the cost of STATCOM there is no specific equation like the SVC (Azadani et al. 2008). Hence, the fourth objective function component in Eq.(5.19) has been defined to having the minimum possible STATCOM sizes regarding to the control of STATCOM, instead of considering the total STATCOM cost (Azadani et al. 2008). Since only one STATCOM has been considered, it is reasonable that:

$$\underbrace{\frac{Cost_{ST}}{Cost_{MAX}} \cong \frac{Q_{ST}}{Q_{ST\max}}}_{For\ One\ STATCOM} \qquad (5.22)$$

where Q_{ST} is the STATCOM size and Q_{STmax} is the maximum possible STATCOM size.

Thus, the fitness function in Eq.(5.19) has been redefined by considering STATCOM size. The new fitness function is given by

$$f(x) = \omega_1 \frac{P_{loss}}{\sum \Delta Loss_{base}} + \omega_2 \frac{L_v}{\sum \Delta V_{base}} + \omega_3 \frac{\lambda_{Crtical(base)}}{\lambda_{Critical}} + \omega_4 \frac{Q_{ST}}{Q_{ST\max}} - \chi_1 . \sum_{i=1}^{nr} bal_i - \chi_2 . \sum_{k=1}^{n} thermal_k - \chi_3 . \sum_{k=1}^{n} voltage_k \qquad (5.23)$$

In the optimum STATCOM placement and sizing method, modal analysis method is first used to determine the critical system buses which are buses with large participation factors. These buses are considered as possible locations for STATCOM installation. Next, the optimal placement and sizing of only one STATCOM among the candidate buses is found by using the IHS and also the GHS algorithms in which the optimal STATCOM set {0,0,…., Q^{ST}_i ,….,0,0} leads to maximum power loss reduction, minimum voltage deviation and maximum eigenvalue in critical mode while considering the STATCOM size.

5.4.1 Application of IHS Algorithm for Optimal Placement and Sizing of STATCOM

The procedures for implementing the IHS algorithm in determining optimal placement and sizing of STATCOM are shown in Figure 5.3 and described as follows:

i. Input system parameters such as bus, branch and generator data.
ii. Calculate the Jacobian matrix and eigenvalues for the base case.
iii. Calculate eigenvectors and bus participation factors for the smallest eigenvalue.
iv. Find buses with large participation factors and consider them as possible locations for STATCOM installation.
v. Randomly add one STATCOM for reactive power compensation at the bus among the candidate buses. Calculate the total power loss, voltage deviation and eigenvalues. Each STATCOM set is considered as a harmony vector. Initialise the arrays of the HM randomly using (3.3). The number of columns in the HM is equal to number of buses in the test system. The optimal parameters of the test system, xL_i and xU_i, are assumed to have minimum and maximum values of STATCOM size in MVar, respectively. The HMS is assumed to be 10.
vi. Improvise a new harmony using the three rules of random selection, memory consideration and pitch adjustment. In this step, the optimal parameters are assumed as follows: HMCR = 90%, PAR_{max}= 0.99, PAR_{min}= 0.4, bw_{max}=1, bw_{min}=0.0001 and NI = 5000.
vii. Run the power flow program to calculate the bus voltages.
viii. Calculate power loss, voltage deviation and eigenvalues.
ix. Check if the STATCOM set (i.e., the new harmony) has a lower fitness function value than the worst harmony in the HM. If yes, the worst harmony is replaced with the new harmony in the HM. Otherwise, generate a new *PAR* and *bw* using (3.7) and (3.8), respectively, and return to step (vi).
x. Determine the optimum STATCOM placement and sizing that provides maximum power loss reduction, maximum voltage stability enhancement and minimum voltage deviation.

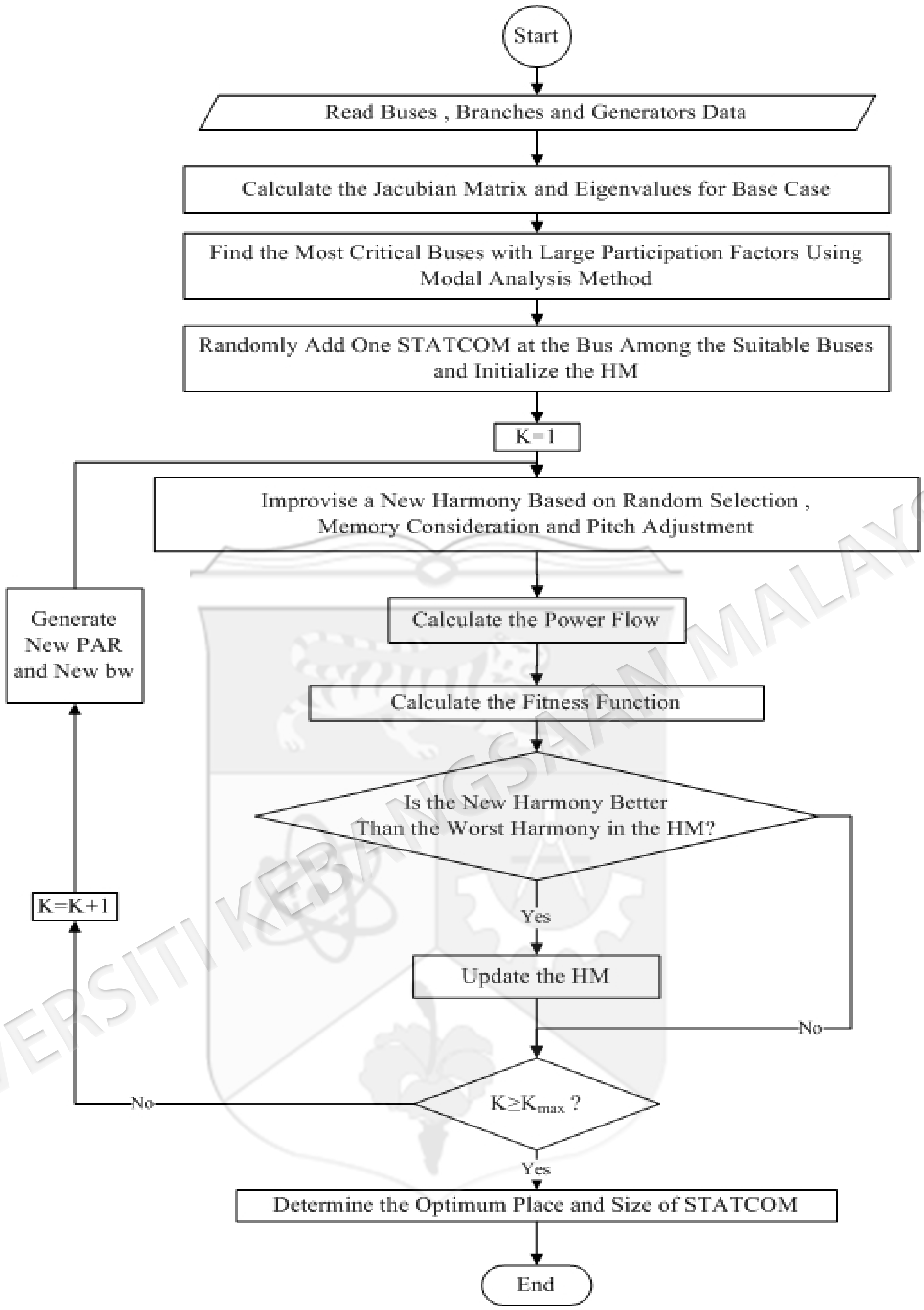

Figure 5.3 Procedures used in solving the optimal STATCOM placement and sizing problem using modal analysis and the IHS algorithm

5.4.2 Application of GHS Algorithm for Optimal Placement and Sizing of STATCOM

The procedures for implementing the GHS algorithm in the optimal placement and sizing of STATCOM are described follows:

i. Input the system parameters such as bus, branch, and generator data.
ii. Form the Jacobian matrix and calculate the eigenvalues for the base case.
iii. Calculate the eigenvectors and determine bus participation factors for the smallest eigenvalue.
iv. Determine buses with large participation factors and consider these buses as possible locations for STATCOM installation.
v. Randomly add one STATCOM for reactive power compensation at the bus among suitable buses. Each STATCOM set is considered a harmony vector. The HM arrays are randomly initialized using (3.3). The number of columns in the HM is equal to the number of buses in the test system. The optimal parameters of the test system, xL_i and xU_i, are assumed to have minimum and maximum values of STATCOM in MVar, respectively. The HMS value is assumed to be 10.
vi. Improvise a new harmony through position updating and genetic mutation. In this step, the genetic mutation probability is assumed as p_m=0.2.
vii. Run the power flow program to calculate power loss, voltage deviation, and the eigenvalues.
viii. Calculate the objective function using (5.22).
ix. Replace the worst harmony in HM with the new harmony.
x. Evaluate whether the stopping criterion (maximum generation ≥5000) is satisfied. If not, return to step (vi) and repeat the procedure.
xi. Determine the optimal Var compensator set (i.e., the best harmony) that provides maximum power loss reduction, minimum voltage deviation, maximum voltage satiability enhancement and minimum STATCOM size.

Figure 5.4 shows a schematic diagram of the procedures used in solving the optimal STATCOM placement and sizing problem using modal analysis and the GHS algorithm.

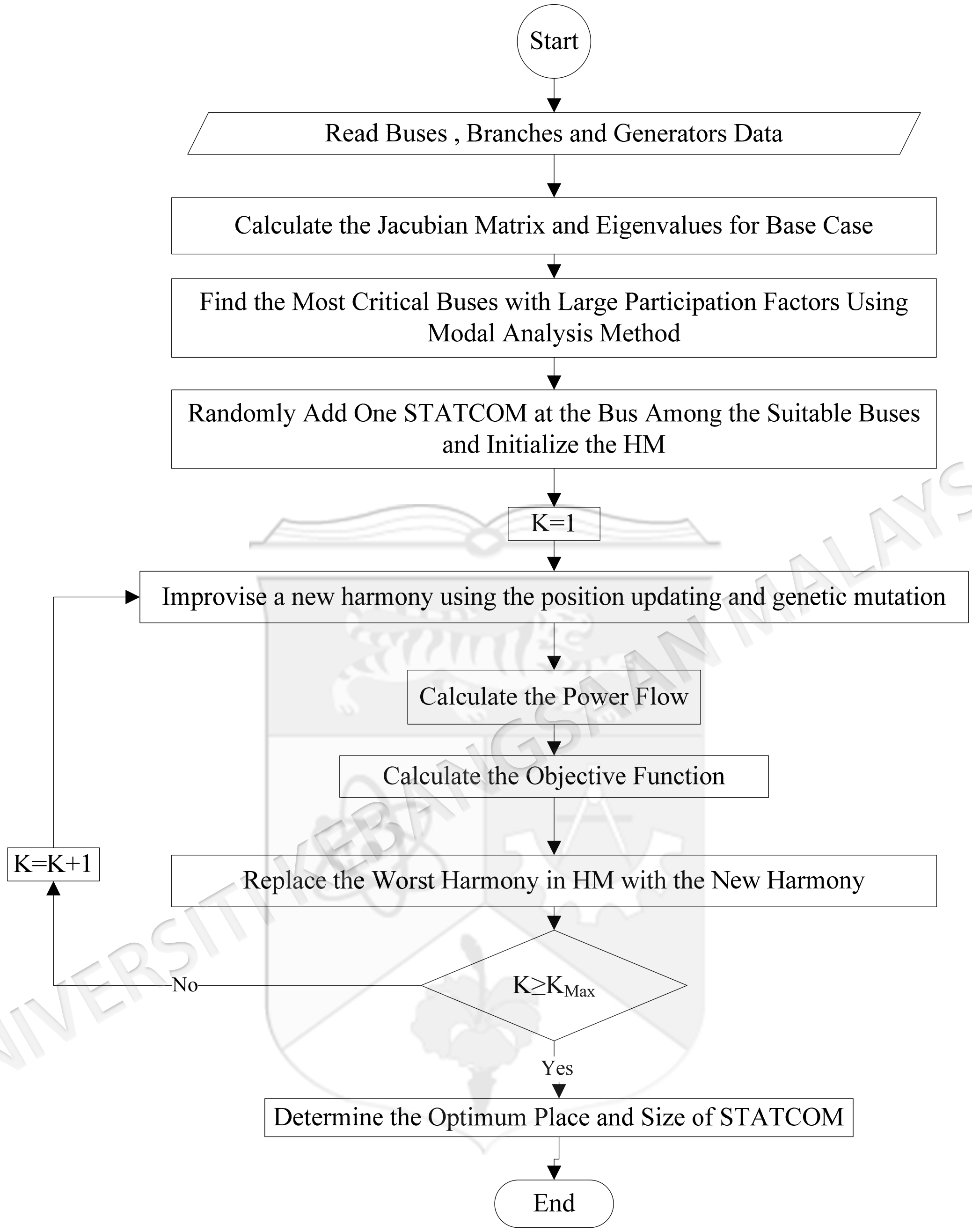

Figure 5.4 Procedures used in solving the optimal STATCOM placement and sizing problem using modal analysis and the GHS algorithm

5.5 SOFTWARE TOOL FOR OPTIMAL PLACEMENT AND SIZING OF SHUNT VAR COMPENSATORS IN POWER SYSTEMS

Due to the limitations of the available power system analysis software tools and lack of heuristic optimization features in these tools, there is a strong motivation for developing a suitable software tool for optimal placement and sizing of shunt Var compensators in distribution and transmission systems incorporating heuristic optimization techniques. For this purpose, a new power system analysis tool called as Optimal Placement of Shunt Var Compensators (OPSVC) has been developed. To date, there is no such power system simulation package developed with features of heuristic optimization algorithms.

The capabilities of the OPSVC are that it can conduct several analyses, such as backward/forward sweep power flow, radial harmonic power flow, optimal placement and sizing of capacitors, SVCs and STATCOMs using different optimization techniques and plotting voltage profile of the studied system before and after installing Var compensators. In this section, the software development of the OPSVC software is discussed by describing the programming language used and the main structure of the software.

5.5.1 Programming Language

The MATLAB programming language is selected to implement the algorithms and routines in the OPSVC software. The MATLAB software which is short for MATrix LABoratory is a powerful and widely used tool for simulation. MATLAB includes tools that allow a program to interactively construct a graphical user interface (GUI) for the program. With this capability, a programmer can design sophisticated data analysis programs that can be operated by relatively inexperienced users (Altintas 2011).

In this work, MATLAB is chosen as the programming tool primarily because it offers several advantages such as graphics facilities, interactive mode of work, simple programming and its wide availability on computing platforms. These factors make Matlab an excellent language for teaching and a powerful tool for solving research and practical problems. MATLAB implements GUI through the graphical user interface development environment (GUIDE) which allows a user to create figure windows containing graphical objects (Altintas 2011). A GUI is a user interface program built with graphical objects such as buttons, text fields, sliders and menus. GUI ensures the communication process between a user and the MATLAB computational engine (Altintas 2011).

5.5.2 Software Structure

All program modules in the OPSVC software have been developed in the MATLAB environment. The step-by-step procedures and calculations involved in the OPSVC are shown in Figure 5.5 and described as follows:

i) Select the power system configuration which is either radial distribution system or transmission system.

ii) Select the test system and the intended analysis. For analysis on a radial distribution system, the analyses include backward/forward sweep power flow, optimal placement and sizing of capacitors without harmonics consideration and optimal placement and sizing of capacitors with harmonics consideration. For analysis on a transmission system, the analyses include power flow, optimal placement and sizing of SVC and optimal placement and sizing of STATCOM.

iii) If the options of optimal placement and sizing of Var compensators are selected, the next steps are to:

  a) Choose the intended optimization technique which may be GA, PSO, HS, IHS and GHS algorithm.
  b) Execute the optimum placement and sizing program.

iv) Display the obtained results and plot the voltage profiles

All the above-mentioned calculations are developed in MATLAB line codes and then integrated with the MATLAB GUI so as to produce a user-friendly interface. The main modules of the OPSVC software are described in Appendix H.

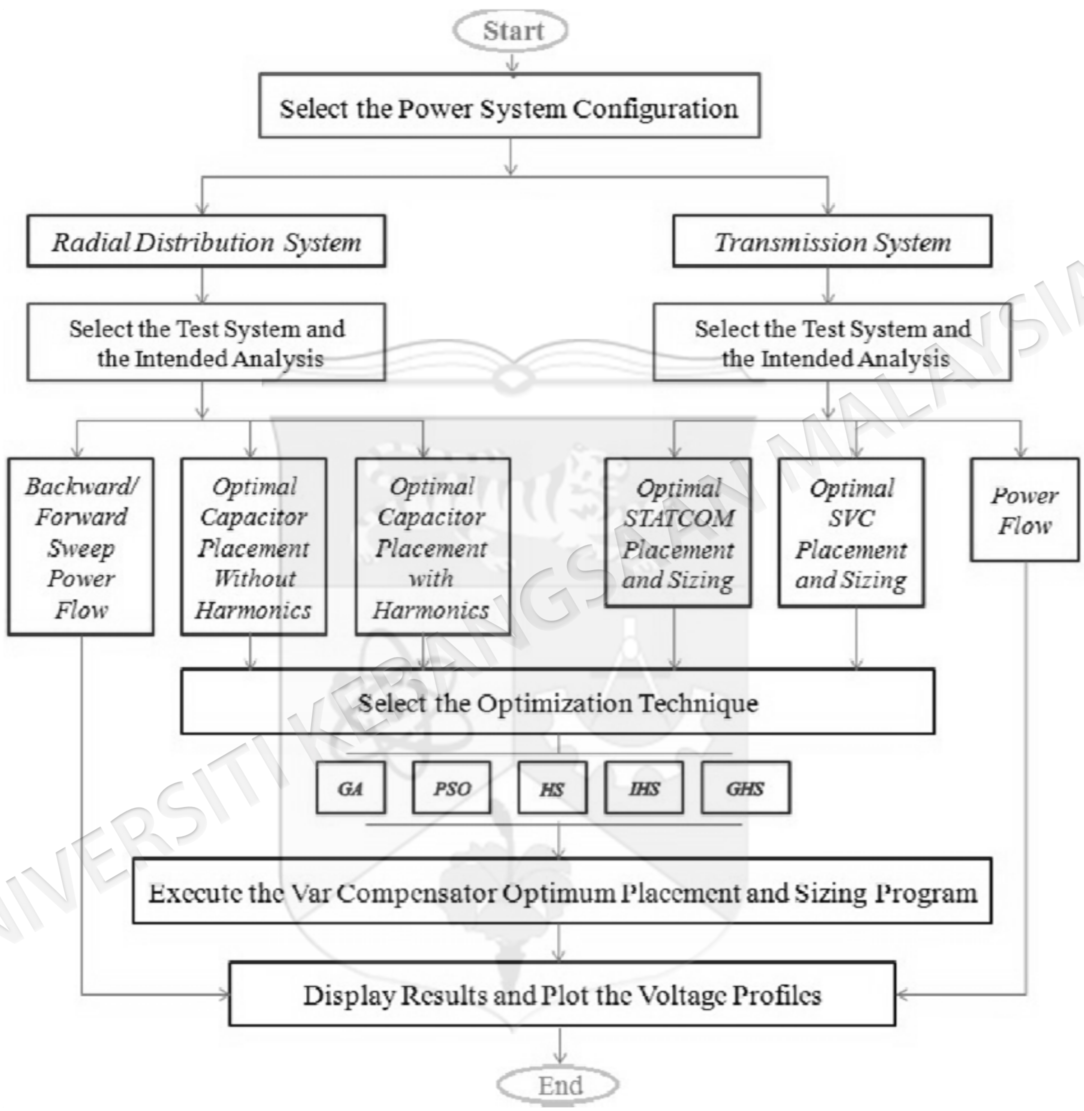

Figure 5.5 Procedure in the OPSVC

5.6 CHAPTER SUMMARY

This chapter presents the application of two heuristic optimization techniques, namely, IHS and GHS algorithms for determining optimal location and size of shunt reactive power compensators such as SVC and STATCOM in a power system. The problem is decomposed into two sub-problems in which the first sub-problem deals with the use of modal analysis method for determining possible locations of SVC or STATCOM. The second sub-problem solves the optimal placement and sizing of SVC or STATCOM by considering a multi-criterion objective function for enhancing voltage stability, improving voltage profile and minimizing power loss and total cost. More over , A MATLAB-based power system software tool incorporated with optimization features, named as OPSVC has been developed for analyzing the optimal placement and sizing of shunt Var compensators in both distribution and transmission systems.

CHAPTER VI

RESULTS AND DISCUSSION

6.1 RESULTS OF OPTIMAL CAPACITOR PLACEMENT AND SIZING IN RADIAL DISTRIBUTION SYSTEMS

The proposed IHS and GHS algorithms have been tested on the 10 bus and 34 bus test systems (Baghzouz & Ertem 1990; Chis et al. 1997; Rao et al. 2011) to evaluate its effectiveness in determining optimal placement of capacitors so as to reduce power loss and total cost. An effective and simple power flow method based on the backward/forward sweep power flow is employed for performing power flow simulations. The performance of the proposed algorithms are also validated on the three-phase 10 bus and 34 bus distribution systems by considering mutual coupling, load unbalance and harmonics. The results of the IHS and GHS algorithms are then compared with the GA, PSO and conventional HS algorithm.

Practical capacitor sizes with the corresponding costs as obtained from Ghose & Goswam (2003) were considered in this study. The relationship between the sizes and yearly costs of the capacitors is as shown in Figure 6.1. Here, the capacitor values are assumed continuous. In this study, the voltage limits are assumed as V_{min}=0.9 p.u. and V_{max}=1.1 p.u. and the equivalent annual cost of power loss (K_P) is selected to be 168 $/(kW-year) (IEEE Std 18-1992).

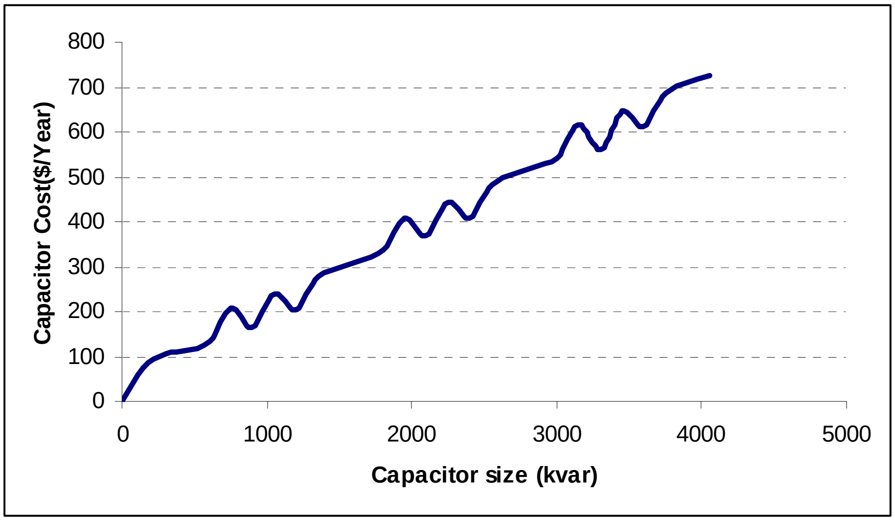

Figure 6.1 Yearly costs of fixed capacitors

6.1.1 Optimal Capacitor Placement Results for the 10 Bus Test System

The performance of the proposed IHS and GHS algorithms in solving the capacitor placement problem is validated on the 10 bus test systems shown in Figure 6.2. The load and line data for the 10 bus system are as shown in Table 6.1.

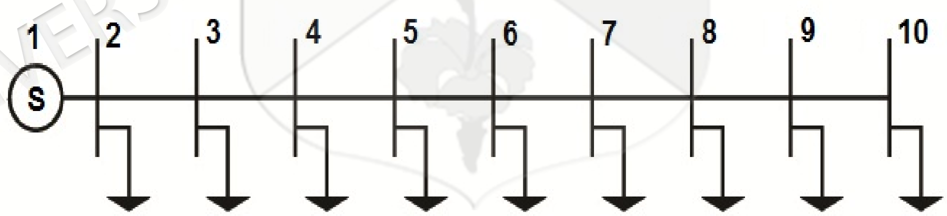

Figure 6.2 The 10 bus test system

The rated line voltage and the total reactive load of the system are 23kV and 4186 kVar, respectively. For reactive power compensation, the maximum capacitor size should not exceed the total reactive load of 4186 kVar (Ghose & Goswam 2003).

Table 6.1 Load and line data of the 10 bus test system

Line No.	Length (Mile)	From, bus i	To , bus i+1	$R_{i,i+1}$ (Ω)	$X_{i,i+1}$ (Ω)	P_L (kW)	Q_L (kVar)
1	0.63	1	2	0.1233	0.4127	1840	460
2	0.88	2	3	0.014	0.605	980	340
3	1.7	3	4	0.7463	1.205	1790	446
4	0.84	4	5	0.6984	0.6084	1598	1840
5	2.3	5	6	1.9831	1.7276	1610	600
6	1.05	6	7	0.9053	0.7886	780	110
7	1.5	7	8	2.0552	1.164	1150	60
8	3.5	8	9	4.7953	2.716	980	130
9	3.9	9	10	5.3434	3.0264	1640	200

Table 6.2 shows the capacitor placement results in terms of capacitor sizes, capacitor locations, power loss, total costs and net saving of the IHS and GHS algorithms compared with the GA, PSO and the conventional HS algorithm. The main objective function of the problem is minimization of total cost which includes power loss cost and capacitor cost. Any reduction in total power loss or total capacitor costs leads to less objective function value. From the results in Table 6.2 , it can be seen that the total capacitor size and also the total capactior cost identified by the IHS and GHS algorithms are greater than GA and the conventional HS algorithm. However, the power loss and total cost is greatly reduced by the IHS algorithm as compared to GA, PSO and conventional HS algorithm. Comparing the results of the IHS and GHS algorithms, the power loss and total cost using the GHS algorithm is lower than the IHS algorithm. In general, the cost saving using the IHS and GHS algorithms are greater than the other optimization techniques.

Table 6.2 Comparison of capacitor placement results of the 10 bus system

Capacitor Location Bus No.	**Before Capacitor Placement**	**Capacitor Size (kVar)**				
		GA	**PSO**	**HS**	**IHS**	**GHS**
2	---	0	0	0	1761	679
3	---	0	3555	294	1636	4042
4	---	0	0	0	1183	0
5	---	1182	4037	2862	1734	2157
6	---	1174	1652	1177	1187	764
7	---	0	0	307	430	0
8	---	0	0	152	0	268
9	---	264	611	138	452	236
10	---	566	0	462	447	314
Total kVar	0	3186	9855	5392	8830	8460
Power Loss (kW)	783.8	696.2	686.0	684.0	668.7	663.4
Power Loss Cost ($/year)	131,675	116,962	115,248	114,912	112,342	111,451
Capacitor Cost($/year)	0	652	1803	1199	1737	1802
Total Cost($/year)	131,675	117,614	117,051	116,111	114,079	113,253
Saving (%)	0	10.7	11.1	11.8	13.4	14.0

6.1.2 Optimal Capacitor Placement Results for the 34 Bus Test System

The proposed IHS and GHS algorithms for solving the capacitor placement problem is also applied on the 34 bus radial distribution systems shown in Figure 6.3. The load and feeder data for the 34 bus system are as shown in Appendix B. The rated line voltage of the system is 11 kV. The results of optimal location and size of shunt capacitors using GA, PSO, HS, IHS and GHS algorithms are shown in Table 6.3.

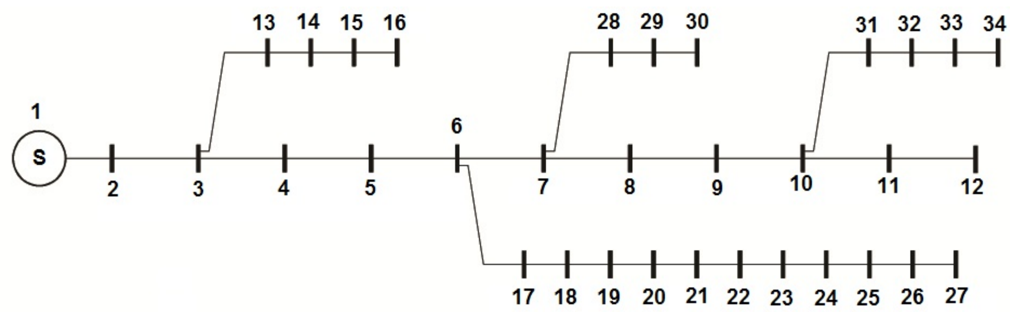

Figure 6.3 The 34 bus test system

Table 6.3 Optimal capacitor placement results of the 34 bus system

Location and Size of Added Capacitors									
GA		**PSO**		**HS**		**IHS**		**GHS**	
Bus	Size (kVar)	Bus	Size (kVar)	Bus	Size (kVar)	Bus	Size (kVar)	Bus	Size (kVar)
8	248	**9**	512	**8**	648	**17**	581	**11**	422
11	751	**19**	781	**19**	1203	**20**	328	**19**	1124
17	288	**20**	479	**20**	197	**22**	794	**20**	276
26	1423	**24**	803	**22**	639	**26**	581	**22**	433

From Table 6.3, it is noted that the optimum location and size of capacitors identified by the different optimization techniques are not the same. Each optimization technique has selected four buses to install the capacitors. It is noted that the voltage magnitudes of all these four buses are lower than 0.97 p.u. based on the power flow results before capacitor placement. This implies that the selected four buses are considered as weak buses with low voltage magnitudes in the system and these buses have been selected by the different optimization techniques for capacitor placement and suitable locations for Var compensation.

Table 6.4 shows a comparison of the optimal capacitor placement results of the IHS and GHS algorithms with the other optimization techniques in terms of power loss, reactive power, capacitor cost, total cost and saving.

Table 6.4 Comparison of capacitor placement results of the 34 bus system

Items	**Before Capacitor Placement**	**GA**	**PSO**	**HS**	**IHS**	**GHS**
Power loss (kW)	221.67	168.8	165.5	161.2	160.2	158.8
Total kVar	0	2710	2575	2687	2284	2255
Capacitor Cost($/y)	0	701.2	636.5	598.7	566.8	556.1
Total Cost ($/y)	37,241	29,060	28,441	27,680	27,480	27,235
Saving (%)	0	22.0	23.6	25.7	26.2	26.9

The results in Table 6.4 show that the GHS algorithm give the greatest reduction in terms of power loss and total costs as compared to GA, PSO, conventional HS and IHS algorithm. In terms of cost saving, the IHS and GHS algorithms give greater saving than the other optimization techniques.

6.1.3 Optimal Capacitor Placement Results for the Unbalanced 10 Bus Test System with Harmonic Consideration

The proposed IHS and GHS algorithms for solving the capacitor placement problem is applied on the three-phase 10 bus distribution system shown in Figure 6.4. This test system is selected for demonstrating the effect of mutual coupling, load unbalance and supply harmonics on the capacitor placement problem.

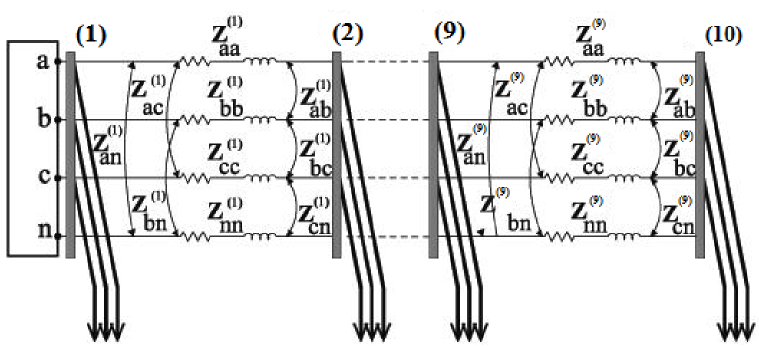

Figure 6.4 The three-phase 10 bus test system

The load data for the unbalanced three-phase 10 bus test system is as shown in Table 6.5. From the table, the load of phase B is 5% higher than the load of phase A and load at phase C is lower by the same percentage, thus keeping the total three-phase loads as in the balanced loading situation (Ghose & Goswam 2003). The line impedances are calculated considering the effect of mutual coupling and the impedance values are as shown in Table 6.6.

Table 6.5 The load data for unbalanced 10 bus test system

Bus No	$P_{L\text{-Phase A}}$ (kW)	$Q_{L\text{-Phase A}}$ (kVar)	$P_{L\text{-Phase B}}$ (kW)	$Q_{L\text{-Phase B}}$ (kVar)	$P_{L\text{-Phase C}}$ (kW)	$Q_{L\text{-Phase C}}$ (kVar)
2	1840	460	1932	483	1748	437
3	980	340	1029	357	931	323
4	1790	446	1879.5	468.3	1700.5	423.7
5	1598	1840	1677.9	1932	1518.1	1748
6	1610	600	1690.5	630	1529.5	570
7	780	110	819	115.5	741	104.5
8	1150	60	1207.5	63	1092.5	57
9	980	130	1029	136.5	931	123.5
10	1640	200	1722	210	1558	190

Table 6.6 Line impedances considering mutual coupling

	Z_{aa}	Z_{bb}	Z_{cc}	Z_{ab}	Z_{ac}	Z_{bc}
R(Ω/mile)	0.7433	0.7526	0.7472	0.1566	0.1536	0.1587
X(Ω/mile)	1.2092	1.1758	1.1959	0.479	0.3865	0.437

In this study, the voltage limits are assumed as V_{min}=0.9 p.u. and V_{max}=1.1 p.u. and the equivalent annual cost of power loss (K_P) is selected to be 168 \$/(kW-year). It is also assumed that the substation voltage contains 3% and 2% of 5-th and 7-th harmonics, respectively (Ghose & Goswam 2003). A harmonic source is at bus 1 and its harmonics data are as shown in Table 6.7. The maximum voltage THD limit is set at 5% (IEEE Std 519-1992).

Table 6.7 The harmonic source data for the unbalanced 10 bus test system

Harmonic Order	1	5	7
Percentage (%)	100	3	2

The optimum shunt capacitor sizes are evaluated by considering harmonic, mutual coupling and load unbalance. Table 6.8 shows the results of optimal capacitor location and size using GHS, IHS and conventional HS algorithms, PSO and GA, by considering mutual coupling, load unbalance and harmonic effects. In this case, power losses at all harmonic orders are added to the fundamental power loss. The results show that by using the GHS algorithm, the total capacitor sizes are the lowest compared to the other optimization techniques and this leads to low capacitor costs.

Tables 6.9 shows a comparison of the optimal capacitor placement results in terms of minimum and maximum voltages, power loss, capacitor cost, total cost and saving. The results of the capacitor placement using the proposed GHS and IHS algorithms are compared with the results using the conventional HS algorithm, PSO, GA and before capacitor placement (BCP). For the case before capacitor placement, no capacitor is installed at any bus in the studied system and no optimization is performed.

From the test results shown in Table 6.9, the following points can be highlighted:

i. The GHS algorithm gives higher voltage magnitudes of both the maximum and minimum bus voltages compared to GA, PSO, conventional HS algorithm and IHS algorithm. Therefore, better voltage improvement can be obtained from the GHS algorithm compared to other optimization techniques.
ii. In terms of power loss and total cost, the GHS algorithm is better than GA, PSO, conventional HS algorithm and IHS algorithm in which the fundamental and total power losses and total cost are greatly reduced.
iii. Comparing the results before and after capacitor placement, it is noted that after implementing optimal capacitor placement, the THD values are less than the THD limit of 5%.

Table 6.8 Capacitor placement results of the unbalanced 10 bus system considering mutual coupling, load unbalance and harmonic effects

Capacitor Location Bus No.	**Capacitor Size (3 phase kVar)**				
	GA	**PSO**	**HS**	**IHS**	**GHS**
2	495	458	157	0	0
3	469	1626	162	1405	0
4	321	1449	1696	632	1356
5	1591	3686	1133	2968	1955
6	1459	0	1215	474	924
7	626	758	1053	0	486
8	0	0	649	760	0
9	472	765	1365	963	477
10	1597	1231	323	484	1808
Total kVar (3-Phase)	21084	29925	23256	23064	21018

Table 6.9 Comparison of results of different optimization techniques for the unbalanced 10 bus system considering mutual coupling, load unbalance and harmonic effects

	BCP	**GA**	**PSO**	**HS**	**IHS**	**GHS**
V_{min} (p.u.)	0.900	0.919	0.929	0.927	0.932	0.934
V_{max} (p.u.)	0.993	0.996	0.997	0.997	0.999	0.999
THD_{max} (%)	5.572	4.89	4.99	4.98	4.98	4.99
Harmonic Power Loss (kW)	97	203	189	178	167	166
Fundamental Power Losses (kW)	3082	2848	2794	2846	2753	2739
Total Power Losses (kW)	3179	3051	2983	3024	2920	2905
Capacitor Cost ($/Year)	0	4578	6021	5091	4818	4332
Total Cost (10^3×$/Year)	534.1	517.2	507.2	513.1	495.4	492.4
Saving (%)	0	3.2	5	3.9	7.2	7.8

6.1.4 Optimal Capacitor Placement Results for the Unbalanced 34 Bus Test System with Harmonics Considerations

Tests were also conducted on the three-phase unbalanced IEEE 34-bus test system shown in Figure 6.5. The IEEE 34-bus test system is an actual distribution system located in Arizona (Carpinelli et al. 2005). For this system, the total number of nodes in the system is 83 and the voltage level of the test network is 24.9 kV. The only substation on the network is located above the node 800. A transformer, 69/24.9 kV is connected between the substation and node 800.

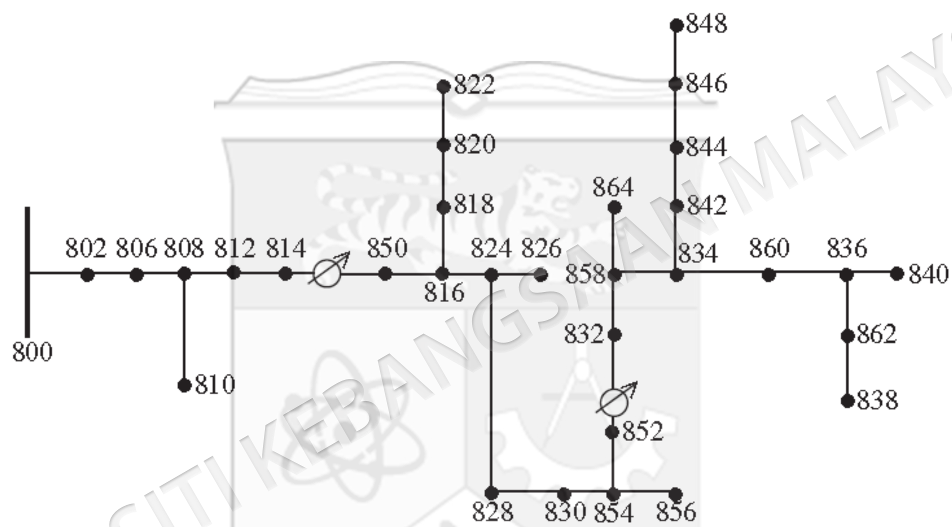

Figure 6.5 Three-phase 34 bus test system

This system contains both single and three phase lines and loads, thus making it suitable for evaluating the proposed optimal capacitor placement method. The single phase lines are lines connected by the nodes; 808–810, 816–818, 818–820, 820–822, 824–826, 854–856, 858–864 and 862–838 while the remaining lines are three phase. The complete network data can be found in Appendix C. The system contains loads that are linear, nonlinear and/or unbalanced. The harmonic producing loads include fluorescent lighting, adjustable speed drives for heat pumps and nonspecific sources such as PCs, TVs, etc. The buses with harmonic producing loads are at nodes; 830, 832, 840, 844, 848 and 860. The harmonic loads are modeled as harmonic current injections which are given in Appendix C. The harmonic load compositions are also given in Appendix C. The load data are chosen so that the voltage distortions do not exceed the IEEE-519 recommended limits before capacitor placement. The voltage distortion limits are assumed as 110% for voltages at the fundamental frequency and 5% for the voltage THD (IEEE Std 519–1992). The optimal location and size of shunt capacitors using GA, PSO, HS, IHS and GHS algorithms are shown in Table 6.10.

Table 6.10 Capacitor placement results of the unbalanced 34 bus system by considering mutual coupling, load unbalance and harmonic effects

Location and Size of Added Capacitors									
GA		**PSO**		**HS**		**IHS**		**GHS**	
Bus	Size (kVar)	Bus	Size (kVar)	Bus	Size (kVar)	Bus	Size (kVar)	Bus	Size (kVar)
806	322	836	455	816	328	808	471	814	613
808	651	840	305	808	635	836	307	836	640
844	486	844	621	844	486	842	612	848	317
860	606	848	611	848	483	848	649	860	313

Form Table 6.10, it is observable that the optimum location and size of capacitors identified by the different optimization techniques are not the same. However, each optimization technique has selected four buses to install the capacitors. Tables 6.11 shows the comparison of the optimal capacitor placement results in terms of minimum and maximum voltages, power loss, capacitor cost, total cost and saving. The results of the optimal capacitor placement using the proposed GHS and IHS algorithms are compared with the results using conventional HS algorithm, PSO, GA and before capacitor placement (BCP).

From the test results shown in Table 6.11, the following points can be summarized:

i. The GHS algorithm gives higher magnitudes for minimum bus voltages compared to GA, PSO, conventional HS and IHS algorithms. Therefore, better voltage improvement can be obtained from the GHS algorithm compared to other optimization techniques.

ii. The GHS algorithm gives lower total power loss and total cost compared to GA, PSO, conventional HS and IHS algorithms.

iii. The voltage THD values of all the optimization techniques are less than 5% after implementing optimal capacitor placement as compared to a voltage THD value of 23.41% before capacitor placement.

Table 6.11 Comparison of results of different optimization techniques for unbalanced 34 bus system by considering mutual coupling, load unbalancing and harmonic effects

	BCP	**GA**	**PSO**	**HS**	**IHS**	**GHS**
V_{min} (p.u.)	0.917	0.922	0.924	0.928	0.930	0.931
V_{max} (p.u.)	0.995	0.997	0.998	0.998	0.999	0.999
THD_{max} (%)	23.41	4.77	4.71	4.88	4.96	4.91
Harmonic Power Loss (kW)	14.7	31.2	25.9	26.7	25.1	24.8
Fundamental Power Loss (kW)	258.3	192.2	191.9	190.6	189.5	189.1
Total Power Loss (kW)	273.0	223.4	217.8	217.3	214.6	213.9
Total kVar	0	6195	5976	5796	6117	5649
Capacitor Cost ($/Year)	0	1553	1496	1484	1545	1508
Total Cost ($/Year)	45,864	39,084	38,087	37,991	37,598	37,443
Saving (%)	0	14.8	17.0	17.2	18.0	18.4

6.1.5 Convergence Characteristics and Accuracy of Different Optimization Techniques for Optimal Placement and Sizing of Capacitors in the Unbalanced 34 Bus System

The accuracy and convergence speed of different optimization techniques in solving the problem of optimal capacitor placement and sizing in radial distribution systems, are compared in this section. The convergence characteristics of the different optimization techniques for the optimal placement and sizing of capacitors in the unbalanced 34 bus test system are shown in Figure 6.6. From the figure, the GHS algorithm converges faster compared with the other optimization techniques.

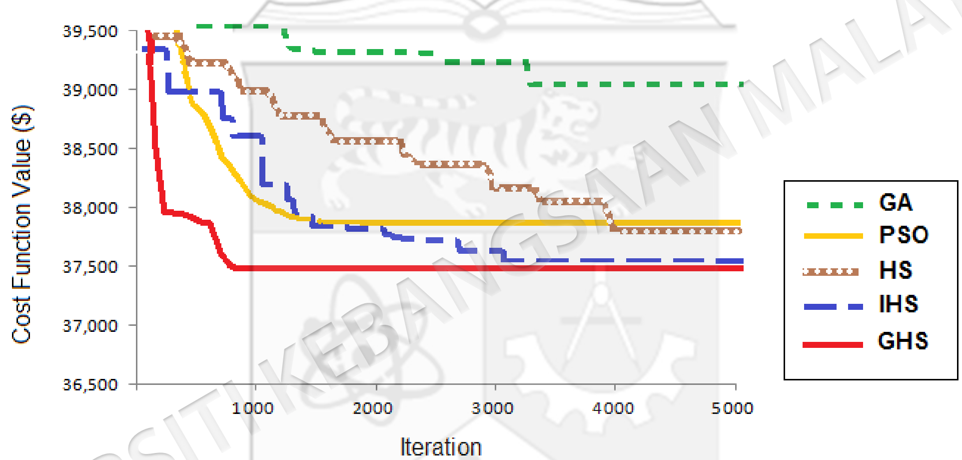

Figure 6.6 Convergence characteristics of different optimization techniques for the optimal placement and sizing of capacitors in the unbalanced 34 bus test system

To evaluate the accuracy of the optimization techniques, consider Table 6.12 which shows the results of the GA, PSO, HS, IHS and GHS algorithms in terms of the minimum, maximum, mean and standard deviation of the cost function values from 50 trials of the aforementioned algorithms. The number of iterations is assumed to be 5000. The optimal GA parameters are selected as follows: population size = 5, crossover= 50% and mutation= 40%. For PSO, the number of particles is set to 5 and the swarm's movability is set to 1.49. Consequently, the optimal parameters of conventional HS algorithm are as follows: HMCR = 90%, PAR=0.4 and bw=0.0001. From Table 6.12, it is observable that the GHS algorithm gives the lowest cost function and standard deviation values compared to other optimization techniques.

This proves that the proposed GHS algorithm for solving the optimal placement and sizing of capacitors in the unbalanced 34-bus test system is more accurate than GA, PSO, conventional HS and IHS algorithms. In terms of computational time, it has been reported that the GHS algorithm notably consumes less average time than the IHS algorithm for solving each problem (Zou et al. 2010 a).

Table 6.12 Accuracy of different optimization techniques for the optimal capacitor placement and sizing for unbalanced 34 bus test system

Cost Function Value ($/Year)	GA	PSO	HS	IHS	GHS
Minimum	39,057.77	38,073.14	37,990.11	37,597.34	37,443.07
Maximum	39,099.12	38,097.81	37,995.97	37,600.18	37,443.35
Mean	39,084.26	38,087.21	37,991.31	37,598.26	37,443.16
Standard Deviation	0.0412	0.0252	0.0051	0.0019	0.0003

6.2 RESULTS OF OPTIMAL SVC PLACEMENT AND SIZING IN TRANSMISSION SYSTEMS

In determining the optimal location and size of SVC in a transmission network , modal analysis is first applied to determine suitable placement of SVC and then IHS and GHS algorithms are applied to determining optimal placement and size of SVC. For the optimization problem formulation, a multi-criterion objective function has been considered to enhance voltage stability, improve voltage profile and minimize power loss and total cost. The results obtained using the proposed IHS and GHS techniques in the 57 bus and 118 bus test systems are compared with other optimization techniques for validation purpose. The 57 bus system shown in Figure 6.7 consists of seven generators with bus 1 as the slack bus, 50 load buses and 80 lines. The system data can be found in Appendix D. At base case condition, the system load is 12.508 p.u. and the system power loss is 28.41 MW (Power Systems Test Case Archive).

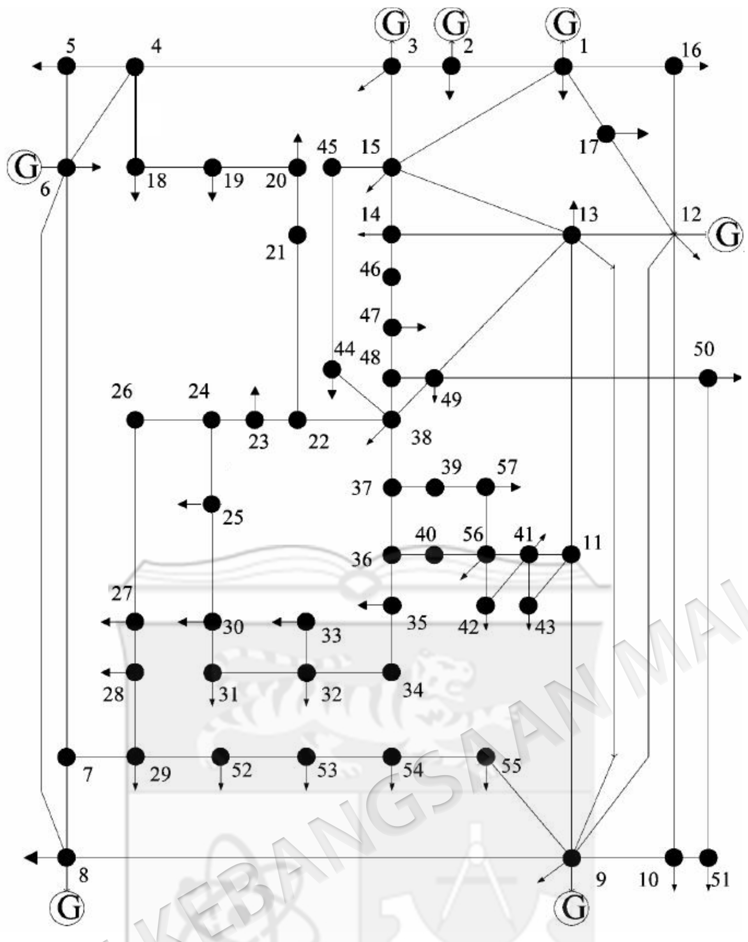

Figure 6.7 Network configuration of the IEEE 57 bus test system

The 118-bus system consists of 54 generators (in which one is the slack node), 64 load buses and 186 lines. The system power loss is 132.86 MW and the system data can be found in Appendix E (Power Systems Test Case Archive).

6.2.1 Optimal SVC Placement Results for the 57 Bus Test System

The eigenvalues of the reduced Jacobian matrix are first generated to obtain the relative proximity of the system to voltage instability. The bus participation factors are then generated for the critical mode to identify the critical buses in the system. The smallest eigenvalue for this system at base case is found to be 0.2344. The bus participation factor values for the smallest eigenvalue of the reduced Jacobian matrix are calculated for all load buses and sorted as shown in Table 6.13.

Table 6.13 The participation factor values of all load buses in the 57 bus test system

Bus No.	Participation Factor	Bus No.	Participation Factor	Bus No.	Participation Factor
31	0.1833	21	0.0067	52	0.0005
33	0.1744	22	0.0067	14	0.0004
32	0.1704	38	0.0057	53	0.0004
30	0.133	20	0.0043	11	0.0002
25	0.1004	44	0.0041	13	0.0002
34	0.0306	27	0.0038	15	0.0002
35	0.0229	41	0.0038	18	0.0002
40	0.0177	48	0.0037	51	0.0002
36	0.0176	47	0.0031	7	0.0001
24	0.0165	19	0.0024	10	0.0001
39	0.0142	49	0.0024	54	0.0001
37	0.014	28	0.0015	4	0
26	0.0138	46	0.0015	5	0
57	0.0114	50	0.0014	16	0
56	0.0092	45	0.0013	17	0
23	0.0072	43	0.0008	55	0
42	0.0070	29	0.0006		

The bus participation factors measure the participation of each bus to the critical mode and the buses with high participation factor values are considered as the critical buses in the power system which is susceptible to voltage instability. In this study, the first ten buses with high participation factor values are considered suitable for SVC installation. From Table 6.13, the suitable buses for SVC installation are buses 24, 25, 30, 31, 32, 33, 34, 35, 36 and 40.

The proposed IHS and GHS algorithms were implemented to determine the optimal location and size of SVC devices in the network. In this study, three SVCs are considered for placement at the appropriate buses of the 57 bus system. From the fitness function constraints, it was assumed that each coefficient value, ω_1, ω_2, ω_3, ω_4, must be between 0 and 1 and the summation of all coefficient values must be 1. In this study, it is decided to give equal importance to the coefficient values for power loss reduction (ω_2), voltage profile improvement (ω_3) and voltage stability enhancement functions (ω_4). Taking into consideration that the SVC cost is of less importance than power loss reduction, voltage profile improvement and voltage stability enhancement functions, the coefficient values in the objective function are selected as

$\omega_1=\omega_2=\omega_3=0.3$ and $\omega_4=0.1$ (coefficient for SVC cost). The penalty factors are usually of large values and are assumed as $\chi_1=100$, $\chi_2=100$, and $\chi_3=100$.

The results obtained from the IHS and GHS algorithms are compared with results obtained using the GA, PSO and the conventional HS algorithm. This optimization study is performed with the restriction that the injected reative power, Q does not exceed 20 MVar. The optimal placement and size of SVCs using the five optimisation techniques are shown in Table 6.14.

Table 6.14 Results of optimal SVC placement and size using different optimization techniques for the 57 bus test system

GA		**PSO**		**HS**		**IHS**		**GHS**	
Bus	SVC (MVar)	Bus	SVC (MVar)	Bus	SVC (MVar)	Bus	SVC (MVar)	Bus	SVC (MVar)
31	9.82	30	3.08	30	3.87	31	7.18	31	10.25
32	1.88	33	8.48	31	8.46	32	5.99	32	4.10
34	6.03	34	3.52	32	3.22	33	5.10	33	5.54

From the Table 6.14, the three buses chosen for SVC placement by the IHS and GHS algorithms are not the same as those determined by the GA, PSO and the conventional HS algorithm. The SVCs using the IHS and GHS algorithms are installed at buses 31, 32 and 33. While the SVCs using GA are installed at buses 31, 32 and 34 and using PSO are installed at buses 30, 33 and 34. The SVCs using the conventional HS algorithm are installed at buses 30, 31 and 32. From the Table 6.13, buses 31, 32 and 33 have high bus participation factor values for the smallest eigenvalue of the test system at base case. Thus, the SVC locations determined using the IHS and GHS algorithm are more effective for enhancing the system voltage stability. In addition, the maximum SVC size determined using the IHS and GHS algorithms is installed at bus 31 which is the most critical bus and most susceptible bus to voltage instability.

For a more detailed analysis of the optimization results, Table 6.15 shows the total power loss, voltage deviation, the smallest eigenvalue and SVC cost after installing the SVC devices. Table 6.15 shows that total power loss and total voltage deviation are reduced after installing SVCs using the five optimization techniques. The eigenvalues increment also illustrates that the system voltage stability is enhanced after installing SVCs. From the table, it can be observed that SVC placement using the GHS algorithm gives the lowest fitness function value, lowest total power loss, highest eigenvalue in critical mode, lowest total SVC cost and least voltage deviation compared to the GA, PSO and HS techniques. However, the result of SVC placement using the IHS algorithm in terms of power loss reduction, voltage deviation minimization, voltage stability enhancement and cost minimization is comparable to the GHS algorithm.

Table 6.15 A comparison of objective function components after SVC installation in the 57 bus test system

Objective function	**Base Case**	**GA**	**PSO**	**HS**	**IHS**	**GHS**
Total Power Losses (MW)	28.41	27.74	27.60	27.91	27.48	27.46
Total Voltage Deviation (pu)	0.265	0.172	0.166	0.167	0.158	0.158
Smallest Eigenvalue	0.234	0.287	0.320	0.332	0.345	0.354
SVC Cost (1000 $)	0.0	71.0	73.7	74.4	70.9	63.6
Fitness function value	1.000	0.754	0.721	0.725	0.694	0.685

The voltage profiles and total voltage deviations for all cases are presented in Figure 6.8 and Figure 6.9, respectively. The deviation from unity voltage magnitude at each bus should be reduced to maximize voltage improvement of the power system. Figure 6.8 shows that after installing SVCs at the selected buses, the voltage profile of the system become closer to 1 pu. The results in Fig 6.9 show that although the voltage deviation drops after SVC placement using the five optimisation techniques, the voltage improvement with the IHS and GHS algorithms are not significantly greater than the other optimization techniques. The maximum voltage drop after installing SVCs is occurred in bus 31 which is the most critical bus.

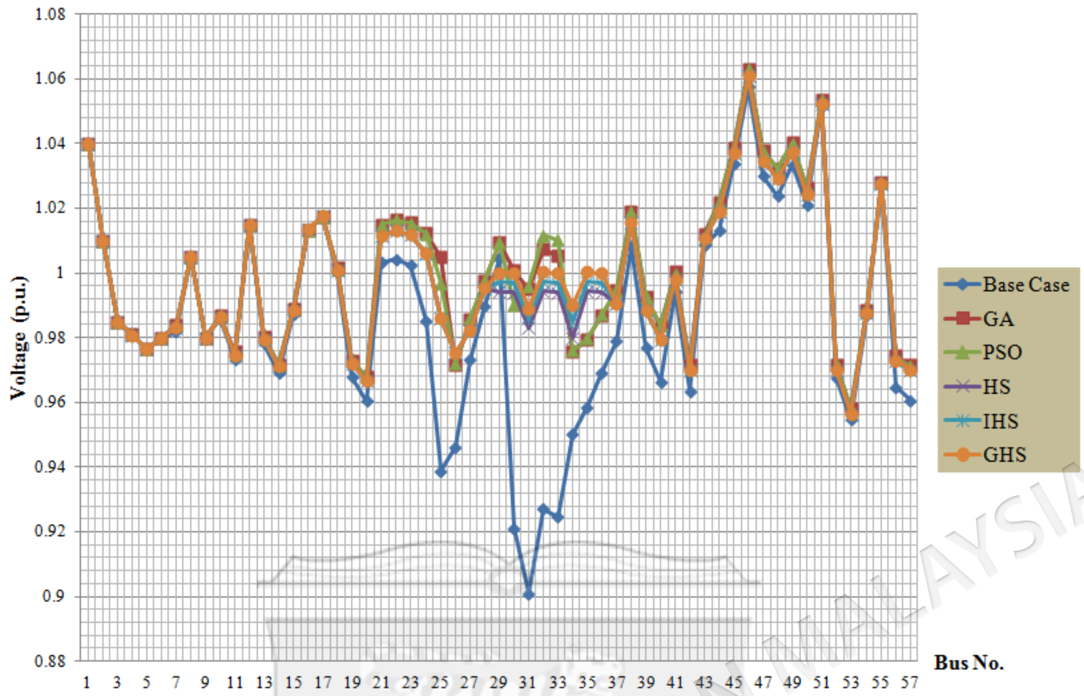

Figure 6.8 Voltage profiles before and after SVC placement in the 57 bus test system

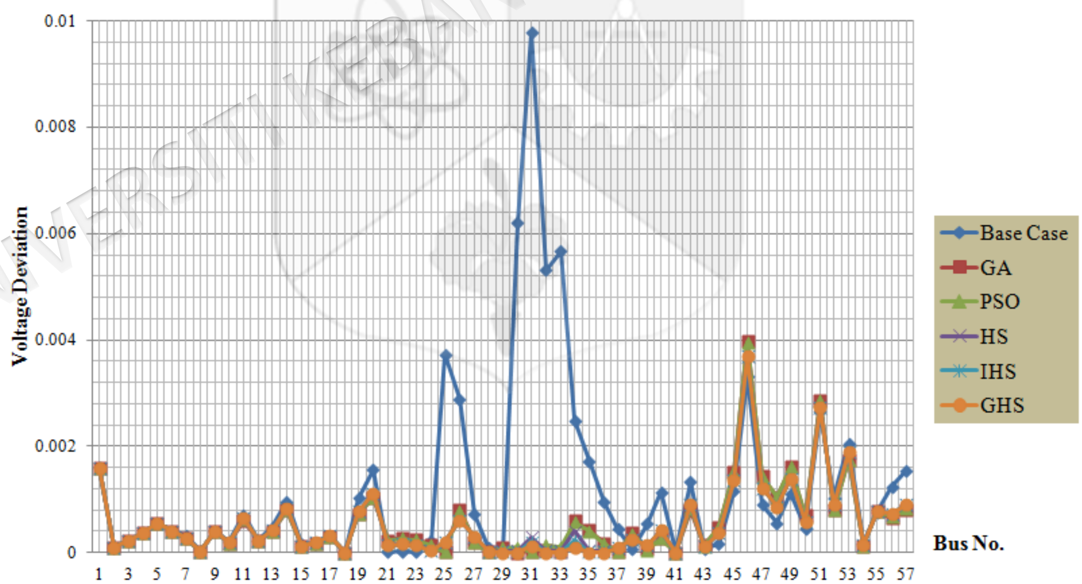

Figure 6.9 Total voltage deviations before and after SVC placement in the 57 bus test system

The convergence characteristics of the different optimization techniques for the optimal placement and sizing of SVCs in 57 bus test system are shown in Figure

6.10. The GHS algorithm not only performs better in finding better solutions, it also converges faster compared with the IHS and other optimization techniques. The optimal parameters of GA are selected as follows: Population Size = 5, Crossover= 50%, Mutation= 40%. For PSO, the number of particles is set to 5 and the swarm's movability is set to 1.49. Consequently, the optimal parameters of conventional HS are selected as follows: HMCR = 90%, PAR=0.4 and bw=0.0001.The number of iterations in all optimization techniques are assumed 5000.

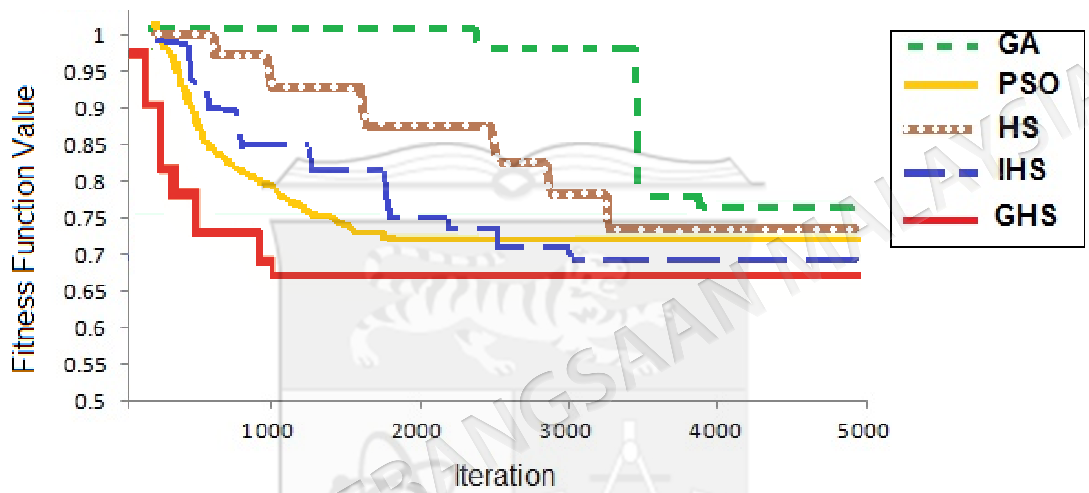

Figure 6.10 Convergence characteristics of different optimization techniques for the optimal placement and sizing of SVCs in the 57 bus test system

For a more detailed analysis of the results, consider Table 6.16 which shows the numerical results of the aforementioned five algorithms. The minimum, maximum, mean and standard deviation of the fitness function values from 50 executions of the GA, PSO, HS, IHS and GHS algorithm are obtained. The number of iterations is assumed 5000. From Table 6.16, it is observable that the minimum, maximum and mean of the fitness function values and standard deviation values using the GHS algorithm are lower than other optimization techniques. The significant difference in the standard deviation values, demonstrate the accuracy of the proposed GHS algorithm in determining optimal placement and sizing of SVCs in the 57 bus test system and that is better than GA, PSO, conventional HS algorithm and IHS algorithm.

Table 6.16 Accuracy of different optimization techniques for the optimal SVC placement and sizing in the 57 bus test system

Fitness Function Value	GA	PSO	HS	IHS	GHS
Minimum	0.7254	0.7205	0.7246	0.6941	0.6849
Maximum	0.7724	0.7284	0.7262	0.6944	0.6851
Mean	0.7541	0.7213	0.7252	0.6943	0.6850
Standard Deviation	4.69e-05	7.83e-05	1.61e-05	2.67e-06	1.22e-07

6.2.2 Optimal SVC Placement Results for the 118 Bus Test System

The smallest eigenvalue of the 118 bus test system at the base case which is without SVC installation is calculated as 3.9425. The bus participation factor values for the smallest eigenvalue of the reduced Jacobian matrix are calculated for all load buses. Among all load buses the bus participation factor values of six buses are sorted and shown in Table 6.17. The bus participation factor values of other load buses are found to be 0. It means that only six buses have participation to the critical mode. From the table, the buses with participation factors correspond to the critical system buses which are at buses 20, 21, 22, 23, 37 and 38. These buses are considered as suitable locations for SVC installation.

Table 6.17 The participation factor values of critical buses in the 118 bus test system

Bus No.	Participation Factor
21	0.4268
22	0.3390
20	0.2274
23	0.0068
37	0.0039
38	0.0014

The proposed IHS and GHS algorithms were implemented to determine the optimal location and size of SVC devices in the network. The coefficient values for the objective functions are assumed to be the same as those in the 57 bus test system. This study is performed with the restriction that the injected Q does not exceed 70 MVar. The results obtained from the IHS and GHS algorithms are compared with results obtained using the GA, PSO and conventional HS algorithm. In this study, three SVCs are considered for placement at the buses with high participation factor values. Table 6.18 shows the results of the optimal location and size of the three SVCs determined by the five optimization techniques mentioned above.

Table 6.18 Results of optimal SVC placement and size using different optimization techniques for the 118 bus test system

GA		**PSO**		**HS**		**IHS**		**GHS**	
Bus	SVC (MVar)	Bus	SVC (MVar)	Bus	SVC (MVar)	Bus	SVC (MVar)	Bus	SVC (MVar)
21	52.45	20	33.08	20	17.78	20	29.12	20	12.11
22	10.46	22	42.18	21	48.36	21	44.22	21	47.25
23	6.17	23	13.12	22	13.22	22	5.34	22	15.47

From the results shown in Table 6.18, the three buses chosen for SVC placement by the HS algorithms are not the same as those determined by the GA and PSO techniques. From the table, the SVC locations determined by the IHS and GHS algorithms at buses 20, 21 and 22 are found to have the largest bus participation factor values. Thus, the SVC locations determined by the IHS and GHS algorithms are more effective for enhancing system voltage stability.

To validate the effectiveness of the IHS and GHS algorithms, the results in terms of total power loss, voltage deviation, smallest eigenvalue and SVC cost after installing the SVC devices are shown in Table 6.19. From the table, it can be observed that the result of SVC placement using the GHS algorithm in terms of power loss reduction, voltage deviation minimization, voltage stability enhancement and cost minimization are better than the IHS and other optimization techniques. In addition, the results show that the GHS algorithm gives the lowest fitness function value compared to the other optimization techniques and this verifies the accuracy of the GHS algorithm in solving the SVC optimal placement and sizing problem.

Table 6.19 A comparison of objective function components after SVC installation in the 118 bus test system

Objective function	Base Case	GA	PSO	HS	IHS	GHS
Total Power Losses (MW)	132.86	132.49	131.30	131.54	130.81	130.03
Total Voltage Deviation (pu)	0.294	0.268	0.265	0.268	0.263	0.261
Smallest Eigenvalue	3.943	5.173	5.217	5.245	5.253	5.265
SVC Cost (1000 $)	0	1163	1139	1113	1090	1036
Fitness function value	1.000	0.842	0.838	0.839	0.837	0.834

The voltage profiles and total voltage deviations for all cases are presented in Figure 6.11 and Figure 6.12, respectively. Figure 6.11 shows that after installing SVCs, the voltage profile of the system become closer to 1 pu. The results in Figure 6.12 show that although the voltage deviation drops after SVC placement, the voltage improvements with the IHS and GHS algorithms are not significantly greater than the other optimization techniques.

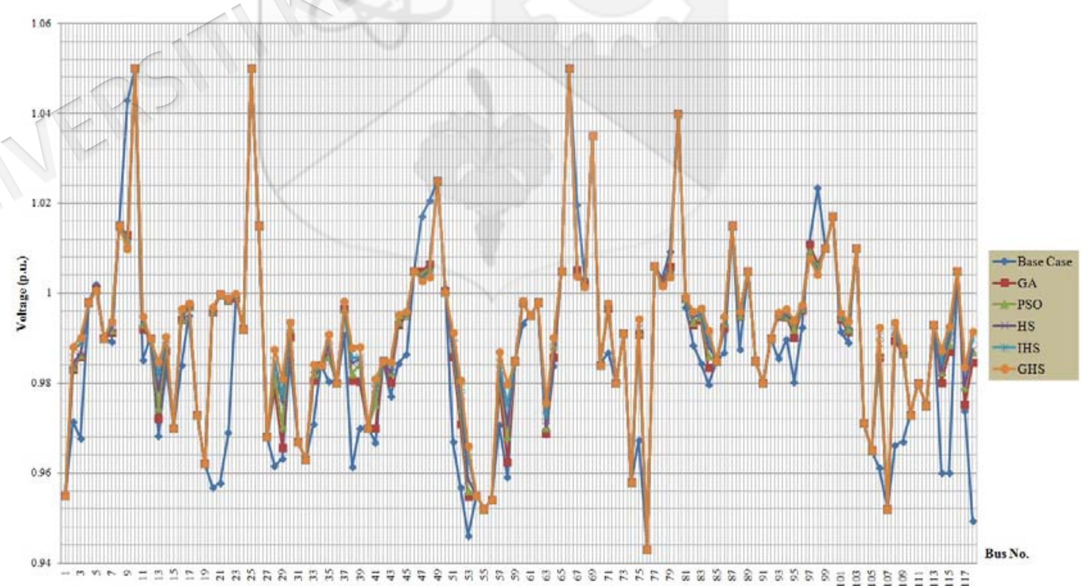

Figure 6.11 Voltage profiles before and after SVC placement in the 118 bus test system

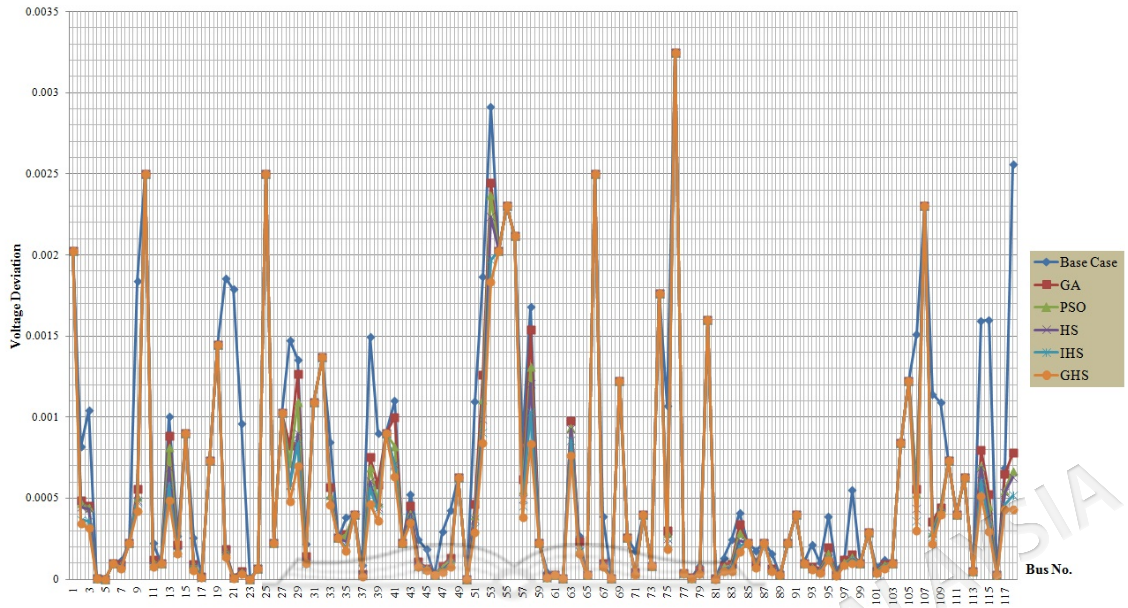

Figure 6.12 Total voltage deviations before and after SVC placement in the 118 bus test system

6.3 RESULTS OF OPTIMAL STATCOM PLACEMENT AND SIZING IN TRANSMISSION SYSTEMS

The IHS and GHS algorithms are used to determine the optimal location and size of only one STATCOM in a transmission network. The suitable buses are for STATCOM placement first identified using the modal analysis and then the proposed IHS and GHS algorithms are used to determine the optimal placement and size of STATCOM compensation required to minimize loss and improve the voltage and voltage stability with respect to the STATCOM size. In this study, it is decided to give equal importance to coefficient values of the power loss reduction (ω_1), voltage profile improvement (ω_2) and voltage stability enhancement (ω_3) functions and less importance to coefficient value of STATCOM size (ω_4). Thus, the coefficient values for the objectives are selected as ω_1=0.3, ω_2=0.3 , ω_3=0.3 and ω_4=0.1 and the penalty factors are assumed as χ_1=100, χ_2=100, and χ_3=100. The results obtained using the proposed IHS and GHS algorithms for the 57 bus and the 118 bus test systems are compared with other optimization techniques for the purpose of evaluating the effectiveness of algorithms.

6.3.1 Optimal STATCOM Placement Results for the 57 Bus Test System

Considering the results of modal analysis shown in Table 6.13, the ten buses with high participation factor values are considered suitable for STATCOM installation. The identified ten buses are buses 24, 25, 30, 31, 32, 33, 34, 35, 36 and 40. Table 7.20 shows the place and size of STATCOM using the five optimisation techniques. The results obtained from the IHS and GHS algorithms are compared with results obtained using the GA, PSO and conventional HS algorithm. Table 6.20 also shows the total power loss, voltage deviation and the smallest eigenvalue after the installation of the STATCOM. This study is performed with the restriction that the injected Q does not exceed 50 MVar.

Table 6.20 A comparison of different optimization techniques for optimal placement and sizing of STATCOM in the 57 bus test system

Objective function	Base Case	GA	PSO	HS	IHS	GHS
Optimum Location (Bus No.)	---	33	32	31	31	31
Size of STATCOM (MVar)	---	17.44	15.35	12.87	12.41	12.37
Total Power Losses (MW)	28.41	28.19	28.02	27.88	27.76	27.74
Total Voltage Deviation	0.265	0.209	0.215	0.181	0.178	0.177
Smallest Eigenvalue	0.234	0.302	0.261	0.291	0.314	0.322
Fitness function value	1.000	0.802	0.839	0.765	0.743	0.736

Table 6.20 shows that STATCOM placement using the GHS algorithm not only produces greater voltage stability enhancement and greater reductions in power loss and voltage deviation than GA, PSO and conventional HS algorithm, but it also gives the lowest fitness function value compared to other optimization techniques. It is also observed that the result of STATCOM placement using the IHS algorithm in terms of power loss reduction, voltage deviation minimization and voltage stability enhancement is comparable to the GHS algorithm. However, the STATCOM size found by the GHS algorithm is lower than that found by the IHS algorithm.

6.3.2 Optimal STATCOM Placement Results for the 118 Bus Test System

The proposed IHS and GHS algorithms were implemented to determine the optimal location and size of only one STATCOM in the 118 bus test system. The coefficient values for the objective functions are assumed to be the same as those in the 57 bus test system. This study is performed with the restriction that the injected Q does not exceed 120 MVar. As shown in Table 6.17, the most critical buses in the system are buses 20, 21, 22, 23, 37 and 38 and these buses are considered as candidate location for STATCOM installation.

Table 6.21 shows a comparison of the optimal STATCOM placement results of the IHS and GHS algorithms with the other optimization techniques in terms of total power loss, voltage deviation, smallest eigenvalue and size of STATCOM. The results in the table show that the GHS algorithm gives the lowest fitness function value and the greatest reduction in terms of power loss and voltage deviation as compared to GA, PSO, conventional HS and IHS algorithms.

Table 6.21 A comparison of different optimization techniques in optimal placement and sizing of STATCOM in the 118 bus test system

Objective function	**Base Case**	**GA**	**PSO**	**HS**	**IHS**	**GHS**
Optimum Location (Bus No.)	---	20	22	21	21	21
Size of STATCOM (MVar)	---	69.11	71.39	64.11	64.17	64.23
Total Power Losses (MW)	132.86	132.57	132.56	131.52	131.43	131.23
Total Voltage Deviation	0.294	0.291	0.290	0.289	0.287	0.285
Smallest Eigenvalue	3.9425	5.108	5.166	5.282	5.284	5.292
Fitness function value	1.000	0.875	0.865	0.857	0.853	0.845

The convergence characteristics of the different optimization techniques for the optimal placement and sizing of STATCOM in the 118 bus test system are shown in Figure 6.13. From the figure, the GHS algorithm converges faster compared with the other optimization techniques.

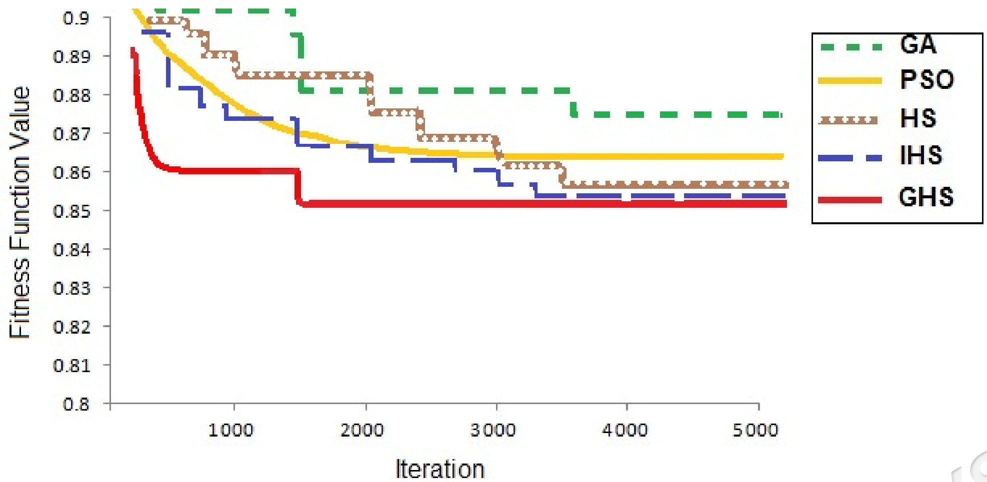

Figure 6.13 Convergence characteristics of different optimization techniques for the optimal placement and sizing of STATCOM in the 118 bus test system

The minimum, maximum, mean and standard deviation of the fitness function values from 50 executions of the GA, PSO, HS, IHS and GHS algorithm are shown in Table 6.22. From the table, it is noted that the GHS algorithm gives the lowest fitness function values and lowest standard deviation values compared to other optimization techniques. This proves that the proposed GHS algorithm for solving the optimal placement and sizing of STATCOM in the 118 bus test system is more accurate than GA, PSO, conventional HS and IHS algorithms.

Table 6.22 Accuracy of different optimization techniques for the optimal STATCOM placement and sizing in the 118 bus test system

Fitness Function Value	GA	PSO	HS	IHS	GHS
Minimum	0.8583	0.8605	0.8567	0.8529	0.8451
Maximum	0.9163	0.8661	0.8581	0.8532	0.8451
Mean	0.8753	0.8651	0.8572	0.8531	0.8451
Standard Deviation	5.80e-04	5.61e-05	1.42e-05	3.78e-06	3.47e-08

6.4 COMPARATIVE STUDY ON THE EFFECTIVENESS OF DIFFERENT VAR COMPENSATION DEVICES

This section presents a comparison on the effectiveness of installing reactive power compensators, such as shunt capacitors, SVC and STATCOM in transmission networks. In the simulation study, the critical or weakest bus was first identified using the modal analysis method and this bus was selected for installing a single shunt capacitor, single SVC and single STATCOM separately. The effects of installing these Var compensation devices on power loss reduction, voltage profile improvement and voltage stability enhancement were examined and compared. The comparative study was performed on the 57 and 118 bus test systems.

6.4.1 Comparative Study Results for the 57 Bus Test System

Form the Table 6.13, the most critical bus in the 57 bus test system is identified as bus 31. This bus is selected to install a Var compensator. The variations in power loss, voltage deviation, and smallest eigenvalue relative to the Var compensator size using the different devices are shown in Figs. 6.14, 6.15 and 6.16, respectively. This study is conducted with the restriction that the injected Q does not exceed 50 MVar in the 57 bus test system.

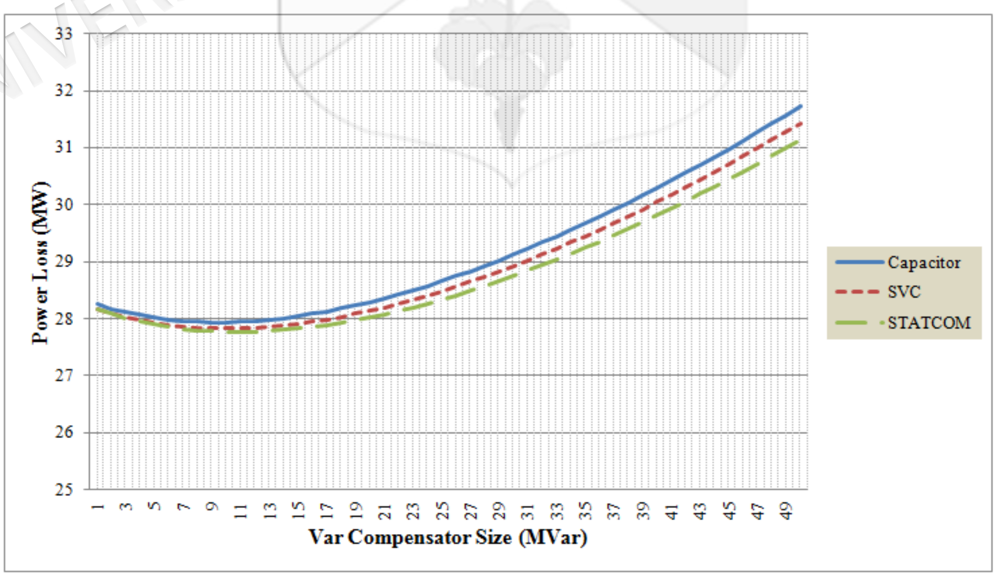

Figure 6.14 Power loss versus Var compensator size after installing different devices in the 57 bus test system

Figure 6.14 shows that the power loss variation curves after installing shunt capacitor, SVC and STATCOM, initially decrease and then increase. The effects of installing shunt capacitor, SVC, and STATCOM with sizes less than 10 MVar are very similar; however, as the sizes increase, the effect of STATCOM on power loss reduction is better than SVC, and the effect of SVC on power loss reduction is better than that of the shunt capacitor.

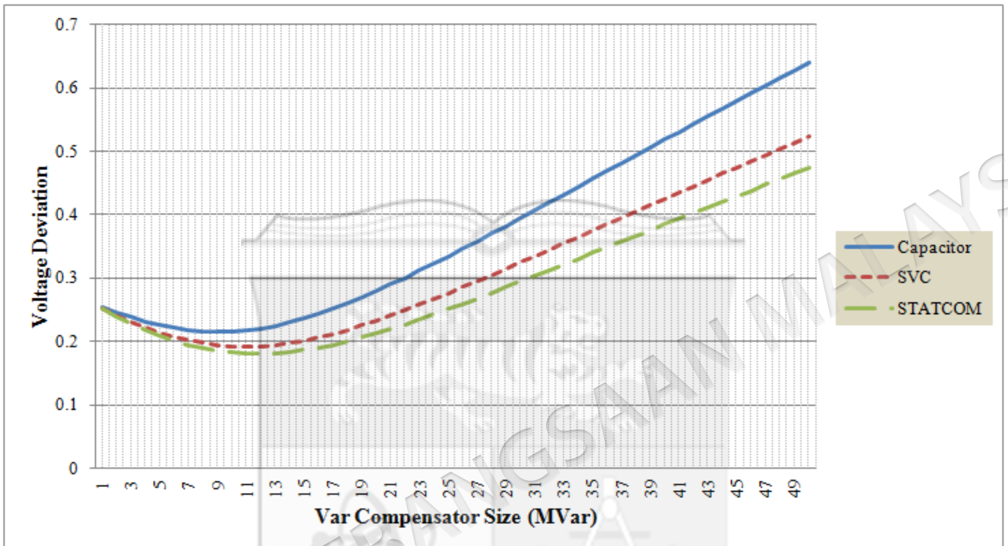

Figure 6.15 Voltage deviation versus Var compensator size after installing different devices in the 57 bus test system

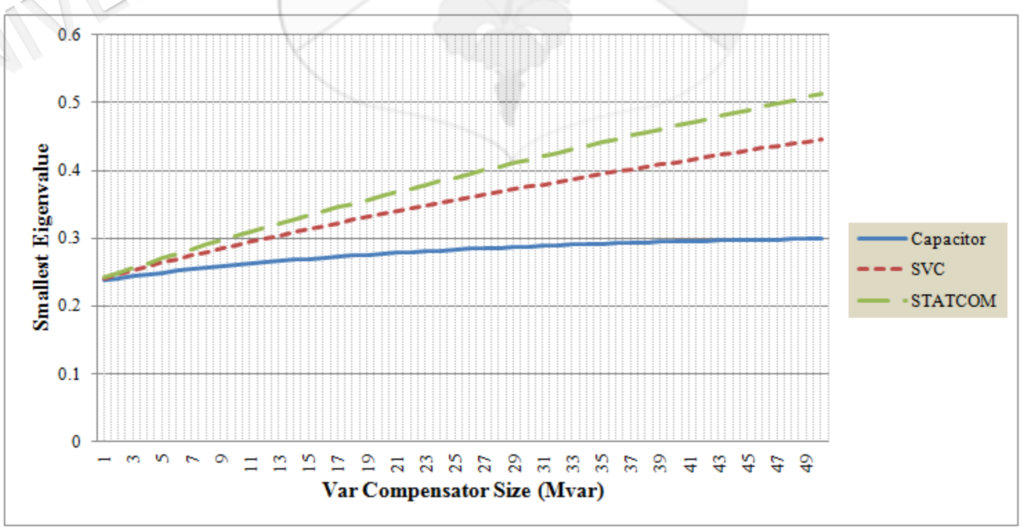

Figure 6.16 Smallest eigenvalue in the critical mode versus Var compensator size after installing the different devices in the 57 bus test system

Figure 6.15 shows that the voltage deviation variation curves after the installation of the shunt capacitor, SVC, and STATCOM initially decrease and then increase. As the Var compensator size increases, the effect of STATCOM on the voltage profile improvement is better than that of SVC, and the effect of SVC is much better than that of the shunt capacitor. From the smallest eigenvalues shown in Figure 6.16, it is noted that the STATCOM gives better voltage stability enhancement than SVC, and the SVC gives better voltage stability enhancement than that of the shunt capacitor. To compare the cost of the Var compensators, Table 6.23 depicts the cost of the compensators (Eslami et al 2011).

Table 6.23 Cost comparison of Var compensators

Var compensation device	**Cost (US $)**
Shunt capacitor	8/kVar
SVC	40/ kVar (controlled portion)
STATCOM	50/ kVar (controlled portion)

To further compare the effectiveness of installing shunt capacitors, SVC and STATCOM in transmission networks, the optimal sizes of these compensators are determined using the GHS algorithm and the objective function defined in (5.19). The total cost is calculated with respect to the type and the cost of each Var compensator shown in Table 6.23. In the calculation of the objective function, the coefficients of the objective function are selected as $\omega_1 = 0.3$, $\omega_2 = 0.3$, $\omega_3 = 0.3$, and $\omega_4 = 0.1$. The results of the optimum sizes for a capacitor, SVC and STATCOM installed at the critical bus are shown in Table 6.24.

Table 6.24 Optimum size for single shunt Var compensator at the critical bus of the 57 bus test system

	Shunt Capacitor	**SVC**	**STATCOM**
Size (MVar)	13.34	12.91	12.37

The results in Table 6.24 show that the optimum size of a shunt capacitor is greater than SVC and STATCOM. This is due to lower cost of shunt capacitor in comparison with SVC and STATCOM. The effect of installing the 13.34 MVar capacitor, 12.91 MVar SVC, and 12.37 MVar STATCOM at the weakest bus of the 57 bus test system are compared in terms of power loss, voltage deviation and voltage stability enhancement as shown in Table 6.25.

Table 6.25 Comparing the effect of different Var compensators installed at the weakest bus of the 57 bus test system

Cases	Base Case	With Capacitor (13.34 MVar)		With SVC (12.91 MVar)		With STATCOM (12.37 MVar)	
			Impr.* (%)		Impr.* (%)		Impr.* (%)
Power Loss (MW)	28.41	28.01	1.4	27.95	1.6	27.74	2.4
Voltage Deviation (p.u)	0.265	0.217	18.1	0.193	27.2	0.177	33.2
The Smallest Eigenvalue	0.2344	0.2612	11.4	0.2997	27.9	0.3221	37.4

**Improvement*

From the results shown in Table 6.25, the following points can be highlighted:

i. The effect of installing a single capacitor, SVC and STATCOM on power loss reduction in the 57 bus test system is not significant in which the power loss reduction is less than 2.5%. It is noted that the effect of installing a single STATCOM on power loss reduction is better than a single SVC, and the effect of installing a single SVC is better than that of a single shunt capacitor.

ii. The effect of the installing a single capacitor, SVC and STATCOM on voltage profile improvement in the 57 bus test system is significant in which the voltage deviation reduction is greater than 18%. It can be seen that the effect of installing of a single STATCOM on voltage profile improvement is better than installing a single SVC and the effect of installing a single SVC is much better than that of a single shunt capacitor.

iii. The effect of the installing a single capacitor, SVC and STATCOM on voltage stability enhancement in the 57 bus test system is substantial in which the smallest eigenvalue improvement is greater than 11%. It is shown that the effect of installing a single STATCOM on voltage stability enhancement is better than a single SVC and the effect of installing a single SVC is better than that of a single shunt capacitor.

6.4.2 Comparative Study Results for the 118 Bus Test System

Consider the highest bus participation factor value for the smallest eigenvalue of the 118 bus test system as shown in Table 6.17. As shown in the table, the critical bus in the 118 bus test system is bus 21 and this bus is selected for installing the Var compensator. The variations in power loss, voltage deviation and smallest eigenvalue relative to the Var compensator size using different devices are shown in Figs. 6.17, 6.18 and 6.19, respectively. This study is conducted with the constraint that the injected Q does not exceed 120 MVar in the 118 bus test system.

From Figs. 6.17 and 6.18, the variation in the curves of both power loss and voltage deviation after installing the shunt capacitor, SVC and STATCOM, initially descend and then ascend. The effect of installing shunt capacitor, SVC and STATCOM on power loss reduction is very similar when the Var compensator size is less than 20 MVar but after the Var compensator size increases, the effect of STATCOM on both power loss reduction and voltage improvement is better than that of SVC and the effect of SVC on power loss reduction and voltage profile improvement is much better than that of the shunt capacitor.

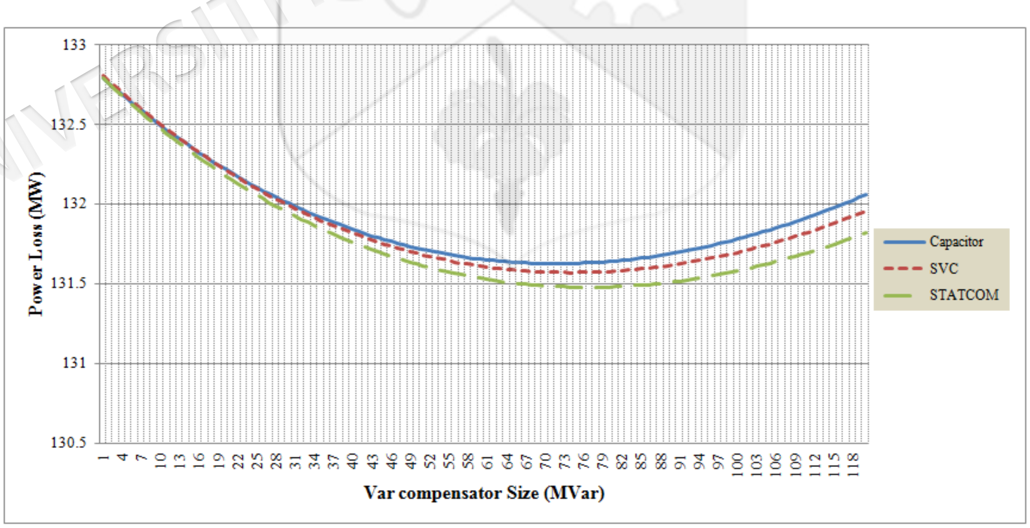

Figure 6.17 Power loss versus Var compensator size after installing different devices in the 118 bus test system

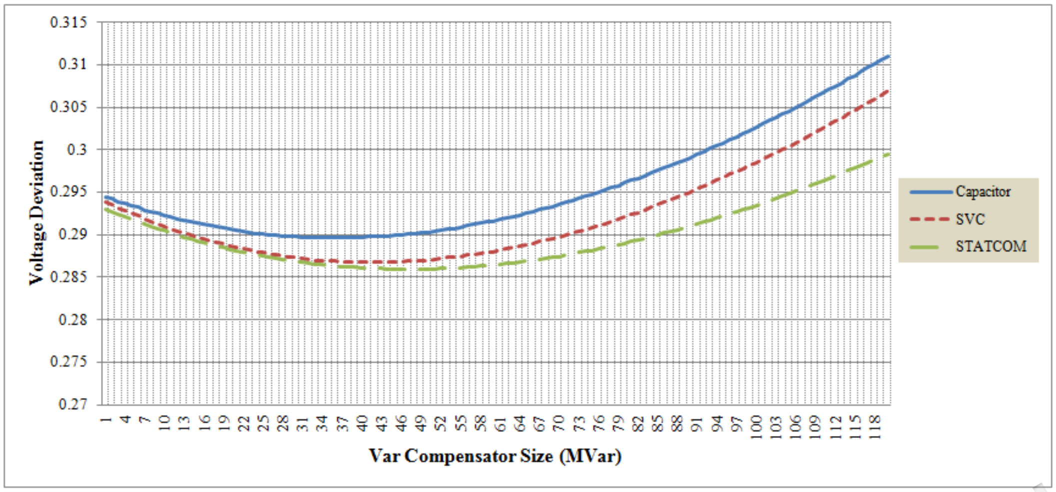

Figure 6.18 Voltage deviation versus Var compensator size after installing the different devices in the 118 bus test system

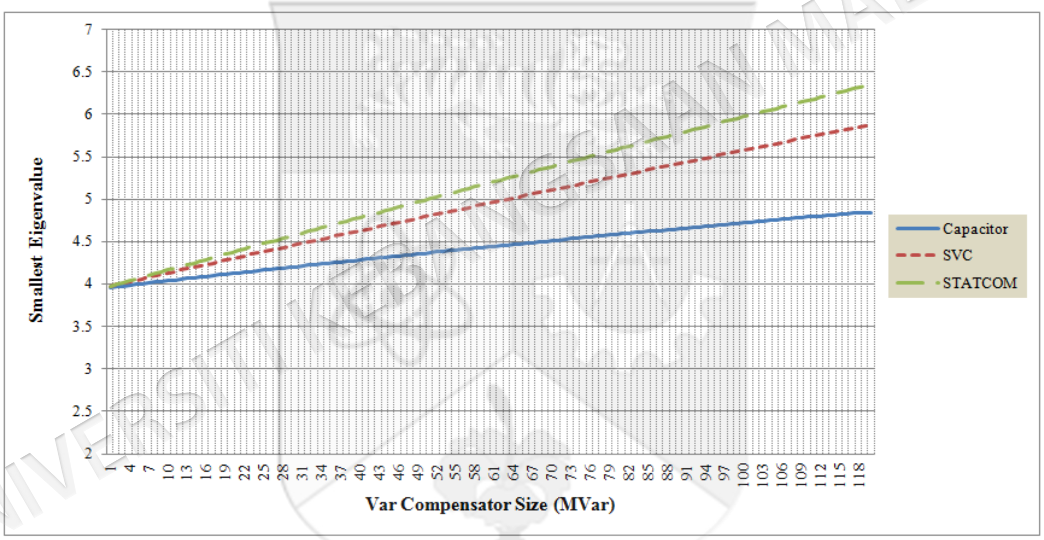

Figure 6.19 Smallest eigenvalue versus Var compensator size after installing different devices in the 118 bus test system

Figure 6.19 shows by increasing the Var compensator size, the STATCOM gives better voltage stability enhancement than the SVC, and the SVC gives better voltage stability enhancement than the shunt capacitor.

Table 6.26 shows the results of the optimum sizes of single capacitor, SVC and STATCOM installed at the critical bus of the 118 bust test system. These optimum sizes were determined using the GHS algorithm and the objective function defined in (5.19), and the coefficients for the objective functions are assumed to be the same as those in the 57 bus test system.

Table 6.26 The optimum size for single shunt Var compensator at the critical bus of the 118 bus test system

	Shunt Capacitor	SVC	STATCOM
Size (MVar)	68.71	65.18	64.23

From the results shown in Table 6.26, the optimum size of single shunt capacitor is greater than SVC and STATCOM due to the fact that the cost of shunt capacitor is less than SVC and STATCOM. The effects of installing the 68.71 MVar capacitor, 65.18 MVar SVC and 64.23 MVar STATCOM at the weakest bus of the 118 bus test system are further compared in terms of power loss, voltage deviation and voltage stability enhancement as shown in Table 6.27.

Table 6.27 Comparing the effect of different Var compensators installed at the weakest bus in the 118 bus test system

Cases	Base Case	With Capacitor (68.71 MVar)		With SVC (65.18 MVar)		With STATCOM (64.23 MVar)	
			Impr.* (%)		Impr.* (%)		Impr.* (%)
Power Loss (MW)	132.86	131.63	0.9	131.59	1.0	131.23	1.2
Voltage Deviation	0.294	0.293	0.3	0.289	1.8	0.285	3.1
The Smallest Eigenvalue	3.943	4.497	14.1	5.030	27.6	5.292	34.2

**Improvement*

From the results shown in Table 6.27, the following points can be highlighted:

i. The effect of installing a single capacitor, SVC and STATCOM on power loss reduction in the 118 bus test system is not very significant because the improvement in power loss reduction is less than 1.2%. Comparing the effect of different Var compensators on power loss reduction, it is shown that the STATCOM gives better power loss than SVC and the SVC gives better power loss reduction than the shunt capacitor.

ii. The effect of installing a single capacitor, SVC, and STATCOM on voltage profile improvement in the 118 bus test system is not very significant because the improvement in voltage deviation reduction is less than 3.2%. It is noted that the STATCOM gives slightly better voltage profile improvement than SVC and that the SVC gives better voltage improvement than the shunt capacitor.

iii. The effect of installing a single capacitor, SVC and STATCOM on voltage stability enhancement in the 118 bus test system is significant because the smallest eigenvalue improvement is greater than 14%. Comparing the effect of different Var compensators on voltage stability enhancement, it is noted that the STATCOM gives better voltage stability improvement than the SVC, and that the SVC gives better voltage stability improvement than the shunt capacitor.

6.5 RESULTS ON THE USE OF THE OPSVC SOFTWARE

To illustrate the use of the developed software tool, OPSVC, some examples for determining optimal placement and sizing of Var compensators in the test systems are considered. The application of OPSVC using the GHS algorithm for determining the optimal location and sizing of shunt capacitors in the three-phase 10 bus test system is illustrated. The 57 bus test system is also considered to illustrate the use of OPSVC in applying the IHS algorithm for optimal SVC placement and sizing in transmission systems**.**

6.5.1 Example of Using OPSVC for Analysis on a Radial Distribution System

The three-phase 10 bus test system is considered to illustrate the use of OPSVC for optimal capacitor placement and sizing in radial distribution systems by considering mutual coupling, load unbalance and harmonics. The GHS algorithm is selected as the optimization technique. Initially, all the required data is entered through the GUI shown in Figure 6.20. In the section of optimization parameters, the number of buses, number of iterations and genetic mutation probability are selected as 10, 5000 and 0.2, respectively. The studied cases are selected as; with mutual coupling and unbalance in loads. The maximum permissible *THD* is also selected as 5%. Then by clicking on the button "Run", the convergence curve is plotted and then the results are shown on the right of the GUI as depicted in Figure 6.20.

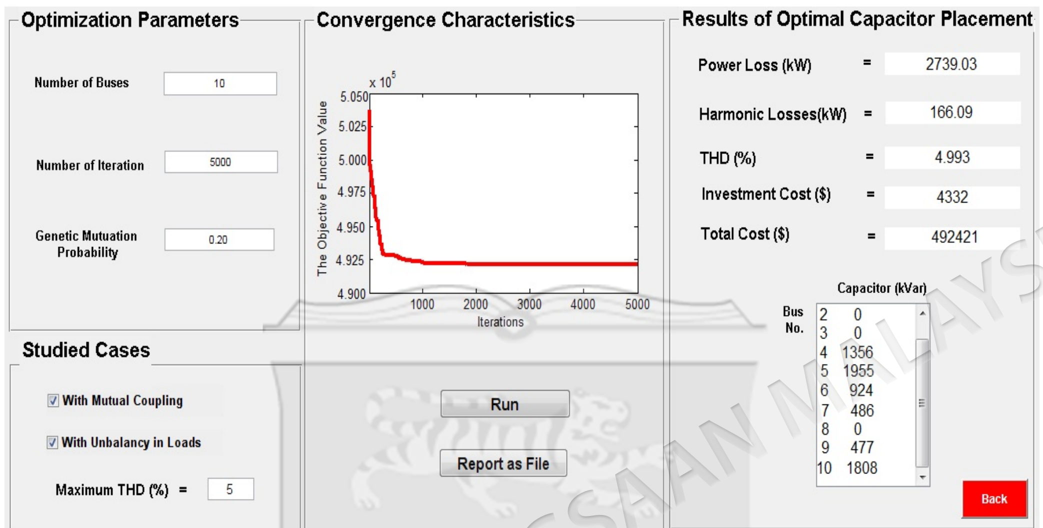

Figure 6.20 Output display of the GUI for optimal capacitor placement in the 10 bus distribution system using the GHS algorithm

Figure 6.20 shows that the obtained capacitor placement results of OPSVC using the GHS algorithm are the same as the results shown in Table 6.8 and Table 6.9. The voltage profile of test system before and after capacitor placement is also plotted as shown in Figure 6.21. From the figure, it can be seen that the voltage improvement after capacitor placement using the GHS algorithm is significant.

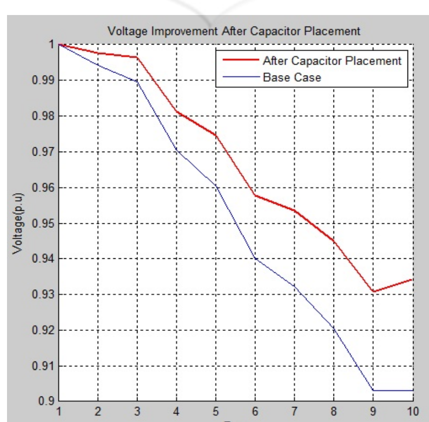

Figure 6.21 Voltage improvement after optimal capacitor placement in the 10 bus distribution system plotted by the OPSVC software

6.5.2 Example of Using OPSVC for Analysis on a Transmission System

The 57 bus test system is considered to illustrate the use of the OPSVC for optimal SVC placement and sizing in transmission systems. In this simulation case, the IHS algorithm is selected as the optimization technique. Initially, all the required data is entered through the GUI shown in Figure 6.22. The optimization parameters are selected as: number of buses =57, number of iterations = 5000, *HMCR* = 95%, PAR_{max}= 0.90, PAR_{min}= 0.4 and bw_{max}=1 , bw_{min}=10^{-6}. The number of SVCs is selected as 3 and the maximum permissible size of SVC is selected as 20MVar. Then by clicking on the button "Run", the convergence curve is plotted and then the results are shown on the right of the GUI in Figure 6.22.

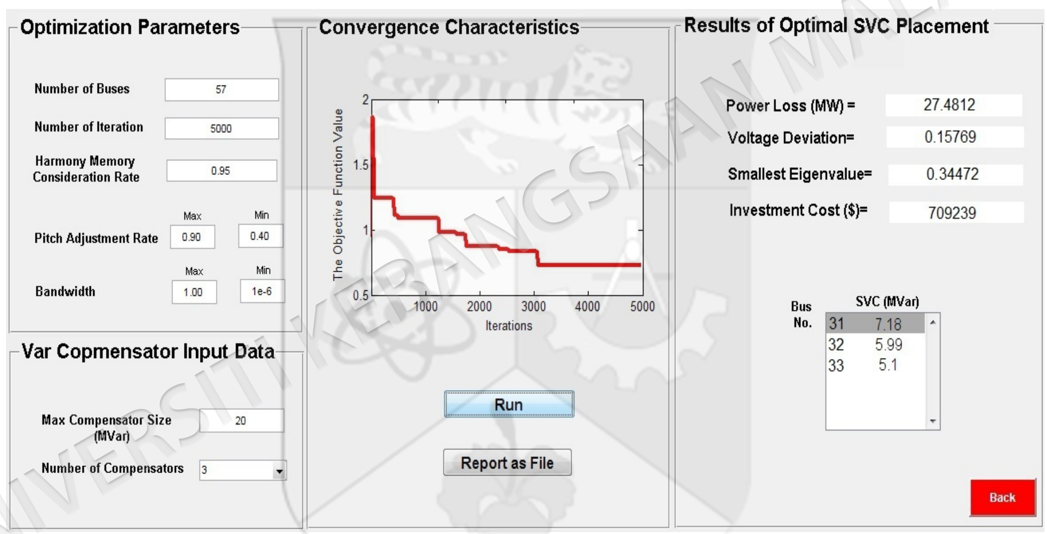

Figure 6.22 Output display of the GUI for optimal SVC placement in the 57 bus test system using the IHS algorithm

Figure 6.22 shows that the obtained SVC placement results of OPSVC using the IHS algorithm are same as the results of Table 6.14 and Table 6.15. From Figure 6.22, the convergence characteristics of the IHS algorithm for the optimal placement and sizing of SVCs in the 57 bus test system are also similar to the results shown in Figure 6.10. The voltage profile and the voltage deviation curves, before and after SVC placement are also plotted as depicted in Figure 6.23 and Figure 6.24, respectively. From the figures, it can be seen that there is a significant voltage improvement at some buses after installing the three SVCs in the 57 bus transmission system.

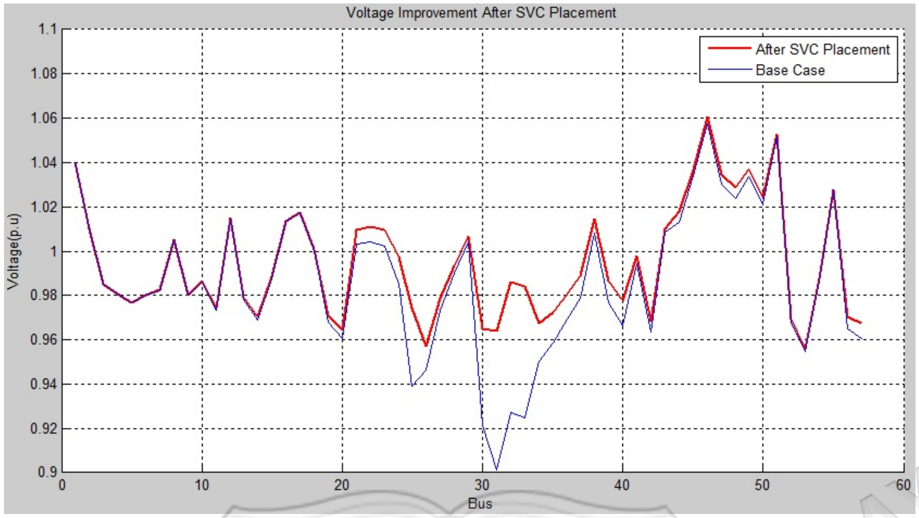

Figure 6.23 Voltage improvement after SVC placement in the 57 bus test system plotted by the OPSVC software

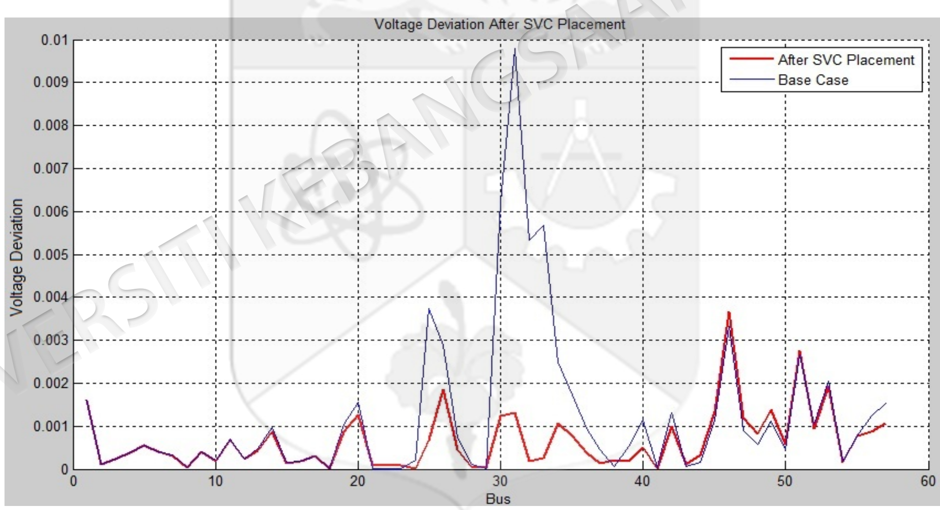

Figure 6.24 Voltage deviation before and after SVC placement in the 57 bus test system plotted by the OPSVC software

6.6 CHAPTER SUMMARY

The proposed IHS and GHS algorithms for determining the optimal location and size of shunt capacitors in radial distribution network have been tested on various distribution networks. Mutual coupling, load unbalance and harmonics supply have been considered for solving the optimal capacitor placement problem. The proposed algorithms have been validated on the three-phase 10-bus and 34-bus radial distribution systems and the tests results showed that the GHS optimization algorithm gives greater reduction in power loss and total costs compared to the GA, PSO, conventional HS and IHS algorithms. The proposed IHS and GHS algorithms are also applied for determining the optimal location and size of SVC and STATCOM in 57 bus and 118 bus transmission networks. The test results showed that the GHS algorithm gives better voltage stability enhancement and greater reduction in power loss, voltage deviation and total cost compared to the GA, PSO, HS and IHS algorithms. It is also shown that the GHS algorithm converges faster compared with the other optimization techniques. In addition, the effectiveness of the most commonly used shunt compensation devices such as shunt capacitor, SVC and STATCOM has been investigated in terms of power loss reduction, voltage profile improvement and voltage stability margin enhancement. The test results showed that the effect installing a single STATCOM in achieving the aforementioned objectives is better than that of a single SVC, and the effect of installing a single SVC is better than that of a single shunt capacitor. However, SVC and STATCOM are expensive compared with shunt capacitor. Finally, the results of using the developed software tool, OPSVC, for optimal placement and sizing of shunt Var compensators in distribution and transmission systems have been presented.

CHAPTER VII

CONCLUSION AND FUTURE WORKS

7.1 CONCLUSION

In this thesis, two metaheuristic optimization techniques named as IHS and novel GHS algorithms have been applied to determine the optimal location and size of shunt reactive power compensators such as shunt capacitors, SVC and STATCOM in power systems. The IHS employs a method for generating new solution vectors that enhances accuracy and convergence of the conventional harmony search algorithm while the GHS algorithm which is inspired by swarm intelligence of the PSO technique, modifies the improvisation step of the HS algorithm, so that a new harmony can mimic the global best harmony in the harmony memory. In addition, the GHS algorithm notably consumes less average time than the IHS algorithm.

To accomplish the first objective of the research which is to implement an effective heuristic optimization technique in terms of speed and accuracy for determining optimal location and size of shunt capacitors in radial distribution systems, the IHS and GHS algorithms have been applied by considering mutual coupling, load unbalance and harmonics. The backward/forward sweep power flow and radial harmonic power flow methods have been developed for calculating the power loss. The proposed algorithms have been validated on the three-phase 10-bus and 34-bus radial distribution systems and the obtained results showed that the IHS and GHS algorithms give greater reduction in power loss and total costs compared to the conventional HS algorithm, PSO and GA. Comparing the performance of IHS and GHS algorithms, it is noted that the GHS algorithm is up to 5 seconds faster in terms of computational time and gives better performance in finding optimal capacitor location and size compared to the IHS algorithm. The simulation results prove that the use of IHS and GHS algorithms which do not require initial value setting for the variables are simpler, faster and more effective than the optimization techniques using GA (Carpinelli et al. 2010), PSO (Ejal & Elhawary 2010), binary PSO (Zhezhelenko et al. 2009) and simulated annealing (Ghose & Goswami 2004). The power loss reduction and net saving after optimal capacitor placement using IHS and GHS algorithms are also greater than the results in all the above-mentioned references.

The second objective is to develop an effective heuristic optimization technique for determining optimal location and size of shunt Var compensators in transmission systems by maximizing power loss reduction and voltage stability margin. To achieve these objectives, IHS and GHS algorithms which are relatively new optimization algorithms have been applied for determining the optimal location and size of SVC and STATCOM in transmission systems. The extent of power loss reduction, voltage profile and voltage stability improvement and total cost reduction are used as measures for evaluating power system performance. The multi-criterion objective function in this optimization problem considers more objective functions and operational constraints compared to other optimal Var compensator placement and sizing methods using GA (Pisica et al. 2009), PSO (Azadani et al. 2008) and EPSO (Eghbal et al. 2009). The effectiveness of the IHS and GHS algorithms in determining optimal location and size of SVC and STATCOM has been validated on the IEEE 57 bus and 118 bus transmission systems. Test results show that the GHS algorithm gives greater voltage stability enhancement and greater reductions in power loss, voltage deviation and total cost compared to GA, PSO, HS and IHS algorithms. Moreover, the GHS algorithm not only performs better in finding optimal solutions but it also converges faster compared with the IHS algorithm.

To address the third objective which is to investigate and determine the most effective reactive compensating device among the shunt capacitor, SVC and STATCOM for power loss reduction, voltage improvement and voltage stability enhancement, modal analysis is applied and a comparative study is implemented. The modal analysis is used to determine the critical or weakest bus from the voltage stability viewpoint and the reactive compensating device is then installed at this bus. A comparative study is then made to investigate the effectiveness of installing a shunt capacitor, SVC and STATCOM in a power system for achieving power loss reduction, voltage profile improvement, and voltage stability margin enhancement. The comparative study has been performed on the 57 and 118 bus transmission systems. The results showed that the effect of installing a STATCOM in achieving the aforementioned objectives is better than SVC, and the effect of installing a SVC is better than that of a single shunt capacitor. However, SVC and STATCOM are expensive compared with shunt capacitor. A comprehensive study has been made to evaluate the effect of installing the shunt capacitor, SVC and STATCOM on power loss reduction, voltage profile improvement and voltage stability enhancement, while the study in Sode-Yome & Mithulananthan (2004) only considers the effect on voltage stability improvement.

7.2 SIGNIFICANT CONTRIBUTIONS OF THE RESEARCH

The major contributions of this thesis are summarized as follows:

i. The proposed IHS and GHS algorithms are easy to implement and can find multiple optimal solutions to constrained multi-objective problem, thereby providing more flexibility in making decisions about the locations of shunt Var compensators. Moreover, the GHS algorithm not only performs better in finding optimal solutions but also converges faster compared with GA, PSO, HS and IHS algorithms.

ii. The solution for optimal capacitor placement and sizing in radial distribution systems is considered practical and realistic because it take into account the unbalanced nature of distribution systems which include mutual coupling effects, unbalanced phase loading and unbalanced distributed loads. Moreover, the presence of harmonic sources in distribution systems has been included in solving the optimal capacitor placement and sizing problem.

iii. A multi-criterion objective function incorporating total cost minimization, voltage stability enhancement, voltage profile improvement and power loss minimization has been considered to solve the optimal location and sizing of shunt Var compensators in a transmission network.

iv. A comprehensive study has been carried out to compare the effectiveness of the most commonly used Var compensation devices, namely, shunt capacitor, SVC, and STATCOM in reducing power loss, improving voltage profile and enhancing voltage stability margin. In addition, a cost–benefit analysis has been carried out to justify the economic viability of the SVC and STACOM.

v. A new power system analysis tool called as Optimal Placement of Shunt Var Compensators (OPSVC) has been developed. The capabilities of the OPSVC are that it can conduct several analyses, such as load flow, optimal placement and sizing of capacitors, SVC and STATCOM using different optimization techniques and plotting voltage profile of the studied system before and after installing the Var compensators.

7.3 SUGGESTIONS FOR FUTURE WORKS

The proposed techniques for optimal placement and sizing of shunt Var compensators in power systems presented in this research have been found very successful. For further development of this research work, some of the possible future works in this area are suggested as follows:

i. In optimal capacitor placement, loads were modeled as constant real and reactive power loads or constant PQ loads. Other load models, namely, constant impedance and constant current load models can also be considered.

ii. In optimal capacitor placement, the energy loss function can be included in the problem formulation if load variations are taken into account.

iii. The developed algorithms can be employed to find the locations and ratings of switched shunt capacitors as well as fixed capacitors.

iv. The proposed IHS and GHS algorithms can be applied to solve mixed integer optimization problems such as optimal allocation and sizing of distributed generators or other types of FACTS devices.

REFERENCES

Abou-Ghazala, A. 2003. Optimal capacitor placement in distribution systems feeding nonlinear loads. *IEEE PowerTech Conference Proceeding*:1-6.

Acha, E., Fuerte-Esquivel, C.R., Ambriz-Perez, H. & Angeles-Camacho, C. 2004. *FACTS Modeling and Simulation in Power Network*. Chichester. John Wiley and Sons Ltd.

Afaghzadeh , H., Valipoor, K.H., Ebtehaj, M. & Ghadimi, H. 2011. Optimal capacitor placement with consideration of voltage source harmonic distortion effect on radial distribution networks using binary particle swarm optimization. *16th Conference on Electrical Power Distribution Networks*:1-6.

Alabduljabbar, A.A. & Milanovi J.V. 2006. Generation Costs Reduction Through Optimal Allocation of FACTS Devices Using Low Discrepancy Sequences. *Power Systems Conference and Exposition*: 946-951.

AlHajri, M., AlRashidi, M. & El-Hawary, M. 2007. A novel discrete particle swarm optimization algorithm for optimal capacitor placement and sizing. *Canadian Conference on Electrical and Computer Engineering*:1286-1289.

Al-Mohammed, A.H. & Elamin, I. 2003. Capacitor Placement In Distribution Systems Using Artificial Intelligent Techniques. *IEEE Power Tech Conference Proceedings*:1-7.

Altintas, A. 2011. A GUI-based education toolbox for power electronics converters using MATLAB/Simulink and SimPowerSystems. *International Journal of Electrical Engineering Education* **48**(1): 1-14.

Annaluru, R., Das, S., Pahwa, A. 2004. Multi-Level Ant Colony Algorithm for Optimal Placement of Capacitors in Distribution Systems. *Congress on Evolutionary Computation*:1932-1937.

Azadani, E.N. , Hosseinian, S.H., Janati , M. & Hasanpor, P. 2008. Optimal Placement of Multiple STATCOM. *12th International Middle-East Power System Conference*:523-528.

Baghaee, H.R., Jannati, M. ,Vahidi, B. , Hosseinian, S.H. & Rastegar, H. 2008. Improvement of Voltage Stability and Reduce Power System Losses by Optimal GA-based Allocation of Multi-type FACTS Devices. *11th International Conference on Optimization of Electrical and Electronic Equipment*: 209-214.

Baghzouz, Y. & Ertem, S. 1990. Shunt capacitor sizing for radial distribution feeders with distorted substation voltages*. IEEE Transaction on Power Delivery* **5**(2):650–657.

Bai, Q. 2010. Analysis of Particle Swarm Optimization Algorithm .*Computer and Information Science* **3**(1):180-184.

Baskarana, J. & Palanisamy, V. 2006. Optimal location of FACTS devices in a power system solved by a hybrid approach. *Nonlinear Analysis* **65**(11) :2094–2102.

Belazzoug, M. & Boudour, M. 2010. FACTS Placement Multiobjective Optimization For Reactive Power System Compensation. *International Multi-Conference on Systems, Signals and Devices*:1-6.

Benabid, R. & Boudour, M. 2007. Optimal Location and Size of SVC and TCSC for Multi-objective Static Voltage Stability Enhancement. *Proceeding of the International Conference on Renewable Energy and Power Systems Quality*:1-6.

Benabid, R., Boudour, M. & Abido, M. A. 2009a. Optimal Placement of FACTS devices for Multiobjective Voltage Stability Problem. *Power Systems Conference and Exposition*:1-11.

Benabid, R., Boudour, M. & Abido, M. A. 2009b. Optimal location and setting of SVC and TCSC devices using non-dominated sorting particle swarm optimization. *Electric Power Systems Research* **79**(12): 1668–1677.

Berizzi, A., Bovo, C. & Ilea, V. 2011. Optimal placement of FACTS to mitigate congestions and inter-area oscillations. *IEEE Trondheim PowerTech*: 1-8.

Bhattacharya, S. K. & Goswami, S. K. 2009. A new fuzzy based solution of the capacitor placement problem in radial distribution system. *Expert Systems with Applications* **36**(3) :4207–4212.

Bonnard, G. 1985. The Problems Posed by Electrical Power Supply to Industrial Installations. *Proceeding of IEE Part B 132*: 335-340.

Carpinelli, G. & Noce, C. 2006. Voltage Regulators and Capacitor Placement in Three-phase Distribution Systems with Non-linear and Unbalanced Loads. *International Journal of Emerging Electric Power Systems* **7**(4):1-17.

Carpinelli, G. , Varilone, P. , Di-Vito , V. & Abur, A. 2005. Capacitor placement in three-phase distribution systems with nonlinear and unbalanced loads. *IEE Proceedings Generation Transmission and Distribution* **152**(1):47-52.

Carpinelli, G., Proto, D., Noce, C., Russo, A. & Varilone, P. 2009. Optimal allocation of capacitors in unbalanced multi-converter distribution systems: A comparison of some fast techniques based on genetic algorithm. *Electric Power Systems Research* **80**(6): 642-650.

Chang, C.F. 2008. Reconfiguration and Capacitor Placement for Loss Reduction of Distribution Systems by Ant Colony Search Algorithm. *IEEE Transactions on Power Systems* **23**(4): 1747-1755.

Chang, C.S. & Huang, J.S. 1997. Optimal SVC placement for voltage stability reinforcement. *Electric Power Systems Research* **42**(3): 165-172.

Chen, T.H., Chen, M.S., Inoue, T., Kotas, P. & Chebli, E.A. 1991. Three-phase cogenerator and transformer models for distribution system analysis. *IEEE Transactions on Power Delivery* **6**(4) :1671-1681.

Chis, M., Salama, M.M.A. & Jayaram, S. 1997. Capacitor placement in distribution system using heuristic search strategies. *IEE Proceedings Generation Transmission and Distribution* **144**(3):225–230.

Coevering, J.V., Stovall, J.P., Hauth, R.L., Tatto, P.J., Railing, B.D. & Johnson, B.K. 1996. The next generation of HVDC- needed R&D, equipment costs, and cost comparisons. *Proceeding of EPRI Conference in Future Power Delivery* :9–10.

Cutsem, T. & Vournas, C. 1998. *Voltage stability of electric power systems*. Springer. Kluwer Academic Publishers.

Das, B.,Verma, P.K. 2001. Artificial neural network-based optimal capacitor switching in a distribution system. *Electric Power Systems Research* **60**(2):55–62.

Das, D .2008. Optimal placement of capacitors in radial distribution system using a Fuzzy-GA method. *Electrical Power and Energy Systems* **30**(6-7):361–367.

Das, D. 2002. Reactive power compensation for radial distribution networks using genetic algorithm. *International Journal of Electrical Power & Energy Systems* **24**(7) :573-581.

Dawkins, R. 1976. *The Selfish Gene*. Oxford University Press.

Del Valle, Y., Hernandez, J.C. ,Venayagamoorthy , G.K. & Harley, R.G. 2006. Optimal STATCOM Sizing and Placement Using Particle Swarm Optimization. *Proceedings of the IEEE Transmission and Distribution Conference and Exposition Latin America* :1-6.

Del Valle, Y., Venayagamoorthy, G. K. & Harley, R.G. 2009. Comparison of Enhanced-PSO and Classical Optimization Methods: a case study for STATCOM placement. *Proceedings of the IEEE 15th International Conference on Intelligent System Applications to Power Systems*: 1-7.

Del-Ser, J., Matinmikko, M., Gil-Lopez, S. & Mustonen, M. 2012. Centralized and distributed spectrum channel assignment in cognitive wireless networks: a harmony search approach. *Applied Soft Computing* **12**(2):921–930.

Dixon , J., Morán, L., Rodríguez, J. & Domke, R. 2006. Reactive Power Compensation Technologies, State of-the-Art Review. *Converter Technology & Electric Traction* **6**:19-24.

Dominguez-Navarro, J. A., Bernal-Agustin, J. L. , Diaz, A. , Requena, D. & Vargas, E.P. 2007.Optimal parameters of FACTS devices in electric power systems applying evolutionary strategies. *Electrical Power and Energy Systems* **29**(1): 83–90.

Dorigo, M. & Maniezzo, V. 1992. Optimization, Learning and Natural Algorithms. *Ph.D. Thesis.Politecnico di Milano.* Italy.

Eberhart, R.C. & Shi, Y. 2000. Comparing inertia weights and constriction factors in Particle Swarm Optimization.*Proceedings of the Congress on Evolutionary Computating*: 84-88.

Eghbal, M., Yorino, N. & Zoka, Y. 2009. Comparative Study on the Application of Modern Heuristic Techniques to SVC Placement Problem. *Journal of Computers* **4**(6):535-541.

Ejal, A. & Elhawary, M.E. 2010. Optimal Capacitor Placement and Sizing in Unbalanced Distribution System With Harmonics Consideration Using

Particle Swarm Optimization. *IEEE Transactions on Power Delivery* **25**(3) :1734-1741.

Ejal, A .2008. Optimal Capacitor Placement and Sizing in Unbalanced Distribution Systems With Harmonics Consideration Using PSO. *Dissertation in Master of Applied Sciences*. Dalhousie University.Halifax. Canada.

Elmitwally, A .2011. Optimal Sizing And Location Of Capacitor Banks In Distorted Distribution Networks With Distributed Wind Generation. *21st International Conference on Electricity Distribution*: 1-4.

Eslami, M., Shareef, H. & Mohamed, A. 2011. Application of artificial intelligent techniques in PSS design:a survey of the state-of-the-art methods. *Przegląd Elektrotechniczny* **87**(4):188-197.

Etemadzadeh, R., Nabavi, R. & Shayanfar, H.A. 2010. Optimal Placement of SVC Based on Line Flow Base Equation Using Mixed Integer Nonlinear Programming. *Proceedings of the IEEE conference*: 1-5.

Farmer, J.D., Packard, N.H. & Perelson, A.S. 1986. The immune system, adaptation, and machine learning. *Physica* **D 22**(1-3): 187-204.

Farsangi, M.M., Nezamabadi-pour, H., Song Y.H. & Lee, K.Y. 2007. Placement of SVCs and Selection of Stabilizing Signals in Power Systems. *IEEE Transactions on Power Systems* **22**(3):1061-1071.

Fogel, L.J., Owens, A.J. & Walsh, M.J. 1966. *Artificial Intelligence Through Simulated Evolution. New York. John Wiley.*

Galiana, G. D. 1996. Assessment and Control of the Impact of FACTS devices on Power System Performance. *IEEE Transactions on Power Systems* **11**(4):1931-1936.

Gallego, R.A., Monticelli, A.J. , Romero, R. 2001. Optimal Capacitor Placement in Radial Distribution Networks. *IEEE Transactions on Power Systems* **16**(4):630-637.

Geem, Z., Kim, J. & Loganathan, G. 2001. A new heuristic optimization algorithm: Harmony search. *Simulation* **76**(2) :60-68.

Ghose, T. & Goswam, S.K. .2003. Effects of unbalances and harmonics on optimal capacitor placement in distribution system. *Electric Power Systems Research* **68**(2):167-173.

Gil-Lopez, S., Del-Ser, J., Salcedo-Sanz, S., Perez-Bellido, A.M., Cabero, J.M. & Portilla-Figueras, J.A. 2012. A hybrid harmony search algorithm for the spread spectrum radar polyphase codes design problem. *Expert System with Applications* **39**(12):11089–11093.

Gitizadeh, M. & Kalantar, M. 2008. A New Approach for Congestion Management via Optimal Location of FACTS Devices in Deregulated Power Systems. Third *International Conference on Electric Utility Deregulation and Restructuring and Power Technologies*:1592-1597.

Glover, F. 1989. Tabu Search, Part I. *ORSA Journal on Computing* **1**(3): 190-206.

Glover, F. 1990. Tabu Search, Part II. *ORSA Journal on Computing* **2**(1) : 4-32.

Goldberg, D. 1989. *Genetic algorithms in search, optimization, and machine learning*. Addison-wesley.

Grudinin, N. & Roytelman, I. 1997. Heading Off Emergencies in Large Electric Grids. *IEEE Spectrum* **34**(4):43-47.

Guo, P., Xuezhi, W. & Han ,Y. 2010. The Enhanced Genetic Algorithms for the Optimization Design. *3rd International Conference on Biomedical Engineering and Informatics* :2991-2994.

Gyugyi, M.L., Shauder, C.D. & Sen , K.K. 1997. Static Synchronous Series Compensator A solid state Approach to the series compensation of transmission line. *IEEE Transactions on Power Delivery* **12**(3):406-417.

Haghdar, K. & Shayanfar, H.A. 2010. Optimal Placement and Sizing of DG and Capacitor for the Loss Reduction via Methods of Generalized Pattern Search and Genetic Algorithm. *Asia-Pacific Power and Energy Engineering Conference*:1-4.

Hernandez, J.C., Del Valle, Y., Venayagamoorthy, G.K. & Harley, R.G. 2006. Optimal Allocation of a STATCOM in a 45 Bus Section of the Brazilian Power System using Particle Swarm Optimization. *Proceedings of the IEEE Swarm Intelligence Symposium*:69-75.

Holland, J.H. 1975a. An introduction with application to biology, control and artificial intelligence Adaptation in Natural and Artificial System. *MIT Press*. Cambridge. MA.

Holland, J.H. 1975b. Adaptation in natural and artificial systems. *The University of Michigan Press*. AnnArbor. Michigan.

Hooshmand, R.A. & Mohkami, H. 2011. New optimal placement of capacitors and dispersed generators using bacterial foraging oriented by particle swarm optimization algorithm in distribution systems. *Electrical Engineering* **93**(1): 43–53.

Hsiao, Y.T. Chen, C. H. & Chien, C.C. 2004. Optimal capacitor placement in distribution systems using a combination fuzzy-GA method. *Electrical Power and Energy Systems* **26**(7) :501–508.

Hu, X., Shi, Y. & Eberhart, R. 2004. Recent advances in particle swarm . *Proceedings of 2004 Congress on Evolutionary Computation* **1** :90-97.

Huang, J.S. & Negnevitsky M. 2008. A Messy Genetic Algorithm Based Optimization Scheme for SVC Placement of Power Systems under Critical Operation Contingence. *International Conference on Computer Science and Software Engineering*: 467-472.

Huang, S. 2000. An immune-based optimization method to capacitor placement in a radial distribution system. *IEEE Transactions on Power Delivery* **15**(2) : 744 - 749.

Huang, T.L., Hsiao, Y.T. , Chang, C.H. & Jiang, J.A. 2008. Optimal placement of capacitors in distribution systems using an immune multi-objective algorithm. *International Journal of Electrical Power & Energy Systems* **30**(3):184–192.

IEEE Std 18–1992. 1992. IEEE Standard for Shunt Power Capacitors. *Institute of Electrical and Electronics Engineers.*

IEEE Std 519–1992. 1992. IEEE Recommended Practices and Requirements for Harmonic Control in Electrical Power Systems. *Institute of Electrical and Electronics Engineers.*

Ishak, S., Abidin, A.F. & Rahinan, T.K.A. 2004. Static Var Compensator Planning Using Artificial Immune System For Loss Minimisation And Voltage Improvement. *National Power & Energy Conference (PECon2004)*: 41-45.

Jumaat, S.A., Musirin, I., Othman, M. M. & Mokhlis, H. 2011. PSO Based Technique for Loss Minimization Considering Voltage Profile and Cost Function. *The 5th International Power Engineering and Optimization Conference (PEOCO2011):* 36-41.

Kannan, S.M. , Rathina, A. , Monica , G. & Slochanal, S.M.R .2008. Fuzzy Logic Based Optimal Capacitor Placement on Radial Distribution Feeders. *Power System Technology and IEEE Power India Conference*:1-6.

Karami, A., Rashidinejad, M. & Gharaveisi, A.A. 2006. Optimal Location of STATCOM for Voltage Security Enhancement via Artificial Intelligent. *IEEE International Conference on Industrial Technology*:2704-2708.

Kazemi, A., Parizad, A. & Baghaee, H.R. 2009. On the use of harmony search algorithm in optimal placement of facts devices to improve power system security. *Proceeding of IEEE EUROCON '09* :570-576.

Kennedy, J. & Eberhart, R. 1995. Particle swarm optimization. *IEEE International Conference on Neural Networks* : 1942-1948.

Khajehzadeh, M., Taha, M.R., El-Shafie , A. & Eslami, M. 2011. A Survey on Meta-Heuristic Global Optimization Algorithms. *Research Journal of Applied Sciences, Engineering and Technology* **3**(6): 569-578.

Khalil, T.M., Youssef, H. K.M. & Abdel Aziz, M.M. 2007. Optimal capacitor placement on radial distribution feeders in presence of nonlinear loads using binary particle swarm optimization. *19th International Conference on Electricity Distribution*: 1-4.

Khandani, F., Soleymani, S. & Mozafari, B. 2011. Optimal Allocation of SVC to Enhance Total Transfer Capability Using Hybrid Genetics Algorithm and Sequential Quadratic Programming. *The 8th Electrical Engineering / Electronics, Computer, Telecommunications and Information Technology (ECTI)* : 861-864.

Kim, T., Lee, Y., Lee, B. & Song, H. 2009. Optimal Capacitor Placement considering Voltage Stability Margin based on improved PSO algorithm. *15th International Conference on Intelligent System Applications to Power Systems*:1-6.

Kirkpatrick, S., Gelatt , C.D. & Vecchi, M. P. 1983. Optimization by simulated annealing. *Science* **220**(4598): 671-680.

Kundur, P. 1994 . *Power System Stability and control*. New York. McGraw-Hill Inc.

Ladjavardi, M., Masoum, M.A.S. 2008. Genetically Optimized Fuzzy Placement and Sizing of Capacitor Banks in Distorted Distribution Networks. *IEEE Transactions on Power Delivery* **23**(1): 449-456.

Laifa, A. & Boudour, M. 2009. Optimal Location of SVC for Voltage Security Enhancement using MOPSO. *Journal of Electrical Systems* **1**: 73-78.

Lee, K. & Geem, Z. 2005. A new meta-heuristic algorithm for continuous engineering optimization: harmony search theory and practice. *Computer Methods in Applied Mechanics and Engineering* **194**(36-38): 3902-3933.

Mahdad, B., Bouktir, T. & Srairi, K. 2006. Strategy of Location and Control of FACTS Devices for Enhancing Power Quality. *IEEE MELECON Conference*: 1068-1072.

Mahdavi, M., Fesanghary, M. & Damangir, E. 2007. An improved harmony search algorithm for solving optimization problems. *Applied Mathematics and Computation* **188**(2):1567–1579.

Majumdar, S., Chakraborty, A.K. & Chattopadhyay, P.K. 2009. Active Power Loss Minimization With FACTS Devices Using SA/PSO Techniques. Third *International Conference on Power Systems*:1-5.

Masoum, M.A.S., Ladjevardi, M., Jafarian, A. & Fuchs, E.F. 2004. Optimal Placement, Replacement and Sizing of Capacitor Banks in Distorted Distribution Networks by Genetic Algorithms. *IEEE Transactions on Power Delivery* **19**(4):1794-1803.

Masoum, M., Jafaraian, A., Ladjevardi, M., Fuchs, E. & Grady, W. 2004. Fuzzy approach for optimal placement and sizing of capacitor banks in the presence of harmonics. *IEEE Transactions on Power Delivery* **19**(2):822-829.

Miller, T.J. 1982. *Reactive power Control in Electric Systems.* New York. John Willey & Sons.

Minguez, R., Milano, F. , Zarate-Minano, R. & Conejo, A.J. 2007. Optimal Network Placement of SVC Devices. *IEEE Transations on Power System* **22**(4):1851-1860.

Mithulananthan, N., Cañizares, C.A. & Reeve, J. 2003. Comparison of PSS, SVC and STATCOM controllers for damping power system oscillation. *IEEE Transations on Power System* **18**(2):786–792.

Mohammadi, A. & Jazaeri, M. 2007. A hybrid particle swarm optimization-genetic algorithm for optimal location of svc devices in power system planning. *42nd International Universities Power Engineering Conference* :1175 - 1181.

Mohkami, H., Hooshmand, R., Khodabakhshian, A. 2011. Fuzzy optimal placement of capacitors in the presence of nonlinear loads in unbalanced distribution networks using BF-PSO algorithm. *Applied Soft Computing* **11**:3634–3642.

Mori, H. & Tsunokawa, S. 2005. Variable Neighborhood Tabu Search for Capacitor Placement in Distribution Systems, *IEEE International Symposium on Circuits and Systems. ISCAS 2005*:4747-4750.

Nakrani, S. & Tovey, C. 2004. On honey bees and dynamic server allocation in internet hosting centers. *Adaptive Behavior* **12**(3-4): 223.

Ng, H., Salama, M. & Chikhani, A. 2000. Classification of capacitor allocation techniques. *IEEE Transactions on Power Delivery* **15**(1): 387-392.

Oo, N. W. 2008. A comparison study on particle swarm and Evolutionary Particle Swarm Optimization using capacitor placement problem. *IEEE 2nd International Power and Energy Conference*:1208-1211 .

Panda, S. & Padhy,N. P. 2008. Optimal location and controller design of STATCOM for power system stability improvement using PSO. *Journal of the Franklin Institute* **345**(2): 166–181.

Parizad, A., Kalantar, M. & Khazali, A. 2009. Application of HSA and GA in Optimal Placement of FACTS Devices Considering Voltage Stability and Losses. *International Conference on Electric Power and Energy Conversion Systems*: 1-7.

Passino, K. 2002. Biomimicry of bacterial foraging for distributed optimization and control. *IEEE Control Systems Magazine* **22**(3):52-67.

Pimentel Filho, M.C., De Lacerda, E.G. M. & Medeiros Junior, M.F. 2009. Capacitor Placement Using Ant Colony Optimization and Gradient .*15th International Conference on Intelligent System Applications to Power Systems*:1-4.

Pirayesh, A., Parastar, A. & Nikoukar, J. 2007. Optimal location of FACTS devices in a power system using modified particle swarm optimization. *42nd International Universities Power Engineering Conference*:1122-1128.

Pisica, I., Bulac, C. ,Toma, L. & Eremia, M. 2009. Optimal SVC Placement in Electric Power Systems Using a Genetic Algorithms Based Method .*IEEE Bucharest Power Tech Conference* :1-6.

Power Systems Test Case Archive. *University of Washington*. ONLINE. http://www.ee.washington.edu/research/pstca/

Prakash, K. & Sydulu, M. 2007. Particle swarm optimization based capacitor placement on radial distribution systems. *IEEE Power Engineering Society General Meeting*:1-5.

Quillen, C.A. 2009. Analysis of Reactive Power Compensation Methods in Distribytion Systems. *Master thesis .Tennessee Technological University*.

Rao, K.S. & Kalyan Kumar, B. 2011. Placement of SVC for Minimizing Losses and Maximizing Total Transfer Capability using Particle Swarm Optimization. *IET Conference Publications*:1-5.

Rao, R.S., Narasimham, S.V.L & Ramalingaraju, M. 2011. Optimal capacitor placement in a radial distribution system using Plant Growth Simulation Algorithm. *Electrical Power and Energy Systems* **33**(5):1133–1139.

Rashedi, E., Nezamabadi-Pour, H. & Saryazdi, S. 2009. GSA: A gravitational search algorithm. *Information Sciences* **179**(13): 2232-2248.

Rechenberg, I. 1965. Cybernetic solution path of an experimental problem. *Royal Aircraft Establishment. brary Translation* 1122.

Reddy, M.D. & Reddy V.C.V. 2008. Capacitor Placement Using Fuzzy and Particle Swarm Optimization Method for Maximum Annual Savings. *ARPN Journal of Engineering and Applied Sciences* **3**(3):25-30.

Rezaee Jordehi, A. & Joorabian , M. 2011. Optimal Placement of Multi-Type FACTS Devices in Power Systems Using Evolution Strategies. *The 5th International Power Engineering and Optimization Conference (PEOCO2011)*:352-357.

Rini , P.D. , Shamsuddin , S.M. & Yuhaniz , S. S. 2011. Particle Swarm Optimization: Technique, System and Challenges. *International Journal of Computer Applications* **14**(1) :19-27.

Saadat, H. 2002. *Power Systems Analysis.* New York. McGraw-Hill.

Salloum, A. 2011. Optimal Location and Sizing of Dynamic VArs for Fast Voltage Collapse . *Master thesis. Arizona State University*.

Samimi, A. & Golkar, M.A. 2011. A novel method for optimal placement of STATCOM in distribution networks using sensitivity analysis by DIgSILENT software. *Asia-Pacific Power Energy Engineering Conference* :1–5.

Santiago, M. & Maldonado, R. 2006. Optimal Placement of FACTS Controllers in Power systems via Evolutionary Strategies. *Proceedings of IEEE international conference on Transmission and Distribution Evolutionary Computation*: 1-6.

Saranjeet, K. 2009. Evolutionary Algorithm Assisted Optimal Placement of FACTS Controllers in Power system. *Master Thesis. Thapar University*.

Saranya, S.G., Muthukumaran, E., Kannan, S.M. & Kalyani, S. 2011. Optimal Capacitor Placement in Radial Distribution Feeders Using Fuzzy-Differential Evolution . *Proceedings of the National Conference on Innovations in Emerging Technology*:85-90.

Saravanan, M., Slochanal, S.M.R., Venkatesh, P., Abraham, J.P.S. 2007. Application of particle swarm optimization technique for optimal location of FACTS devices considering cost of installation and system loadability. *Electric Power System Research* **77**(3-4):276–283.

Sharma, C. 2007. Ganness MG. Determination of power system voltage stability using modal analysis. *IEEE International Conference Power Engineering, Energy and Electrical Drives* :381–387.

Shaygan, M., Seifossadat, S.G.H. & Razaz, M. 2011. Study the Effects of STATCOM on the Static Voltage Stability Improvement and Reduction of Active and Reactive Losses .*International Review of Electrical Engineering* **6**(4) :1862-1869.

Shi, Y. & Eberhart, R. 1998. A modified particle swarm optimizer. Proceedings of the IEEE Congress on Evolutionary Computation: 69-73.

Shyr, W. J., 2008. Introduction and Comparison of Three Evolutionary-Based Intelligent Algorithms for Optimal Design. *Third International Conference on Convergence and Hybrid Information Technology*: 879-884.

Smith, S.F. 1980. A learning system based on genetic adaptive algorithms. *Ph.D. Thesis*. University of Pittsburgh.

Sode-Yome, A. & Mithulananthan, N. 2004. Comparison of shunt capacitor, SVC and STATCOM in static voltage stability margin enhancement. *International Journal of Electrical Engineering Education* **41**(2):158–171.

Sreedharan,S., Ongsakul, W. Singh, J.G. Buayai, K. & Wartana, I.M. 2011. PSO Based Tuning of FACTS Controllers for Maximizing the Wind Energy Penetration in Power Systems. *IEEE PES Innovative Smart Grid Technologies*:287-293.

Stevenson,W.D. & Jr. 1982. *Elements of Power System Analysis*. New York. McGraw- Hill Book Company. 4th Edition.

Sundareswaran, K., Bharathram, P., Siddharth, M.,Vaishnavi, G., Shrivastava, N.A. & Sarma , H. 2009. Voltage Profile enhancement through optimal placement of FACTS devices using Queen-Bee-Assisted GA. *Third International Conference on Power Systems*: 1-5.

Sundareswaran, K., Hariharan, B. ,Parasseri, F.P. Antony, D.S. & Subair, B. 2009. Optimal Placement of Static VAr Compensators (SVC's) Using Particle Swarm Optimization. International Conference on Power, Control and Embedded Systems (ICPCES):1-4.

Sundareswaran, K., Srinivasarao Nayak, P., Venkatesh, D. & Hariharan, B. 2011. Optimal Placement of FACTS Devices using Probabilistic Particle Swarm Optimization. *IEEE PES Innovative Smart Grid Technologies*: 1-6.

Swarnkar, A., Gupta, N. & Niazi, K.R. 2010. Optimal Placement of Fixed and Switched Shunt Capacitors for Large-Scale Distribution Systems using Genetic Algorithms. *Innovative Smart Grid Technologies Conference*:1-8.

Tabatabaei, S.M. & Vahidi, B. 2011. Bacterial foraging solution based fuzzy logic decision for optimal capacitor allocation in radial distribution system. *Electric Power Systems Research* **81**(4):1045–1050.

Talebi, M.A., Kazemi, A. ,Gholami, A. & Rajabi, M. 2005. Optimal placement of Static VAR Compensators in distribution feeders for load balancing by genetic algorithm. *18th International Conference and Exhibition on Electricity Distribution*: 1-6.

Tao, L., Si-yuan,W. & Jie , Z. 2010. Power quality analysis based on ETAP software. *Journal of Electric Power Science and Technology* 1: 1-6.

Tavakoli Bina, M. , Rezaei Siahbidi , J. & Kanzi, K. 2005. Application of Averaging Technique to the Power System Optimum Placement and Sizing of Static Compensators. *The 7th International Power Engineering Conference*:1-6.

Taylor, C. 1994. *Power system voltage stability*. New York. MC Graw Hill.

Taylor, C. W. 1999. Improving Grid Behavior. *IEEE Spectrum* **36**(6):40-45.

Teng, J. & Chang, C.Y. 2007. Backward/Forward Sweep-Based Harmonic Analysis Method for Distribution System. *IEEE Transaction on Power Delivery* **22**(3):1665-1672.

Teng, J. 2000. A network-topology-based three-phase load flow for distribution systems. *Proc Natl. Sci. Counc. ROC (A)* **24** :259-264.

Thukaram, D. & Lomi, A. 2000. Selection of static VAR compensator location and size for system voltage stability improvement. *Electric Power System Research* **54**(2):139–150.

Tibin, J., Sini, X., Chitra, S. Cherian, V. I. & Sreedharan, S. 2011. PSO Based Optimal Placement and Setting of FACTS Devices for Improving the Performance of Power Distribution System. *Bonfring International Journal of Power Systems and Integrated Circuits* **1**:60-64.

Tinney , W. & Hart, C. 1972. Power flow solution by Newton's method. *IEEE Transactions on Power Apparatus and Systems* **86**(6).

Varshney, S., Srivastava, L. & Pandit , M. 2011. Comparison of PSO Models for Optimal Placement and Sizing of Statcom. Second International Conference on Sustainable Energy and Intelligent System :346-351.

Wanner, E., Mathys, R. & Hausler, M. 1983 .Compensation Systems for Industry. *Brown Boveri Review* **70** :330-340.

Wu, Q. H., Lu, Z. , Li, M. S. & Ji, T.Y. 2008. Optimal Placement of FACTS Devices by A Group Search Optimizer with Multiple Producer, Evolutionary Computation, *IEEE World Congress on Computational Intelligence*: 1033-1039.

Yang , W. & Li, Q.Q. 2004. Survey on particle swarm optimization algorithm. *Journal of Engineering Science* **6**(5):87-94.

Yu, X.M. , Xiong, X.Y. & Wu, Y.W. 2004. A PSO-based approach to optimal capacitor placement with harmonic distortion consideration. *Electric Power Systems Research* **71**(1):27–33.

Zhang, W., Li, F. & Tolbert, L.M. 2006. Optimal Allocation of Shunt Dynamic Var Source SVC and STATCOM: A Survey. *Department of Electrical and Computer Engineering. the University of Tennessee. Knoxville*: 1-6.

Zhang, X.P. & Rehtanz, C. & Pal, B. 2006. *Flexible AC Transmission systems Modelling and Control*. Berlin. Springer.

Zhang, Y. & Milanovic, J.V. 2007. Voltage Sag Cost Reduction With Optimally Placed FACTS Devices. *9th International Conference on Electrical Power, Quality and Utilisation*: 1-6.

Zhezhelenko, I.V., Gorpinich, A.V. & Khalil, T.M .2009. Optimal Capacitor Placement in Distribution System Considering Mutual Coupling, Load Unbalancing and Harmonics. *20th International Conference on Electricity Distribution*:1-4.

Zou, D., Gao, L., Li, S., Wu, J. & Wang, X. 2010. A novel global harmony search algorithm for task assignment problem. *Journal of Systems and Software* **83**(10):1678–1688.

Zou, D., Gao, L., Wu, J., Li, S. & Li, Y. 2010. A novel global harmony search algorithm for reliability problems. *Computers & Industrial Engineering* **58**(2):307–316.

APPENDIX A

PARTIAL DERIVATIVES FOR STATCOM MODEL

Partial derivatives for the static compensator (STATCOM) model are:

$$\frac{\partial P_k}{\partial \theta_k} = -Q_k - V_k^2 G_{vR} \tag{A.1}$$

$$\frac{\partial P_k}{\partial \delta_{vR}} = V_k V_{vR}[G_{vR} \sin(\theta_k - \delta_{vR}) - B_{vR} \cos(\theta_k - \delta_{vR})] \tag{A.2}$$

$$\frac{\partial P_{vR}}{\partial \delta_{vR}} = -Q_{vR} - V_{vR}^2 B_{vR} \tag{A.3}$$

$$\frac{\partial P_{vR}}{\partial \theta_k} = V_k V_{vR}[G_{vR} \sin(\delta_{vR} - \theta_k) - B_{vR} \cos(\delta_{vR} - \theta_k)] \tag{A.4}$$

$$\frac{\partial P_k}{\partial V_k} V_k = P_k + V_k^2 G_{vR} \tag{A.5}$$

$$\frac{\partial P_k}{\partial V_{vR}} V_{vR} = V_k V_{vR}[G_{vR} \cos(\theta_k - \delta_{vR}) - B_{vR} \sin(\theta_k - \delta_{vR})] \tag{A.6}$$

$$\frac{\partial P_{vR}}{\partial V_k} V_{vR} = P_{vR} + V_{vR}^2 G_{vR} \tag{A.7}$$

$$\frac{\partial P_{vR}}{\partial V_k} V_k = V_k V_{vR}[G_{vR} \cos(\delta_{vR} - \theta_k) - B_{vR} \sin(\delta_{vR} - \theta_k)] \tag{A.8}$$

$$\frac{\partial Q_k}{\partial \theta_k} = P_k - V_k^2 G_{vR} \tag{A.9}$$

$$\frac{\partial Q_k}{\partial \delta_{vR}} = -V_k V_{vR}[G_{vR} \cos(\theta_k - \delta_{vR}) + B_{vR} \sin(\theta_k - \delta_{vR})] \tag{A.10}$$

$$\frac{\partial Q_{vR}}{\partial \delta_{vR}} = P_{vR} - V_{vR}^2 G_{vR} \tag{A.11}$$

$$\frac{\partial Q_{vR}}{\partial \theta_k} = -V_k V_{vR}[G_{vR} \cos(\delta_{vR} - \theta_k) + B_{vR} \sin(\delta_{vR} - \theta_k)] \tag{A.12}$$

$$\frac{\partial Q_k}{\partial V_k} V_k = Q_k - V_k^2 B_{vR} \tag{A.13}$$

$$\frac{\partial Q_k}{\partial V_{vR}} V_{vR} = V_k V_{vR} [G_{vR} \sin(\theta_k - \delta_{vR}) - B_{vR} \cos(\theta_k - \delta_{vR})] \tag{A.14}$$

$$\frac{\partial Q_{vR}}{\partial V_k} V_{vR} = Q_{vR} - V_{vR}^2 B_{vR} \tag{A.15}$$

$$\frac{\partial Q_{vR}}{\partial V_k} V_k = -V_k V_{vR} [G_{vR} \sin(\delta_{vR} - \theta_k) - B_{vR} \cos(\delta_{vR} - \theta_k)] \tag{A.16}$$

APPENDIX B

IEEE 34 BUS TEST SYSTEM DATA

Table B.1 Load and line data of the 34 bus test system

Bus Number	Load		Sectional Parameters				Length (km)
			Bus Number		Impedance(Ω/km)		
	P(kW)	Q(kvar)	From	To	R	X	
2	230	142.5	1	2	0.195	0.08	0.6
3	0	0	2	3	0.195	0.08	0.55
4	230	142.5	3	4	0.299	0.083	0.55
5	230	142.5	4	5	0.299	0.083	0.55
6	0	0	5	6	0.299	0.083	0.5
7	0	0	6	7	0.524	0.09	0.6
8	230	142.5	7	8	0.524	0.09	0.4
9	230	142.5	8	9	0.524	0.09	0.6
10	0	0	9	10	0.524	0.09	0.4
11	230	142.5	10	11	0.524	0.09	0.25
12	137	84	11	12	0.524	0.09	0.2
13	72	45	3	13	0.524	0.09	0.3
14	72	45	13	14	0.524	0.09	0.4
15	72	45	14	15	0.524	0.09	20
16	13.5	7.5	15	16	0.524	0.09	0.1
17	230	142.5	6	17	0.299	0.083	0.6
18	230	142.5	17	18	0.299	0.083	0.55
19	230	142.5	18	19	0.378	0.086	0.55
20	230	142.5	19	20	0.378	0.086	0.5
21	230	142.5	20	21	0.378	0.086	0.5
22	230	142.5	21	22	0.524	0.09	0.5
23	230	142.5	22	23	0.524	0.09	0.5
24	230	142.5	23	24	0.524	0.09	0.6
25	230	142.5	24	25	0.524	0.09	0.4
26	230	142.5	25	26	0.524	0.09	0.25
27	137.5	85	26	27	0.524	0.09	0.2
28	75	48	7	28	0.524	0.09	0.3
29	75	48	28	29	0.524	0.09	0.3
30	75	48	29	30	0.524	0.09	0.3
31	57	34.5	10	31	0.524	0.09	0.3
32	57	34.5	31	32	0.524	0.09	0.4
33	57	34.5	32	33	0.524	0.09	0.3
34	57	34.5	33	34	0.524	0.09	0.2

APPENDIX C

UNBALANCED 34 BUS TEST SYSTEM DATA

Table C.1 Line data of the unbalanced 34 bus test system

Node A	Node B	Length(ft.)	Config.
800	802	2580	300
802	806	1730	300
806	808	32230	300
808	810	5804	303
808	812	37500	300
812	814	29730	300
814	850	10	301
816	818	1710	302
816	824	10210	301
818	820	48150	302
820	822	13740	302
824	826	3030	303
824	828	840	301
828	830	20440	301
830	854	520	301
832	858	4900	301
832	888	0	XFM-1
834	860	2020	301
834	842	280	301
836	840	860	301
836	862	280	301
842	844	1350	301
844	846	3640	301
846	848	530	301
850	816	310	301
852	832	10	301
854	856	23330	303
854	852	36830	301
858	864	1620	302
858	834	5830	301
860	836	2680	301
862	838	4860	304
888	890	10560	300

Table C.2 Transformer data of the unbalanced 34 bus test system

	kVA	kV-high	kV-low	R - %	X - %
Substation:	2500	69 - D	24.9 -Gr. W	1	8
XFM -1	500	24.9 - Gr.W	4.16 - Gr. W	1.9	4.08

Table C.3 Distributed loads of the unbalanced 34 bus test system

Node A	Node B	Load Model	Ph-1 kW	Ph-1 kVAr	Ph-2 kW	Ph-2 kVAr	Ph-3 kW	Ph-3 kVAr
802	806	Y-PQ	0	0	30	15	25	14
808	810	Y-I	0	0	16	8	0	0
818	820	Y-Z	34	17	0	0	0	0
820	822	Y-PQ	135	70	0	0	0	0
816	824	D-I	0	0	5	2	0	0
824	826	Y-I	0	0	40	20	0	0
824	828	Y-PQ	0	0	0	0	4	2
828	830	Y-PQ	7	3	0	0	0	0
854	856	Y-PQ	0	0	4	2	0	0
832	858	D-Z	7	3	2	1	6	3
858	864	Y-PQ	2	1	0	0	0	0
858	834	D-PQ	4	2	15	8	13	7
834	860	D-Z	16	8	20	10	110	55
860	836	D-PQ	30	15	10	6	42	22
836	840	D-I	18	9	22	11	0	0
862	838	Y-PQ	0	0	28	14	0	0
842	844	Y-PQ	9	5	0	0	0	0
844	846	Y-PQ	0	0	25	12	20	11
846	848	Y-PQ	0	0	23	11	0	0
Total			262	133	240	120	220	114

Table C.4 Spot loads of the unbalanced 34 bus test system

Node	Load Model	Ph-1 kW	Ph-1 kVAr	Ph-2 kW	Ph-2 kVAr	Ph-3 kW	Ph-4 kVAr
860	Y-PQ	20	16	20	16	20	16
840	Y-I	9	7	9	7	9	7
844	Y-Z	135	105	135	105	135	105
848	D-PQ	20	16	20	16	20	16
890	D-I	150	75	150	75	150	75
830	D-Z	10	5	10	5	25	10
Total		344	224	344	224	359	229

Table C.5 Overhead line configurations of the unbalanced 34 bus test system

Config.	Phasing	Phase ACSR	Neutral ACSR	Spacing Type
300	B A C N	1/0	1/0	Three-Phase, 4 wire
301	B A C N	#2 6/1	#2 6/1	Three-Phase, 4 wire
302	A N	#4 6/1	#4 6/1	Single-Phase, 2 wire
303	B N	#4 6/1	#4 6/1	Single-Phase, 2 wire
304	B N	#2 6/1	#2 6/1	Single-Phase, 2 wire

Impedances of the unbalanced 34 bus test system are as follow:

Configuration 300:

Z (R +jX) in ohms per mile

1.3368	1.3343	0.2101	0.5779	0.2130	0.5015
		1.3238	1.3569	0.2066	0.4591
				1.3294	1.3471

B in micro Siemens per mile

5.3350	-1.5313	-0.9943
	5.0979	-0.6212
		4.8880

Configuration 301:

Z (R +jX) in ohms per mile

1.9300	1.4115	0.2327	0.6442	0.2359	0.5691
		1.9157	1.4281	0.2288	0.5238
				1.9219	1.4209

B in micro Siemens per mile

5.1207	-1.4364	-0.9402
	4.9055	-0.5951
		4.7154

Configuration 302:

Z (R +jX) in ohms per mile

2.7995	1.4855	0.0000	0.0000	0.0000	0.0000
		0.0000	0.0000	0.0000	0.0000
				0.0000	0.0000

B in micro Siemens per mile

4.2251	0.0000	0.0000
	0.0000	0.0000
		0.0000

Configuration 303:

Z (R +jX) in ohms per mile

0.0000	0.0000	0.0000	0.0000	0.0000	0.0000
		2.7995	1.4855	0.0000	0.0000
				0.0000	0.0000

B in micro Siemens per mile

0.0000	0.0000	0.0000
	4.2251	0.0000
		0.0000

Configuration 304:

Z (R +jX) in ohms per mile

0.0000	0.0000	0.0000	0.0000	0.0000	0.0000
		1.9217	1.4212	0.0000	0.0000
				0.0000	0.0000

B in micro Siemens per mile

0.0000	0.0000	0.0000
	4.3637	0.0000
		0.0000

Table C.6 Current spectra of harmonic loads

Harmonic Order	Fluorescent		ASD		Other	
	Mag. (pu)	Angle (deg)	Mag. (pu)	Angle (deg)	Mag. (pu)	Angle (deg)
1	1	-41.2	1	-1.5	1	-35
2	0	0	0	0	0	0
3	0.08	273.4	0.2168	0.7	0.0028	-105.8
4	0	0	0	0	0.038	-167.4
5	0.0428	339	0.00608	110.8	0.0008	-275.5
6	0	0	0	0	0.0332	-42.6
7	0.0084	137.7	0.0276	151.9	0	0
8	0	0	0	0	0.002	-275.5
9	0.0056	263.2	0.0172	-95	0	0
10	0	0	0	0	0	0
11	0.0036	39.8	0.0144	-13.9	0	0
12	0	0	0	0	0	0
13	0.0024	182.4	0.0116	95.2	0	0
14	0	0	0	0	0	0
15	0.002	287	0.01	-182.7	0	0

Table C.7 Harmonic loads location and composition

Bus No.	Harmonic load composition					
830	15%	fluorescent	20%	ASD	15%	other
832	30%	fluorescent	0%	ASD	60%	other
840	20%	fluorescent	20%	ASD	20%	other
844	15%	fluorescent	20%	ASD	15%	other
848	0%	fluorescent	0%	ASD	60%	other
860	10%	fluorescent	10%	ASD	20%	other

APPENDIX D

IEEE 57 BUS TEST SYSTEM DATA

Table D.1 Bus data of IEEE 57 bus test system

Bus	Type	P_d (MW)	Q_d(MVar)	Bus	Type	P_d (MW)	Q_d(MVar)
1	S	55	17	*30*	L	3.6	1.8
2	G	3	88	*31*	L	5.8	2.9
3	G	41	21	*32*	L	1.6	0.8
4	L	0	0	*33*	L	3.8	1.9
5	L	13	4	*34*	L	0	0
6	G	75	2	*35*	L	6	3
7	L	0	0	*36*	L	0	0
8	G	150	22	*37*	L	0	0
9	G	121	26	*38*	L	14	7
10	L	5	2	*39*	L	0	0
11	L	0	0	*40*	L	0	0
12	G	377	24	*41*	L	6.3	3
13	L	18	2.3	*42*	L	7.1	4.4
14	L	10.5	5.3	*43*	L	2	1
15	L	22	5	*44*	L	12	1.8
16	L	43	3	*45*	L	0	0
17	L	42	8	*46*	L	0	0
18	L	27.2	9.8	*47*	L	29.7	11.6
19	L	3.3	0.6	*48*	L	0	0
20	L	2.3	1	*49*	L	18	8.5
21	L	0	0	*50*	L	21	10.5
22	L	0	0	*51*	L	18	5.3
23	L	6.3	2.1	*52*	L	4.9	2.2
24	L	0	0	*53*	L	20	10
25	L	6.3	3.2	*54*	L	4.1	1.4
26	L	0	0	*55*	L	6.8	3.4
27	L	9.3	0.5	*56*	L	7.6	2.2
28	L	4.6	2.3	*57*	L	6.7	2
29	L	17	2.6				

Table D.2 Generator data of IEEE 57 bus test system

Bus	P_g(MW)	Q_g(MVar)	Q_{max}(MVar)	Q_{min}(MVar)	V_g (pu)
1	128.9	-16.1	200	-140	1.04
2	0	-0.8	50	-17	1.01
3	40	-1	60	-10	0.985
6	0	0.8	25	-8	0.98
8	450	62.1	200	-140	1.005
9	0	2.2	9	-3	0.98
12	310	128.5	155	-150	1.015

Table D.3 Branch data of IEEE 57 bus test system

Bus (From)	Bus (To)	R (Ω)	X (Ω)	B (Ω)	Bus (From)	Bus (To)	R (Ω)	X (Ω)	B (Ω)
1	2	0.0083	0.028	0.129	7	29	0	0.0648	0
2	3	0.0298	0.085	0.0818	25	30	0.135	0.202	0
3	4	0.0112	0.0366	0.038	30	31	0.326	0.497	0
4	5	0.0625	0.132	0.0258	31	32	0.507	0.755	0
4	6	0.043	0.148	0.0348	32	33	0.0392	0.036	0
6	7	0.02	0.102	0.0276	34	32	0	0.953	0
6	8	0.0339	0.173	0.047	34	35	0.052	0.078	0.0032
8	9	0.0099	0.0505	0.0548	35	36	0.043	0.0537	0.0016
9	10	0.0369	0.1679	0.044	36	37	0.029	0.0366	0
9	11	0.0258	0.0848	0.0218	37	38	0.0651	0.1009	0.002
9	12	0.0648	0.295	0.0772	37	39	0.0239	0.0379	0
9	13	0.0481	0.158	0.0406	36	40	0.03	0.0466	0
13	14	0.0132	0.0434	0.011	22	38	0.0192	0.0295	0
13	15	0.0269	0.0869	0.023	11	41	0	0.749	0
1	15	0.0178	0.091	0.0988	41	42	0.207	0.352	0
1	16	0.0454	0.206	0.0546	41	43	0	0.412	0
1	17	0.0238	0.108	0.0286	38	44	0.0289	0.0585	0.002
3	15	0.0162	0.053	0.0544	15	45	0	0.1042	0
4	18	0	0.555	0	14	46	0	0.0735	0
4	18	0	0.43	0	46	47	0.023	0.068	0.0032
5	6	0.0302	0.0641	0.0124	47	48	0.0182	0.0233	0
7	8	0.0139	0.0712	0.0194	48	49	0.0834	0.129	0.0048
10	12	0.0277	0.1262	0.0328	49	50	0.0801	0.128	0
11	13	0.0223	0.0732	0.0188	50	51	0.1386	0.22	0
12	13	0.0178	0.058	0.0604	10	51	0	0.0712	0
12	16	0.018	0.0813	0.0216	13	49	0	0.191	0
12	17	0.0397	0.179	0.0476	29	52	0.1442	0.187	0
14	15	0.0171	0.0547	0.0148	52	53	0.0762	0.0984	0
18	19	0.461	0.685	0	53	54	0.1878	0.232	0
19	20	0.283	0.434	0	54	55	0.1732	0.2265	0
21	20	0	0.7767	0	11	43	0	0.153	0
21	22	0.0736	0.117	0	44	45	0.0624	0.1242	0.004
22	23	0.0099	0.0152	0	40	56	0	1.195	0
23	24	0.166	0.256	0.0084	56	41	0.553	0.549	0
24	25	0	1.182	0	56	42	0.2125	0.354	0
24	25	0	1.23	0	39	57	0	1.355	0
24	26	0	0.0473	0	57	56	0.174	0.26	0
26	27	0.165	0.254	0	38	49	0.115	0.177	0.003
27	28	0.0618	0.0954	0	38	48	0.0312	0.0482	0
28	29	0.0418	0.0587	0	9	55	0	0.1205	0

APPENDIX E

IEEE 118 BUS TEST SYSTEM DATA

Table E.1 Bus data of IEEE 118 bus test system

Bus	Type	P_d (MW)	Q_d (MVar)	Bus	Type	P_d (MW)	Q_d (MVar)	Bus	Type	P_d (MW)	Q_d (MVar)
1	G	51	27	***41***	L	37	10	***81***	L	0	0
2	L	20	9	***42***	G	96	23	***82***	L	54	27
3	L	39	10	***43***	L	18	7	***83***	L	20	10
4	G	39	12	***44***	L	16	8	***84***	L	11	7
5	L	0	0	***45***	L	53	22	***85***	G	24	15
6	G	52	22	***46***	G	28	10	***86***	L	21	10
7	L	19	2	***47***	L	34	0	***87***	G	0	0
8	G	28	0	***48***	L	20	11	***88***	L	48	10
9	L	0	0	***49***	G	87	30	***89***	G	0	0
10	G	0	0	***50***	L	17	4	***90***	G	163	42
11	L	70	23	***51***	L	17	8	***91***	G	10	0
12	G	47	10	***52***	L	18	5	***92***	G	65	10
13	L	34	16	***53***	L	23	11	***93***	L	12	7
14	L	14	1	***54***	G	113	32	***94***	L	30	16
15	G	90	30	***55***	G	63	22	***95***	L	42	31
16	L	25	10	***56***	G	84	18	***96***	L	38	15
17	L	11	3	***57***	L	12	3	***97***	L	15	9
18	G	60	34	***58***	L	12	3	***98***	L	34	8
19	G	45	25	***59***	G	277	113	***99***	G	42	0
20	L	18	3	***60***	L	78	3	***100***	G	37	18
21	L	14	8	***61***	G	0	0	***101***	L	22	15
22	L	10	5	***62***	G	77	14	***102***	L	5	3
23	L	7	3	***63***	L	0	0	***103***	G	23	16
24	G	13	0	***64***	L	0	0	***104***	G	38	25
25	G	0	0	***65***	G	0	0	***105***	G	31	26
26	G	0	0	***66***	G	39	18	***106***	L	43	16
27	G	71	13	***67***	L	28	7	***107***	G	50	12
28	L	17	7	***68***	L	0	0	***108***	L	2	1
29	L	24	4	***69***	S	0	0	***109***	L	8	3
30	L	0	0	***70***	G	66	20	***110***	G	39	30
31	G	43	27	***71***	L	0	0	***111***	G	0	0
32	G	59	23	***72***	G	12	0	***112***	G	68	13
33	L	23	9	***73***	G	6	0	***113***	G	6	0
34	G	59	26	***74***	G	68	27	***114***	L	8	3
35	L	33	9	***75***	L	47	11	***115***	L	22	7
36	G	31	17	***76***	G	68	36	***116***	G	184	0
37	L	0	0	***77***	G	61	28	***117***	L	20	8
38	L	0	0	***78***	L	71	26	***118***	L	33	15
39	L	27	11	***79***	L	39	32				
40	G	66	23	***80***	G	130	26				

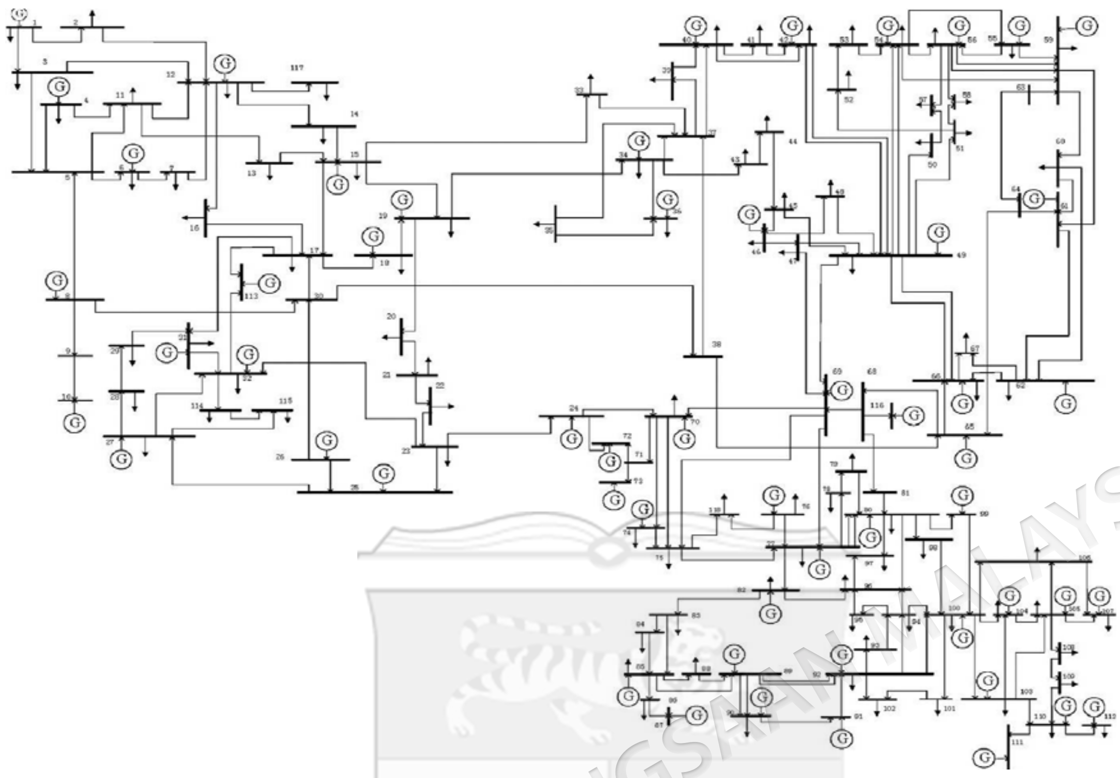

Figure E.1 Network diagram for the 118 bus test system

Table E.2 Generator data of IEEE 118 bus test system

Bus	P_g (MW)	Q_g (MVar)	Q_{max} (MVar)	Q_{min} (MVar)	V_g (pu)	Bus	P_g (MW)	Q_g (MVar)	Q_{max} (MVar)	Q_{min} (MVar)	V_g (pu)
1	0	0	15	-5	0.955	***65***	391	0	200	-67	1.005
4	0	0	300	-300	0.998	***66***	392	0	200	-67	1.05
6	0	0	50	-13	0.99	***69***	516.4	0	300	-300	1.035
8	0	0	300	-300	1.015	***70***	0	0	32	-10	0.984
10	450	0	200	-147	1.05	***72***	0	0	100	-100	0.98
12	85	0	120	-35	0.99	***73***	0	0	100	-100	0.991
15	0	0	30	-10	0.97	***74***	0	0	9	-6	0.958
18	0	0	50	-16	0.973	***76***	0	0	23	-8	0.943
19	0	0	24	-8	0.962	***77***	0	0	70	-20	1.006
24	0	0	300	-300	0.992	***80***	477	0	280	-165	1.04
25	220	0	140	-47	1.05	***85***	0	0	23	-8	0.985
26	314	0	1000	-1000	1.015	***87***	4	0	1000	-100	1.015
27	0	0	300	-300	0.968	***89***	607	0	300	-210	1.005
31	7	0	300	-300	0.967	***90***	0	0	300	-300	0.985
32	0	0	42	-14	0.963	***91***	0	0	100	-100	0.98
34	0	0	24	-8	0.984	***92***	0	0	9	-3	0.99
36	0	0	24	-8	0.98	***99***	0	0	100	-100	1.01
40	0	0	300	-300	0.97	***100***	252	0	155	-50	1.017
42	0	0	300	-300	0.985	***103***	40	0	40	-15	1.01
46	19	0	100	-100	1.005	***104***	0	0	23	-8	0.971
49	204	0	210	-85	1.025	***105***	0	0	23	-8	0.965
54	48	0	300	-300	0.955	***107***	0	0	200	-200	0.952
55	0	0	23	-8	0.952	***110***	0	0	23	-8	0.973
56	0	0	15	-8	0.954	***111***	36	0	1000	-100	0.98
59	155	0	180	-60	0.985	***112***	0	0	1000	-100	0.975
61	160	0	300	-100	0.995	***113***	0	0	200	-100	0.993
62	0	0	20	-20	0.998	***116***	0	0	1000	-1000	1.005

Table E.3 Branch data of IEEE 118 bus test system

Bus (From)	Bus (To)	R (Ω)	X (Ω)	B (Ω)	Bus (From)	Bus (To)	R (Ω)	X (Ω)	B (Ω)
1	***3***	0.0129	0.0424	0.01082	***64***	***61***	0	0.0268	0
4	***5***	0.00176	0.00798	0.0021	***38***	***65***	0.00901	0.0986	1.046
3	***5***	0.0241	0.108	0.0284	***64***	***65***	0.00269	0.0302	0.38
5	***6***	0.0119	0.054	0.01426	***49***	***66***	0.018	0.0919	0.0248
6	***7***	0.00459	0.0208	0.0055	***49***	***66***	0.018	0.0919	0.0248
8	***9***	0.00244	0.0305	1.162	***62***	***66***	0.0482	0.218	0.0578
8	***5***	0	0.0267	0	***62***	***67***	0.0258	0.117	0.031
9	***10***	0.00258	0.0322	1.23	***65***	***66***	0	0.037	0
4	***11***	0.0209	0.0688	0.01748	***66***	***67***	0.0224	0.1015	0.02682

Continued…

...Continued

5	***11***	0.0203	0.0682	0.01738	***65***	***68***	0.00138	0.016	0.638
11	***12***	0.00595	0.0196	0.00502	***47***	***69***	0.0844	0.2778	0.07092
2	***12***	0.0187	0.0616	0.01572	***49***	***69***	0.0985	0.324	0.0828
3	***12***	0.0484	0.16	0.0406	***68***	***69***	0	0.037	0
7	***12***	0.00862	0.034	0.00874	***69***	***70***	0.03	0.127	0.122
11	***13***	0.02225	0.0731	0.01876	***24***	***70***	0.00221	0.4115	0.10198
12	***14***	0.0215	0.0707	0.01816	***70***	***71***	0.00882	0.0355	0.00878
13	***15***	0.0744	0.2444	0.06268	***24***	***72***	0.0488	0.196	0.0488
14	***15***	0.0595	0.195	0.0502	***71***	***72***	0.0446	0.18	0.04444
12	***16***	0.0212	0.0834	0.0214	***71***	***73***	0.00866	0.0454	0.01178
15	***17***	0.0132	0.0437	0.0444	***70***	***74***	0.0401	0.1323	0.03368
16	***17***	0.0454	0.1801	0.0466	***70***	***75***	0.0428	0.141	0.036
17	***18***	0.0123	0.0505	0.01298	***69***	***75***	0.0405	0.122	0.124
18	***19***	0.01119	0.0493	0.01142	***74***	***75***	0.0123	0.0406	0.01034
19	***20***	0.0252	0.117	0.0298	***76***	***77***	0.0444	0.148	0.0368
15	***19***	0.012	0.0394	0.0101	***69***	***77***	0.0309	0.101	0.1038
20	***21***	0.0183	0.0849	0.0216	***75***	***77***	0.0601	0.1999	0.04978
21	***22***	0.0209	0.097	0.0246	***77***	***78***	0.00376	0.0124	0.01264
22	***23***	0.0342	0.159	0.0404	***78***	***79***	0.00546	0.0244	0.00648
23	***24***	0.0135	0.0492	0.0498	***77***	***80***	0.017	0.0485	0.0472
23	***25***	0.0156	0.08	0.0864	***77***	***80***	0.0294	0.105	0.0228
26	***25***	0	0.0382	0	***79***	***80***	0.0156	0.0704	0.0187
25	***27***	0.0318	0.163	0.1764	***68***	***81***	0.00175	0.0202	0.808
27	***28***	0.01913	0.0855	0.0216	***81***	***80***	0	0.037	0
28	***29***	0.0237	0.0943	0.0238	***77***	***82***	0.0298	0.0853	0.08174
30	***17***	0	0.0388	0	***82***	***83***	0.0112	0.03665	0.03796
8	***30***	0.00431	0.0504	0.514	***83***	***84***	0.0625	0.132	0.0258
26	***30***	0.00799	0.086	0.908	***83***	***85***	0.043	0.148	0.0348
17	***31***	0.0474	0.1563	0.0399	***84***	***85***	0.0302	0.0641	0.01234
29	***31***	0.0108	0.0331	0.0083	***85***	***86***	0.035	0.123	0.0276
23	***32***	0.0317	0.1153	0.1173	***86***	***87***	0.02828	0.2074	0.0445
31	***32***	0.0298	0.0985	0.0251	***85***	***88***	0.02	0.102	0.0276
27	***32***	0.0229	0.0755	0.01926	***85***	***89***	0.0239	0.173	0.047
15	***33***	0.038	0.1244	0.03194	***88***	***89***	0.0139	0.0712	0.01934
19	***34***	0.0752	0.247	0.0632	***89***	***90***	0.0518	0.188	0.0528
35	***36***	0.00224	0.0102	0.00268	***89***	***90***	0.0238	0.0997	0.106
35	***37***	0.011	0.0497	0.01318	***90***	***91***	0.0254	0.0836	0.0214
33	***37***	0.0415	0.142	0.0366	***89***	***92***	0.0099	0.0505	0.0548
34	***36***	0.00871	0.0268	0.00568	***89***	***92***	0.0393	0.1581	0.0414
34	***37***	0.00256	0.0094	0.00984	***91***	***92***	0.0387	0.1272	0.03268
38	***37***	0	0.0375	0	***92***	***93***	0.0258	0.0848	0.0218
37	***39***	0.0321	0.106	0.027	***92***	***94***	0.0481	0.158	0.0406
37	***40***	0.0593	0.168	0.042	***93***	***94***	0.0223	0.0732	0.01876
30	***38***	0.00464	0.054	0.422	***94***	***95***	0.0132	0.0434	0.0111
39	***40***	0.0184	0.0605	0.01552	***80***	***96***	0.0356	0.182	0.0494
40	***41***	0.0145	0.0487	0.01222	***82***	***96***	0.0162	0.053	0.0544
40	***42***	0.0555	0.183	0.0466	***94***	***96***	0.0269	0.0869	0.023
41	***42***	0.041	0.135	0.0344	***80***	***97***	0.0183	0.0934	0.0254
43	***44***	0.0608	0.2454	0.06068	***80***	***98***	0.0238	0.108	0.0286
34	***43***	0.0413	0.1681	0.04226	***80***	***99***	0.0454	0.206	0.0546
44	***45***	0.0224	0.0901	0.0224	***92***	***100***	0.0648	0.295	0.0472

Continued…

...Continued

45	***46***	0.04	0.1356	0.0332	***94***	***100***	0.0178	0.058	0.0604
46	***47***	0.038	0.127	0.0316	***95***	***96***	0.0171	0.0547	0.01474
46	***48***	0.0601	0.189	0.0472	***96***	***97***	0.0173	0.0885	0.024
47	***49***	0.0191	0.0625	0.01604	***98***	***100***	0.0397	0.179	0.0476
42	***49***	0.0715	0.323	0.086	***99***	***100***	0.018	0.0813	0.0216
42	***49***	0.0715	0.323	0.086	***100***	***101***	0.0277	0.1262	0.0328
45	***49***	0.0684	0.186	0.0444	***92***	***102***	0.0123	0.0559	0.01464
48	***49***	0.0179	0.0505	0.01258	***101***	***102***	0.0246	0.112	0.0294
49	***50***	0.0267	0.0752	0.01874	***100***	***103***	0.016	0.0525	0.0536
49	***51***	0.0486	0.137	0.0342	***100***	***104***	0.0451	0.204	0.0541
51	***52***	0.0203	0.0588	0.01396	***103***	***104***	0.0466	0.1584	0.0407
52	***53***	0.0405	0.1635	0.04058	***103***	***105***	0.0535	0.1625	0.0408
53	***54***	0.0263	0.122	0.031	***100***	***106***	0.0605	0.229	0.062
49	***54***	0.073	0.289	0.0738	***104***	***105***	0.00994	0.0378	0.00986
49	***54***	0.0869	0.291	0.073	***105***	***106***	0.014	0.0547	0.01434
54	***55***	0.0169	0.0707	0.0202	***105***	***107***	0.053	0.183	0.0472
54	***56***	0.00275	0.00955	0.00732	***105***	***108***	0.0261	0.0703	0.01844
55	***56***	0.00488	0.0151	0.00374	***106***	***107***	0.053	0.183	0.0472
56	***57***	0.0343	0.0966	0.0242	***108***	***109***	0.0105	0.0288	0.0076
50	***57***	0.0474	0.134	0.0332	***103***	***110***	0.03906	0.1813	0.0461
56	***58***	0.0343	0.0966	0.0242	***109***	***110***	0.0278	0.0762	0.0202
51	***58***	0.0255	0.0719	0.01788	***110***	***111***	0.022	0.0755	0.02
54	***59***	0.0503	0.2293	0.0598	***110***	***112***	0.0247	0.064	0.062
56	***59***	0.0825	0.251	0.0569	***17***	***113***	0.00913	0.0301	0.00768
56	***59***	0.0803	0.239	0.0536	***32***	***113***	0.0615	0.203	0.0518
55	***59***	0.04739	0.2158	0.05646	***32***	***114***	0.0135	0.0612	0.01628
59	***60***	0.0317	0.145	0.0376	***27***	***115***	0.0164	0.0741	0.01972
59	***61***	0.0328	0.15	0.0388	***114***	***115***	0.0023	0.0104	0.00276
60	***61***	0.00264	0.0135	0.01456	***68***	***116***	0.00034	0.00405	0.164
60	***62***	0.0123	0.0561	0.01468	***12***	***117***	0.0329	0.14	0.0358
61	***62***	0.00824	0.0376	0.0098	***75***	***118***	0.0145	0.0481	0.01198
63	***59***	0	0.0386	0	***76***	***118***	0.0164	0.0544	0.01356
63	***64***	0.00172	0.02	0.216					

APPENDIX F

MATLAB CODES FOR BACKWARD/FORWARD SWEEP POWER FLOW IN DISTRIBUTION SYSTEMS

```
clc
clear all
load newline.mat
load newload.mat
Z_base=V_base^2/S_base;
powerload=newload3/S_base;
sample_number=1;
w=2*pi*50;
line = newline;
load_power = powerload;
line=line/Z_base;
line2=line;
Size_line=size(line);
Size_load_power=size(load_power);
[line_number,xxx]=size(find(line~= 0));
[xxx,load_power_number]=size(find(load_power~= 0));
 jj=1;

%%%%%%%%%%%%%%%%%%%%%%%%%%%%%%%%%%%%%%%
%%%%%%%%%  for BIBC   %%%%%%%%%%%%%%%%%%%%%%%%%%%%%%%%%%%%%%

  BIBC=zeros(line_number,Size_load_power(1,2)-1);

  for i=1:line_number
    for j=1:Size_load_power(1,2)-1
      if line(i,j)~= 0
        B1=j;
        if i==1 && j==1
          BIBC(i,j)=1;
        else
          BIBC(:,j)=BIBC(:,i-1);
          BIBC(B1,j)=1;
        end
      end
    end
  end


  for i=2:Size_load_power(1,2)

    if load_power(1,i)== 0
      BIBC(:,i-1)=0;
    end
  end

%%%%%%%%%     for BCBV     %%%%%%%%%%%%%%%%%%%%%%%%%%%%%%%%%%%%

  BCBV=zeros(line_number,Size_load_power(1,2)-1);
```

```
for i=1:line_number
   for j=1:Size_load_power(1,2)-1
      if line(i,j)~= 0
         B1=j;
         if i==1 && j==1
            BCBV(i,j)=line(i,j);
         else
            BCBV(j,:)=BCBV(i-1,:);
            BCBV(B1,j)=line(i,j);
         end
      end
   end
end

% %%%%%%%%%%%%%%   main  load flow       %%%%%%%%%%%%%%%%%

DLF=BCBV*BIBC;
V1=ones(Size_load_power(1,2)-1,1);
V_bus=ones(Size_load_power(1,2)-1,1);
I=zeros(Size_load_power(1,2)-1,1);
Iaa=zeros(Size_load_power(1,2)-1,1);
i=1;
telorance=1;


while i<=200   % maximum iterations
   for j=1:Size_load_power(1,2)-1
      I(j,1)=conj(load_power(1,j+1)/V_bus(j,1));
   end
   I_test(:,i)=I;
   V_bus= V1-(DLF*I);
   V_test(:,i)=V_bus;


   if i<=1
      telorance= 1;   % convergence condition

   else
      telorance= abs(abs(I_test(line_number,i))-abs(I_test(line_number,i-1)));


   end
   if abs(telorance) <= 1e-5
%           fprintf('Power flow sloution found for %gth sample in "%g" iterations\n',jj,i)
       break
   end
      i=i+1;
end
if i==201
   fprintf('No solution, the algorithm is not converge\n')
    return
end

V_bus_size=size(V_bus);
v_bus_shift=zeros(V_bus_size(1,1)+1,1);
v_bus_shift(1,1)=1;
```

```
  for i=2: V_bus_size(1,1)+1
     v_bus_shift(i,1)=V_bus(i-1,1);
  end

  V_bus=v_bus_shift;

  I_bus_shift=zeros(V_bus_size(1,1)+1,1);
  I_bus_shift(1,1)=(V_bus(1,1)-V_bus(2,1))/line(1,1);

  for i=2: V_bus_size(1,1)+1
     I_bus_shift(i,1)=I(i-1,1);
  end

 I_bus=I_bus_shift;

%%%%%%  calculate the loads Impedance)

  V_bus_size=size(V_bus);
  Z_loads=zeros(Size_load_power(1,2),1);

  for i=1:V_bus_size(1,1)
     if load_power(1,i) ~= 0
        Z_loads(i,1)=(V_bus(i,1))/conj(load_power(1,i)/V_bus(i,1));
     else
        Z_loads(i,1)=0;
     end
  end
   %%%%%%% Total losses calculation
%%%%%%%%%%%%%%%%%%%%%%%%%%%%%%%%%%%%%%%%%%%%

 Branch_I=BIBC*I;
  B_I=Branch_I.^2;
  BT=transpose(B_I);
  hhhh=(size(line2));
  ttt=(hhhh(1,1));
  line3=zeros(1,ttt);
     for hhh=1:1:ttt
        for yyy=1:ttt
           for kkk=1:ttt
              if line2(hhh,yyy)~=0
                 line3(1,yyy)=line2(hhh,yyy);
              end
           end
        end
     end

     loss=BT.*line3;
     loss_size=size(loss);
     sum_loss=0;
     total_loss=0;
     for kk=1:loss_size(1,2)
         sum_loss=loss(1,kk);
         total_loss=total_loss+sum_loss;
        end
     loss;
     total_loss;
     total_losses=abs(total_loss)*100e6
```

APPENDIX G

MATLAB CODES FOR HARMONIC POWER FLOW IN DISTRIBUTION SYSTEMS

```
clc
clear all
load newline3.mat
load newload3.mat
w=2*pi*50;
line = newline;
load_power = powerload;
source2=newsource5;
Z_base=V_base^2/S_base;
% load_power=load_power/S_base;
line=line/Z_base;
line2=line;
Size_line=size(line);

Size_load_power=size(load_power);
[line_number,xxx]=size(find(line~= 0));
[xxx,load_power_number]=size(find(load_power~= 0));


jj=1;
%%%%%%%%%%%%%%%%%%%%%%%%%%%%%%%%%%%%%%%%%%%%%%
%%%%%%%%%  for BIBC   %%%%%%%%%%%%%%%%%%%%%%%%%%%%%%%%%%%%%%%%%%%

  BIBC=zeros(line_number,Size_load_power(1,2)-1);

  for i=1:line_number
    for j=1:Size_load_power(1,2)-1
      if line(i,j)~= 0
        B1=j;
        if i==1 && j==1
          BIBC(i,j)=1;
        else
          BIBC(:,j)=BIBC(:,i-1);
          BIBC(B1,j)=1;
        end
      end
    end
  end


  for i=2:Size_load_power(1,2)

    if load_power(1,i)== 0
      BIBC(:,i-1)=0;
    end
  end

%%%%%%%%%      for BCBV      %%%%%%%%%%%%%%%%%%%%%%%%%%%%%%
```

```
BCBV=zeros(line_number,Size_load_power(1,2)-1);


for i=1:line_number
    for j=1:Size_load_power(1,2)-1
        if line(i,j)~= 0
            B1=j;
            if i==1 && j==1
                BCBV(i,j)=line(i,j);
            else
                BCBV(j,:)=BCBV(i-1,:);
                BCBV(B1,j)=line(i,j);
            end
        end
    end
end



% %%%%%%%%%%%%%%%   main  load flow       %%%%%%%%%%%%%%%%%

DLF=BCBV*BIBC;
V1=ones(Size_load_power(1,2)-1,1);
V_bus=ones(Size_load_power(1,2)-1,1);
I=zeros(Size_load_power(1,2)-1,1);
Iaa=zeros(Size_load_power(1,2)-1,1);
i=1;
telorance=1;


while i<=200   % maximum iterations
    for j=1:Size_load_power(1,2)-1
        I(j,1)=conj(load_power(1,j+1)/V_bus(j,1));
    end
    I_test(:,i)=I;
    V_bus= V1-(DLF*I);
    V_test(:,i)=V_bus;


    if i<=1
        telorance= 1;   % convergence condition

    else
        telorance= abs(abs(I_test(line_number,i))-abs(I_test(line_number,i-1)));


    end
    if abs(telorance) <= 1e-5
%           fprintf('Power flow sloution found for %gth sample in "%g" iterations\n',jj,i)
         break
    end
        i=i+1;
end
if i==201
    fprintf('No solution, the algorithm is not converge\n')
     return
end
```

```
  V_bus_size=size(V_bus);
  v_bus_shift=zeros(V_bus_size(1,1)+1,1);
  v_bus_shift(1,1)=1;

  for i=2: V_bus_size(1,1)+1
    v_bus_shift(i,1)=V_bus(i-1,1);
  end

  V_bus=v_bus_shift;

  I_bus_shift=zeros(V_bus_size(1,1)+1,1);
  I_bus_shift(1,1)=(V_bus(1,1)-V_bus(2,1))/line(1,1);

  for i=2: V_bus_size(1,1)+1
    I_bus_shift(i,1)=I(i-1,1);
  end

 I_bus=I_bus_shift;

%%%%%%  calculate the loads Impedance)

  V_bus_size=size(V_bus);
  Z_loads=zeros(Size_load_power(1,2),1);

  for i=1:V_bus_size(1,1)
    if load_power(1,i) ~= 0
      Z_loads(i,1)=(V_bus(i,1))/conj(load_power(1,i)/V_bus(i,1));
    else
      Z_loads(i,1)=0;
    end
  end
  %%%%%%% Total losses calculation
%%%%%%%%%%%%%%%%%%%%%%%%%%%%%%%%%%%%%%%%%%

 Branch_I=BIBC*I;
  B_I=Branch_I.^2;
  BT=transpose(B_I);
  hhhh=(size(line2));
  ttt=(hhhh(1,1));
  line3=zeros(1,ttt);
    for hhh=1:1:ttt
      for yyy=1:ttt
        for kkk=1:ttt
          if line2(hhh,yyy)~=0
            line3(1,yyy)=line2(hhh,yyy);
          end
        end
      end
    end

    loss=BT.*line3;
    loss_size=size(loss);
    sum_loss=0;
    total_loss=0;
    for kk=1:loss_size(1,2)
       sum_loss=loss(1,kk);
       total_loss=total_loss+sum_loss;

    end
```

```
      loss;
      total_loss;
      total_losses=abs(total_loss)*100e6 ;
%%%%%%%%%%%%%%%%%%%%%%%%%%%%%%%%%%%%%%%%%%%%%%%%%%%%%%%%%%%%%%%%%%%%%%%%
%
%%%%%%%%%%  harmonic load flow   %%%%%%%%%%%%%%%%%%%%
%%%%%%%%%%%%%%%%%%%%%%%%%%%%%%%%%%%%%%%%%%%%%%%%%%%%%%%%%%%%%%%%%%%%%%%%
%%%
   Vbus_abs=abs(V_bus);
   h=1; Iindcator = [];
   line_1=real(line)+1j*imag(line)*h;
   Z_loads_1=real(Z_loads)+1j*imag(Z_loads)*h;
   load_1=Z_loads_1';
   max_line=length(line_1); k=0;
   for row=1:max_line
      for column=1:max_line
         if line_1(row,column)~=0
            k=k+1;
            lokasi = [row; (column+1)];
            Iindcator = [Iindcator, lokasi];
            Iline_h(k)=(V_bus(row)-V_bus(column+1))/line_1(row,column);
         end
      end
   end
   Itot1 = abs(Iline_h);
   for mm=1:5
      if mm==1
         h=5;
         source=abs(source2(mm,:)).*I_bus';
      end
      if mm==2
         h=7;
         source=abs(source2(mm,:)).*I_bus';
      end
      if mm==3
         h=11;
         source=abs(source2(mm,:)).*I_bus';
      end
      if mm==4
         h=13;
         source=abs(source2(mm,:)).*I_bus';
      end
      if mm==5
         h=17;
         source=abs(source2(mm,:)).*I_bus';
      end


      line=(real(line_1)+1j*imag(line_1)*h);
      Z_loads=(real(Z_loads_1)+1j*imag(Z_loads_1)*h);
      loads = Z_loads';



%%%%%%%%%%%%%%%%%%%%%%%%%%%%%%%%%%%%%%%%%%%%%%%%%%%%%%%%%%%%%%%%%%%%%%%%
%%%%%%
   Size_line=size(line);
   Size_load=size(loads);
   Size_source=size(source);
```

```
[line_number,xxx]=size(find(line~= 0));
[xxx,load_number]=size(find(loads~= 0));
[xxx,source_number]=size(find(source~= 0));
parallel_number=source_number+load_number;

%%%%%%%%  for A   %%%%%%%%%%%%%%%%%%%%%%%%%%%%%%%%%%%%%%

A2=zeros(line_number,parallel_number);
A1=A2;
load_number1=load_number;
source_number1=source_number;
for i=Size_line:-1:1
   for j=Size_line:-1:1
      if line(i,j)~= 0
         if source(1,j+1)~= 0
            A1(i,source_number1)=1;
            if source_number1 ~= 1
                source_number1=source_number1-1;
            end
         end
         if loads(1,j+1)~= 0
            A1(i,load_number1+source_number)=1;
            load_number1=load_number1-1;
         end
      end
   end
end


for i=Size_line:-1:2
   for j=Size_line:-1:1
      if line(i,j)~= 0
         for k=1:Size_line
            if line(k,i-1)~= 0            %% means these 2 line are conected to each other
               for m=1:parallel_number
                  if A1(j,m)~= 0
                     A1(i-1,m)=A1(j,m);
                  end
               end
            end
         end
      end
   end
end

A2=A1;

%%%%%%%%%%%%%%%%%%%%    for HA   %%%%%%%%%%%%%%%%%%%%%%%%%%

HA=zeros(line_number,parallel_number);
nn=0;
HA(1,:)=line(1,1);

for i=2:1:Size_line
   for j=1:1:Size_line
      if line(i,j)~= 0
          for k=1:Size_line
            if line(k,i-1)~= 0
```

```
                HA(j,:)=HA(i-1,:)+line(i,j)*A2(j,:);
              end
            end
          end
        end
      end

%%%%%%%%%%%%%%%%%%   for HAss   %%%%%%%%%%%%%%%%%%%%%
  HAss=zeros(load_number);
  i=1;
  j=1;
  for n=1:Size_load(1,2)
    if loads(1,n)~= 0
      while j<=load_number
        HAss(i,j)=HA(n-1,source_number+j);
        j=j+1;

      end
      i=i+1;
      j=1;
    end
  end

%%%%%%%%%%%%%%  for HAsh   %%%%%%%%%%%%%%%%%%%%%%%%

  HAsh=zeros(load_number,source_number);
  i=1;
  j=1;

  for n=1:Size_load(1,2)
    if loads(1,n)~= 0
      while j<=source_number
        HAsh(i,j)=HA(n-1,j);
        j=j+1;
      end
      i=i+1;
      j=1;
    end
  end

%%%%%%%%%%%%%%%%%   for Zs and HLF   %%%%%%%%%%%%%%%%%%%%%%%%%%%%

  Zs=zeros(load_number);
  i=1;

  for n=1:Size_load(1,2)
    if loads(1,n)~= 0
      Zs(i,i)=loads(1,n);
      i=i+1;
    end
  end

  HLF=HAss+Zs;

%%%%%%%%%%%%%%%%%%   finding currents of parallel elements  %%%%%%
  Ih=zeros(source_number,1);
  i=1;

  for n=1:Size_source(1,2)
```

```
    if source(1,n)~= 0
      Ih(i,1)=source(1,n);
      i=i+1;
    end
  end

  Is=(HLF)^-1 * -HAsh*Ih;

%%%%%%%%%%%%  Harmonic load flow    %%%%%%%%%%%%%%%%%%%%%%%%%%%%

  Ii=zeros(parallel_number,1);
  size_Ih=size(Ih);
  size_Is=size(Is);
  k=1;
  for i=1:parallel_number
    if i<= size_Ih(1,1)
      Ii(i,1)=Ih(i,1);
    else
      if k<= load_number
      Ii(i,1)=Is(k,1);
      k=k+1;
      end
    end
  end

  V_bus_h=HA*Ii;

  V_bus_h_size=size(V_bus_h);
  v_bus_h_shift=zeros(V_bus_h_size(1,1)+1,1);
  v_bus_h_shift(1,1)=0;

  for i=2: V_bus_h_size(1,1)+1
    v_bus_h_shift(i,1)=V_bus_h(i-1,1);
  end

  V_bus_h=v_bus_h_shift;

  V_mag=abs(V_bus_h);
  V_ang=angle(V_bus_h)*180/pi;
  V_size=size(V_bus_h);
  for i=1:V_size(1,1)
    % fprintf('V%g=   %g , %g\n',i,V_mag(i,1),V_ang(i,1));
  end

%%%%%%%%   injected current to each bus  %%%%%%%%%

  for i=1:V_size(1,1)
    if source(1,i)~= 0
      I_harmonic_load(i,1)=V_bus_h(i,:)/Z_loads(i,1);
    else
      I_harmonic_load(i,1)=0;
    end
  end

  I_ingected=source'-I_harmonic_load;

  if mm==1
    V_bus_h_total_abs_5th(jj,:)=abs(V_bus_h');
    I_ingected_total_abs_5th(jj,:)=abs(I_ingected');
```

```
  end
  if mm==2
    V_bus_h_total_abs_7th(jj,:)=abs(V_bus_h');
    I_ingected_total_abs_7th(jj,:)=abs(I_ingected');
  end
  if mm==3
    V_bus_h_total_abs_11th(jj,:)=abs(V_bus_h');
    I_ingected_total_abs_11th(jj,:)=abs(I_ingected');
  end
  if mm==4
    V_bus_h_total_abs_13th(jj,:)=abs(V_bus_h');
    I_ingected_total_abs_13th(jj,:)=abs(I_ingected');
  end
  if mm==5
    V_bus_h_total_abs_17th(jj,:)=abs(V_bus_h');
    I_ingected_total_abs_17th(jj,:)=abs(I_ingected');
  end

  V_bus_h_total(jj+(mm-1)*sample_number,:)=abs(V_bus_h');
  I_ingected_total(jj+(mm-1)*sample_number,:)=abs(I_ingected');

  % fprintf('sample No. %g for %gth harmonic generated.\n',jj,h);
  line_1=real(line)+1j*imag(line)*h;
  max_line=length(line_1); k=0;
    for row=1:max_line
      for column=1:max_line
        if line_1(row,column)~=0
          k=k+1;
          Iline_h(k)=(V_bus(row)-V_bus(column+1))/line_1(row,column);
        end
      end
    end

    Itot1 = [Itot1; abs(Iline_h)];

  end

  Itot1 = [Iindcator;Itot1];

% end

% fprintf('    ****   All  done   ****.\n');
% Vbus_abs
%%%%%%%%   THDv and THDi calculation
%%%%%%%%%%%%%%%%%%%%%%%%%%%%%%%%%%%%%%%%%%%%%
V_bus_h_total_abs=abs(V_bus_h_total);
V_bus_fundamental=abs(V_bus)';
VFUND=V_bus_fundamental;
AA=V_bus_h_total_abs;
BB=AA.^2;
THDV=(sqrt(sum(BB,1))./VFUND)*100;   %%% THDV bus voltage
% VTHD=[1:83;THDV]
% VTHD3=THDV(3)
AVE_THDV=sum(THDV)/83;
GG=Itot1(4:8,:);
HH=GG.^2;
THDI=(sqrt(sum(HH,1))./Itot1(3,:))*100;  %%THDi branch current
ITHD=[Iindcator;THDI];
```

APPENDIX H

MAIN MODULES OF THE OPSVC SOFTWARE

This section describes the main routines in the OPSVC software which consists of five main modules, namely test system selection, power flow analysis, optimization and voltage profile plotting.

H.1 Test System Selection Module

Figures H.2, H.3 and H.4 show the interfaces of the OPSVC for test system selection. From the main interface of the OPSVC, as shown in Figure H.2, a user can select the appropriate button depending on the intended system configuration for analyses. There are two system configurations for analyses, which are radial distribution systems and transmission systems.

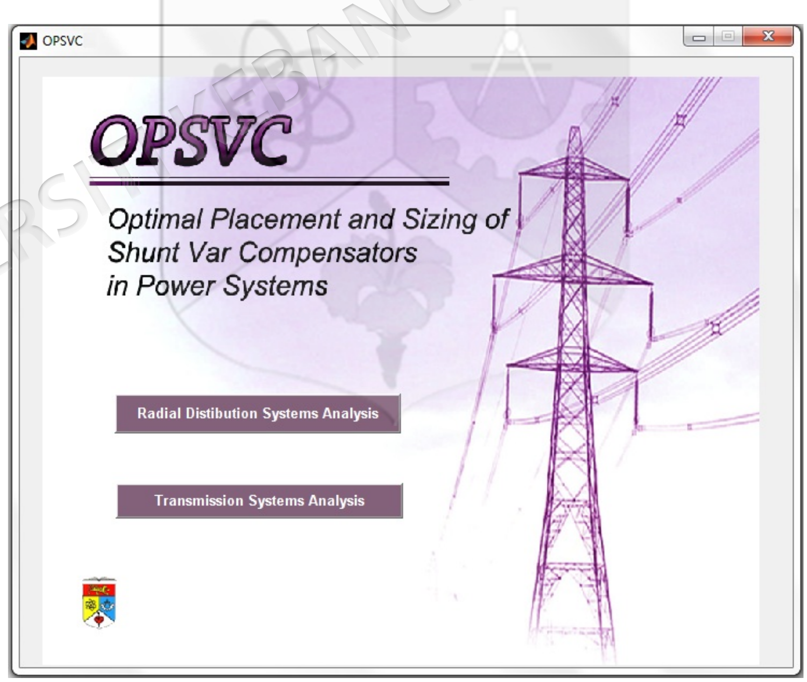

Figure H.2 The main page of the OPSVC software tool

For the radial distribution system interface as shown in Figure H.3, a user has to specify the test system and the intended analysis which may be selected from the backward/forward sweep power flow, optimal placement and sizing of capacitors without harmonics consideration and optimal placement and sizing of capacitors with harmonics consideration. If a user selects the optimal placement and sizing analyses, an optimization technique must be selected from the GA, PSO, HS algorithm, IHS algorithm and GHS algorithm. If a user selects the optimal placement and sizing analysis with harmonic consideration, a harmonic source file is required to be selected.

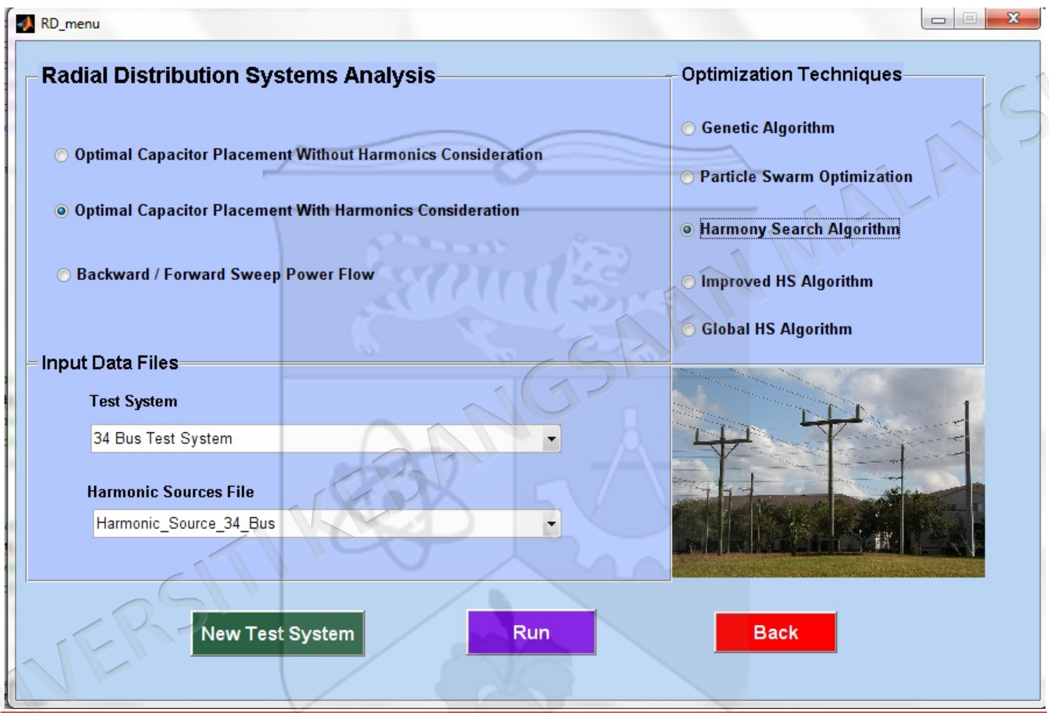

Figure H.3 Interface for radial distribution system analysis

In the OPSVC software tool, distribution system analysis can be performed on four test radial distribution systems, namely, the 10 bus system, 34 bus system, three-phase 10 bus system with harmonic sources and three-phase 34 bus system with harmonic sources. The line and load data of each test distribution system are already embedded in a file which is saved as "*.rdt". For example the file "34_Bus_Test_system.rdt" consists of 34 bus radial distribution system data. The data of harmonic sources are already embedded in a file which has been saved as "*.rdh". For example the file "Harmonic_Source_34_Bus.rdh" consists of the harmonic sources data for the 34 bus radial distribution system. A user can make a new test distribution system by creating a new "rdt" file. For this purpose, a user must click on the “New Test System” and form the line matrix and load matrix of the new system.

In the transmission system interface as shown in Figure H.4, a user has to specify the test system and the intended analysis. The analyses include power flow, optimal placement and sizing of SVCs and optimal placement and sizing STATCOM. If a user selects the optimal placement and sizing analyses, an optimization technique must be selected from the GA, PSO, HS algorithm, IHS algorithm and GHS algorithm.

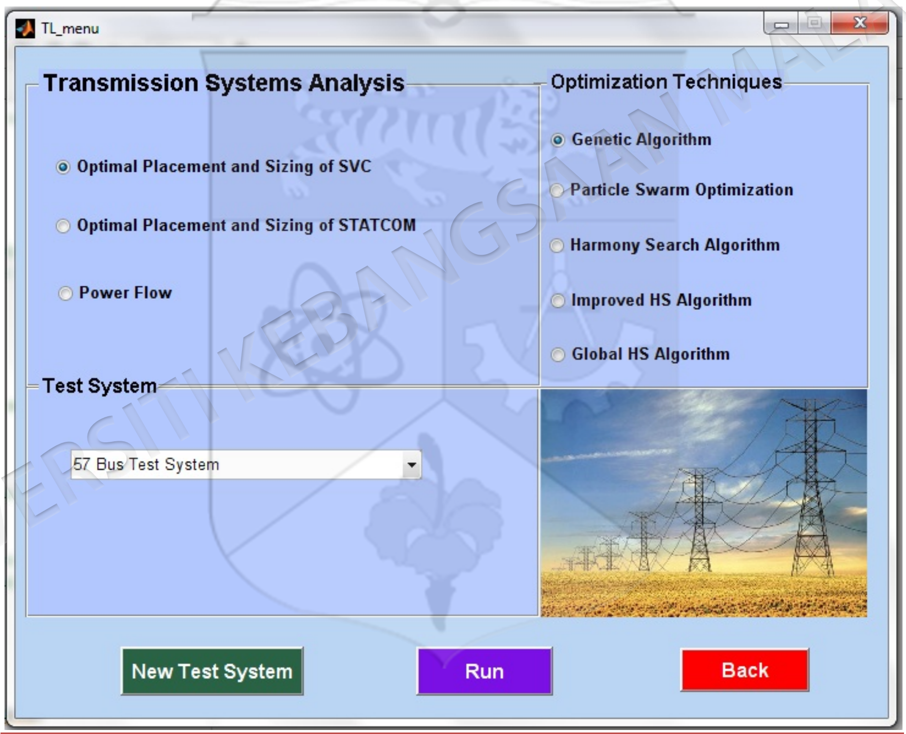

Figure H.4 Interface for transmission system analysis

In OPSVC, two transmission systems, namely, the IEEE 57 bus system and the IEEE 118 bus system are considered as default test systems for transmission system analysis. The line, load and generator data of the transmission test system are embedded in a file which has been saved as "*.tlt". For example the file "57_Bus_Test_System.tlt" consists of 57 bus transmission system data. A user can make a new transmission test system by clicking on the “New Test System” and create a new "tlt" file.

H.2 Power Flow Module

The widely used power flow solver based on the standard Newton Raphson technique is incorporated in the software tool. The background theory of the Newton Raphson power flow technique can be found in Tinney & Hart (1972); Stevenson & Jr (1982); Saadat (2002). By performing power flow analysis, the bus voltage magnitudes, $|V_i|$ and angles, δ_i can be determined.

For radial distribution networks, a simple power flow technique named as the backward/forward sweep power flow (Teng 2000) is used because the method does not require the formation of the Jacobian matrix. Besides, a simple harmonic power flow that uses the backward and forward sweep method (Teng & Chang 2007) has also been developed to calculate harmonic branch currents and harmonic nodal voltages. Figure H.5 shows the output interface of the OPSVC software after performing power flow analysis on a test radial distribution system. The backward/forward sweep power flow and harmonic radial power flow which have been described in Chapter 4 , are used together to calculate the voltage magnitude, voltage angle and THD at each bus.

Figure H.6 shows the power flow output for the 57 bus transmission system. The Newton Raphson technique is used to calculate the voltage magnitude and voltage angle of each bus. The 57 bus transmission system data can be found in Appendix D.

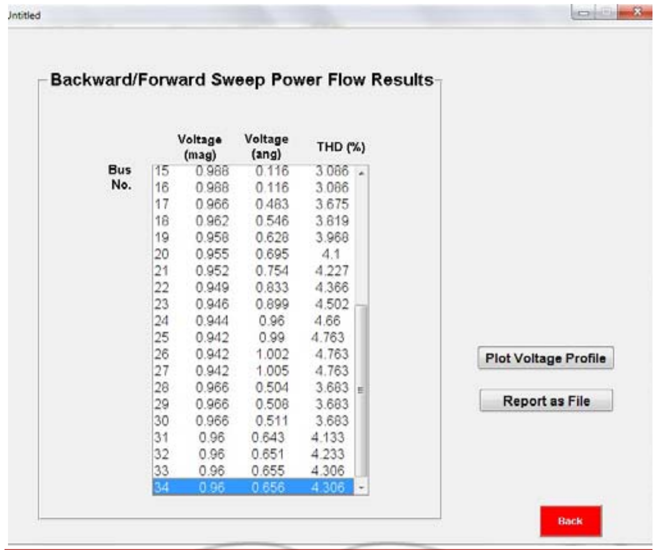

Figure H.5 The power flow output for a test radial distribution system

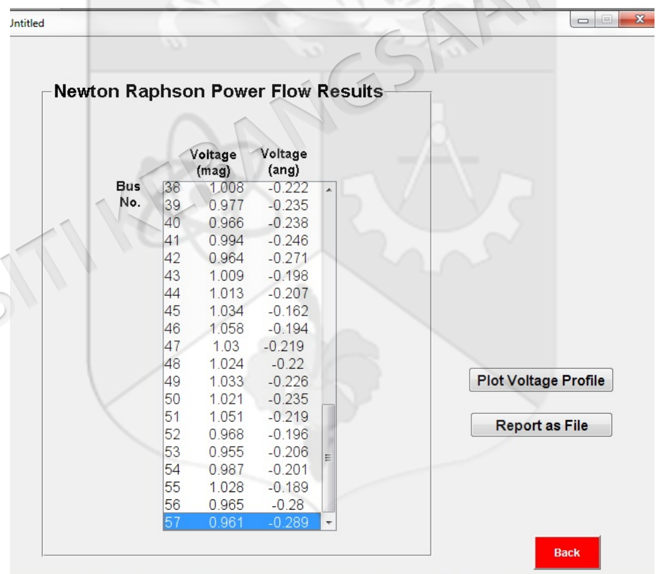

Figure H.6 The power flow output for the 57 bus transmission system

In both transmission and distribution power flow analyses, the results of line power flow have not been displayed on the GUI, but have been calculated and saved in a text file. A user can access all the power flow results by clicking on the "Report as File". Figure H.7 shows the line power flow results of the 57 bus transmission system which are reported in the form of a text file.

Line Power Flow - Notepad

File Edit Format View Help

47	1.030	-12.526
48	1.024	-12.615
49	1.033	-12.960
50	1.021	-13.444
51	1.051	-12.570
52	0.968	-11.207
53	0.955	-11.817
54	0.987	-11.531
55	1.028	-10.843
56	0.965	-16.053
57	0.961	-16.565

Line Power Flow Results

Line	From	To	From Bus Injection		To Bus Injection		Loss	
#	Bus	Bus	P (MW)	Q (MVAr)	P (MW)	Q (MVAr)	P (MW)	Q (MVAr)
1	1	2	102.24	74.95	-100.93	-84.07	1.317	4.44
2	2	3	97.93	-4.68	-95.13	4.53	2.801	7.99
3	3	4	60.21	-8.01	-59.79	5.72	0.423	1.38
4	4	5	13.78	-4.46	-13.65	2.26	0.130	0.27
5	4	6	14.14	-5.13	-14.05	2.11	0.095	0.33
6	6	7	-17.83	0.50	17.89	-2.81	0.067	0.34
7	6	8	-42.48	-6.57	43.13	5.22	0.644	3.28
8	8	9	178.40	19.79	-175.23	-9.02	3.169	16.17
9	9	10	17.26	-9.00	-17.13	5.36	0.133	0.60
10	9	11	12.94	2.76	-12.89	-4.67	0.049	0.16
11	9	12	2.54	-15.85	-2.44	8.64	0.104	0.47
12	9	13	2.33	-1.49	-2.32	-2.39	0.003	0.01
13	13	14	-10.28	23.15	10.37	-23.89	0.092	0.30
14	13	15	-48.94	4.88	49.62	-4.89	0.683	2.21
15	1	15	149.11	34.60	-145.19	-24.71	3.922	20.05
16	1	16	79.38	-0.87	-76.73	7.12	2.647	12.01
17	1	17	93.47	3.93	-91.55	1.79	1.929	8.75
18	3	15	33.91	-16.88	-33.69	12.33	0.226	0.74
19	4	18	13.98	2.54	-13.98	-1.45	-0.000	1.10
20	4	18	17.89	1.33	-17.89	0.05	-0.000	1.38

Figure H.7 The line power flow results for 57 bus transmission system

H.3 Optimization Module

Five heuristic optimization techniques, namely, GA, PSO, HS algorithm, IHS algorithm and GHS algorithm are used to solve the optimal shunt Var compensators problem. The detailed implementation procedures of these optimization techniques for finding the optimal solutions have been described in Chapter 3. Figure H.8 shows the interface of optimal capacitor placement in a radial distribution system. This GUI form includes four sections: optimization parameters, studied cases, convergence characteristics and results of optimal capacitor placement. In the “optimization parameters” section, a user has to specify the required parameters of the selected optimization technique. In the “studied cases” section, a user can consider mutual coupling and load unbalance for solving the problem. For cases considering harmonics, the maximum value of THD has to be defined.

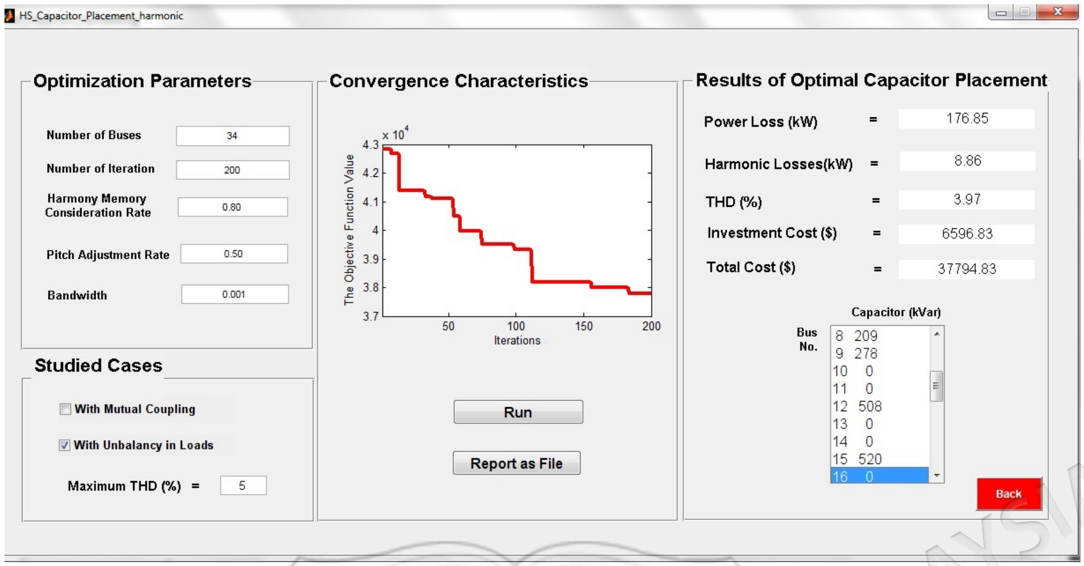

Figure H.8 The interface for solving optimal capacitor placement problem

While the program is running, the convergence curve is plotted as shown in Figure H.8. When the optimization procedure is completed, the optimal capacitor locations and sizes are displayed on the interface. The power loss, harmonic power loss, THD, investment cost and total cost after installing capacitors are also displayed on the interface.

Figure H.9 shows the interface for solving the optimal Var compensator placement problem. This GUI has four sections, namely, optimization parameters, Var compensator input data, convergence characteristics and results of optimal SVC/STATCOM placement. In the section "Var compensators input data", a user has to specify the maximum range of Var compensators in MVar and also the number of Var compensator.

While the program is running, the convergence characteristic is plotted and when the optimization procedure is completed, the obtained optimal SVC or STATCOM location and size are displayed on the GUI. The power loss, voltage deviation, the smallest eigenvalue and investment cost after installing the Var compensators are also displayed on the interface.

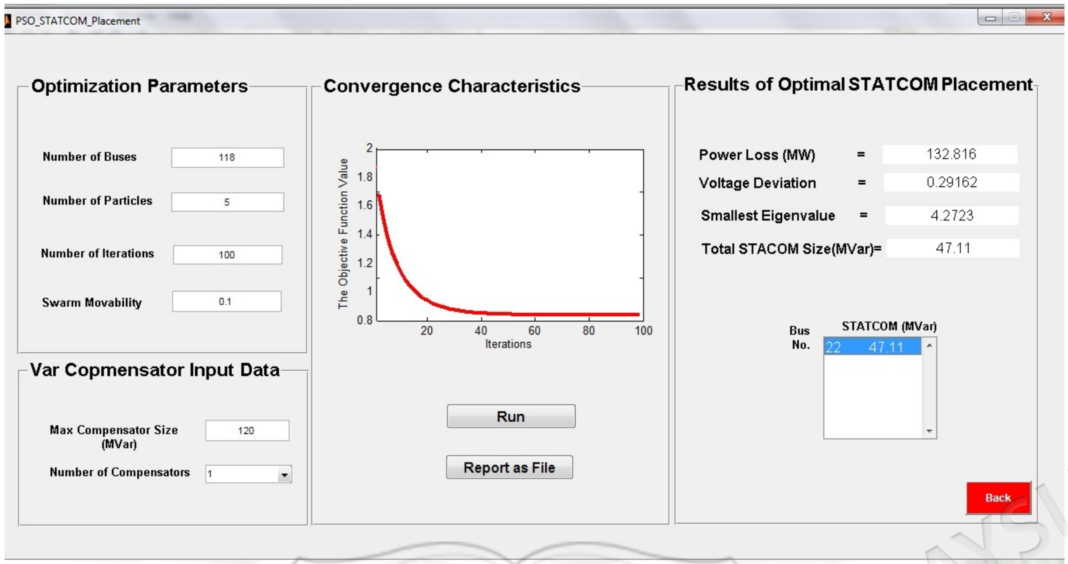

Figure H.9 The interface for solving optimal Var compensator placement problem

H.4 **Voltage Profile Plotting** Module

In each analysis, after running the program, voltage profile of the studied system is plotted. Figure 6.10 shows an example of the voltage profile before and after capacitor installation. Since voltage deviation minimization is one of the objective function in the optimal placement and sizing of shunt Var compensators in transmission systems, the OPSVC software can also plot the total voltage deviation curves before and after installation of Var compensators as shown in Figure H.11.

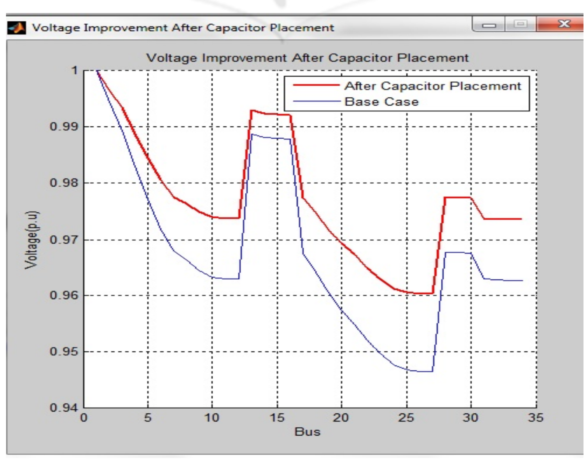

Figure H.10 Voltage profile before and after capacitor installation

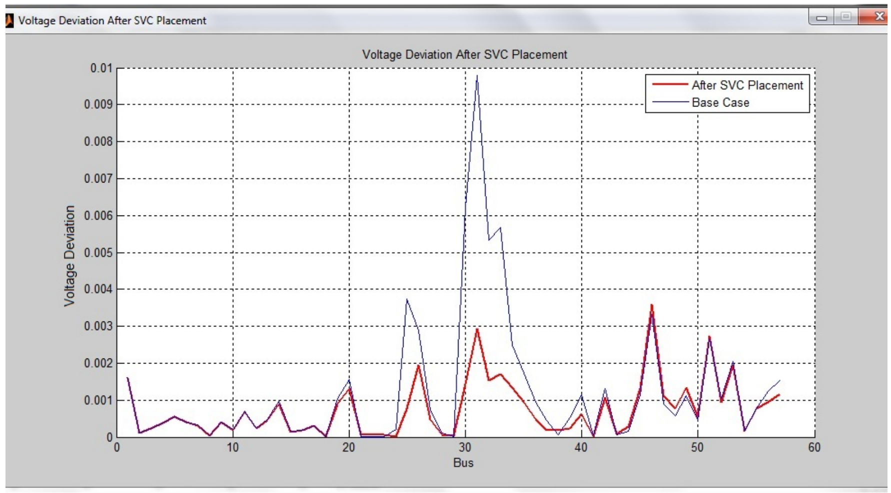

Figure H.11 Voltage deviation curves before and after installation of Var compensator

APPENDIX I

LIST OF PUBLICATIONS

Journal Papers

Sirjani, R., Mohamed, A., Shareef, H. 2012. Optimal Allocation of Shunt Var Compensators in Power Systems Using a Novel Global Harmony Search Algorithm. *International Journal of Electrical Power and Energy Systems* **43**(1): 562-572.

Sirjani, R., Mohamed, A., Shareef, H. 2012. Heuristic Optimization Techniques to Determine Optimal Capacitor Placement and Sizing in Radial Distribution Networks: A Comprehensive Review . *Przeglad Elektrotechniczny* **88**(7a):1-7.

Sirjani, R., Mohamed, A., Shareef, H. 2012. Optimal placement and sizing of Static Synchronous Compensators in power systems using an Improved Harmony Search Algorithm. *International Review of Electrical Engineering* **7**(2): 4183-4193.

Sirjani, R., Mohamed, A., Shareef, H. 2011. Optimal placement and sizing of Static Var Compensators in power systems using Improved Harmony Search Algorithm. *Przeglad Elektrotechniczny* **87**(7): 214-218.

Sirjani, R., Mohamed, A., Shareef, H. 2011. Optimal Capacitor Placement in Three-Phase Distribution Systems Using Improved Harmony Search Algorithm. *International Review of Electrical Engineering* **6**(4B): 1783-1793.

Sirjani, R., Mohamed, A., Shareef, H. 2011. Optimal Capacitor Placement in a Distribution Network with Nonlinear Loads Using Harmony Search Algorithm. *Australian Journal of Basic and Applied Sciences* **5**(6): 461-474.

Sirjani, R., Mohamed, A., Shareef, H. 2010. Optimal Capacitor Placement in a Radial Distribution System Using Harmony Search Algorithm. *Journal of Applied Sciences* **10**(23): 2996-3006.

Sirjani, R., Mohamed, A., Shareef, H. 2012. Optimal Placement and Sizing of Shunt FACTS Devices in Power Systems Using Heuristic Optimization Techniques: a Comprehensive Survey. *Przeglad Elektrotechniczny Przeglad Elektrotechniczny* **88**(10b): 335-341.

Sirjani, R., Mohamed, A., Shareef, H. 2012. Comparative Study of the Effectiveness of Different Var Compensation Devices in Large-Scale Power Networks. *Journal of Central South University of Technology*. **Accepted for Publication**

Conference Proceedings

Sirjani, R., Mohamed, A., Shareef, H. 2011. An Improved Harmony Search Algorithm for Optimal Capacitor Placement in Radial Distribution Systems. *The 5th International Power Engineering and Optimization Conference* :323-328.

Sirjani, R., Mohamed, A., Shareef, H. 2011. Improved Harmony Search Algorithm for Optimal Placement and Sizing of Static Var Compensators in Power Systems. *First International Conference on Informatics and Computational Intelligence* :295-300.

Sirjani, R., Mohamed, A., Shareef, H. 2011. A Hybrid BCO/HS Algorithm for Optimal Placement and Sizing of Static Var Compensators in Power Systems. *11th WSEAS/IASME International Conference on Electric Power Systems, High Voltages, Electric Machines* : 54-59.

Sirjani, R., Mohamed, A., Shareef, H. 2010. Optimal Capacitor Placement in Distribution Systems Using Ant Colony Optimization. *Regional Engineering Postgraduate Conference* :1-7.